

LA-14389

Approved for public release;  
distribution is unlimited.

---

## Property and Lifetime Prediction in Aged U-Nb Alloys: A Statistical Assessment

Edited by Mable Amador, Group IRM-CAS.  
Photocomposition by Deidre A. Plumlee, Group IRM-CAS.

Los Alamos National Laboratory, an affirmative action/  
equal opportunity employer, is operated by Los Alamos  
National Security, LLC, for the National Nuclear Security  
Administration of the U.S. Department of Energy under  
contract DE-AC52-06NA25396.



This report was prepared as an account of work sponsored by an agency of the U.S. Government. Neither Los Alamos National Security, LLC, the U.S. Government nor any agency thereof, nor any of their employees make any warranty, express or implied, or assume any legal liability or responsibility for the accuracy, completeness, or usefulness of any information, apparatus, product, or process disclosed, or represent that its use would not infringe privately owned rights. Reference herein to any specific commercial product, process, or service by trade name, trademark, manufacturer, or otherwise does not necessarily constitute or imply its endorsement, recommendation, or favoring by Los Alamos National Security, LLC, the U.S. Government, or any agency thereof. The views and opinions of authors expressed herein do not necessarily state or reflect those of Los Alamos National Security, LLC, the U.S. Government, or any agency thereof. Los Alamos National Laboratory strongly supports academic freedom and a researcher's right to publish; as an institution, however, the Laboratory does not endorse the viewpoint of a publication or guarantee its technical correctness.

LA-14389  
Issued: February 2009

---

## Property and Lifetime Prediction in Aged U-Nb Alloys: A Statistical Assessment

Robert E. Hackenberg

Geralyn M. Hemphill

This page left blank intentionally.

## TABLE OF CONTENTS

<b>LIST OF ACRONYMS AND SYMBOLS .....</b>	<b>ix</b>
<b>ABSTRACT.....</b>	<b>1</b>
<b>1. INTRODUCTION.....</b>	<b>2</b>
<b>2. EXPERIMENTAL DATA SETS.....</b>	<b>3</b>
2.1. Model Fitting .....	3
2.2. Model Validation .....	4
2.2.1. Nonbanded U-5.6Nb and U-7.7Nb .....	5
2.2.2. Banded U-6Nb .....	5
<b>3. STATISTICAL EVALUATION METHOD .....</b>	<b>6</b>
3.1. Sources and Magnitudes of Scatter .....	6
3.2. Previous Analysis Method .....	7
3.2.1. Modeling Approach .....	7
3.2.2. Failure Criterion and Lifetime Prediction .....	9
3.3. Current Analysis Method .....	11
3.3.1. Statistical Modeling Overview .....	11
3.3.2. Model Evaluation .....	12
3.3.3. Model Fitting .....	14
3.3.4. Model Predictions and Statistical Intervals .....	15
<b>4. RESULTS AND DISCUSSION .....</b>	<b>16</b>
4.1. Model Fitting—General Comments .....	16
4.1.1. Quality of Fitting .....	16
4.1.2. Comparison of Parameters and Aging Responses .....	18
4.1.3. Modeling Assumptions .....	19
4.2. Model Fitting—Specific Properties .....	21
4.2.1. Total Elongation .....	21
4.2.2. Uniform Elongation .....	21
4.2.3. First-Yield Strength .....	21
4.2.4. First-Yield Modulus .....	22
4.2.5. Second-Yield Strength .....	22
4.2.6. Ultimate Tensile Strength .....	22
4.2.7. Vickers Hardness .....	22
4.3. Model Validation .....	22
4.4. Lifetime Predictions .....	24
4.5. Evaluation of Age-Sensitive Properties for Surveillance .....	25
4.6. Recommendations for Future Work .....	26
<b>5. CONCLUSIONS .....</b>	<b>28</b>
<b>ACKNOWLEDGEMENTS .....</b>	<b>29</b>
<b>REFERENCES.....</b>	<b>29</b>
<b>APPENDIX 1: SOURCES AND MAGNITUDES OF SCATTER.....</b>	<b>101</b>
<b>APPENDIX 2: MODEL FITS AND PREDICTIONS ON AN ALTERNATE DEFINITION OF HARDNESS REPLICATES .....</b>	<b>105</b>
<b>APPENDIX 3: MODEL EVALUATION .....</b>	<b>111</b>
<b>APPENDIX 4: BACKGROUND ON NONLINEAR MODELS .....</b>	<b>121</b>

## LIST OF TABLES

Table 2.1.	Tensile Data from Each Replicate of Nonbanded U-5.6Nb. ....	31
Table 2.2.	Vickers Microhardness Linescan Data from Nonbanded U-5.6Nb. ....	33
Table 2.3.	Tensile Data from Each Replicate of Nonbanded U-7.7Nb.. ....	35
Table 2.4.	Vickers Microhardness Linescan Data from Nonbanded U-7.7Nb. ....	37
Table 2.5.	Tensile Validation Data for Nonbanded U-7.7Nb. ....	39
Table 2.6.	Vickers Hardness Validation Data for Nonbanded U-5.6Nb. ....	40
Table 2.7.	Vickers Hardness Validation Data for Nonbanded U-7.7Nb. ....	41
Table 2.8.	Chemical Analysis Results of Banded U-6Nb from the Validation Experiments. ....	42
Table 2.9.	Tensile Validation Data for Banded U-6Nb. ....	43
Table 2.10.	Vickers Hardness Validation Data for Banded U-6Nb. ....	44
Table 3.1.	Property Values at the Start and End (Peak) of Age-Hardening. ....	48
Table 3.2.	Kinetic Parameters for U-5.6Nb Obtained from the Previous Study. ....	49
Table 3.3.	Kinetic Parameters for U-7.7Nb Obtained from the Previous Study. ....	49
Table 3.4.	Lifetimes for U-5.6Nb and U-7.7Nb Obtained from the Previous Study ....	49
Table 3.5.	Analytic Method Comparison between the Previous and Present Studies. ....	50
Table 3.6.	Total Elongation Kinetic Parameters for U-5.6Nb. ....	51
Table 3.7.	Total Elongation Kinetic Parameters for U-7.7Nb. ....	51
Table 3.8.	Uniform Elongation Kinetic Parameters for U-5.6Nb. ....	51
Table 3.9.	Uniform Elongation Kinetic Parameters for U-7.7Nb. ....	51
Table 3.10.	First-Yield Strength Kinetic Parameters for U-5.6Nb. ....	52
Table 3.11.	First-Yield Strength Kinetic Parameters for U-7.7Nb. ....	52
Table 3.12.	First-Yield Modulus Kinetic Parameters for U-5.6Nb. ....	52
Table 3.13.	First-Yield Modulus Kinetic Parameters for U-7.7Nb ....	52
Table 3.14.	Second-Yield Strength Kinetic Parameters for U-5.6Nb. ....	53
Table 3.15.	Second-Yield Strength Kinetic Parameters for U-7.7Nb. ....	53
Table 3.16.	Ultimate Tensile Strength Kinetic Parameters for U-5.6Nb. ....	53
Table 3.17.	Ultimate Tensile Strength Kinetic Parameters for U-7.7Nb. ....	53
Table 3.18.	Vickers Hardness Kinetic Parameters for U-5.6Nb. ....	54
Table 3.19.	Vickers Hardness Kinetic Parameters for U-7.7Nb. ....	54
Table 4.1.	Results for Three Quality-of-Model-Fitting Metrics Evaluated for each Property in U-5.6Nb ....	55
Table 4.2.	Results for Three Quality-of-Model-Fitting Metrics Evaluated for each Property in U-7.7Nb. ....	55
Table 4.3.	Residual Standard Errors and Ancillary Quantities ....	55
Table 4.4.	Summary of Activation Energies Q from Model Fitting of the Previous Study and This Study. ....	56
Table 4.5.	Summary of A Parameter ( $= 1/dx$ ) from Model Fitting of the Previous Study and This Study. ....	56
Table 4.6.	Summary of B Parameter ( $= x_0$ at 300°C) from Model Fitting of the Previous Study and This Study. ....	56
Table 4.7.	Experimentally Measured and Predicted Mean TE Values for Various U-Nb Alloys for Current and Future Model Validation. ....	57
Table 4.8.	Experimentally Measured and Predicted Mean UE Values for Various U-Nb Alloys for Current and Future Model Validation. ....	58

Table 4.9.	Experimentally Measured and Predicted Mean 1YS Values for Various U-Nb Alloys for Current and Future Model Validation. ....	59
Table 4.10.	Experimentally Measured and Predicted Mean 1YM Values for Various U-Nb Alloys for Current and Future Model Validation. ....	60
Table 4.11.	Experimentally Measured and Predicted Mean 2YS Values for Various U-Nb Alloys for Current and Future Model Validation. ....	61
Table 4.12.	Experimentally Measured and Predicted Mean UTS Values for Various U-Nb Alloys for Current and Future Model Validation. ....	62
Table 4.13.	Experimentally Measured and Predicted Mean HV Values for Various U-Nb Alloys for Current and Future Model Validation. ....	63
Table 4.14.	Lifetime Predictions for U-5.6Nb. ....	64
Table 4.15.	Lifetime Predictions for U-7.7Nb. ....	64
Table 4.16.	Threshold of Fractional and Absolute Property Changes, and Associated Aging Times at 40°C where a Statistically Significant Aging Response is Expected to be Experimentally Observable in Banded U-6Nb. ....	65
Table 4.17.	Threshold of Fractional and Absolute Property Changes, and Associated Aging Times at 40°C where a Statistically Significant Aging Response is Expected to be Experimentally Observable in Nonbanded U-5.6Nb. ....	65
Table 4.18.	Threshold of Fractional and Absolute Property Changes, and Associated Aging Times at 40°C where a Statistically Significant Aging Response is Expected to be Experimentally Observable in Nonbanded U-7.7Nb. ....	65
Table 4.19.	Notional Tensile Property Equivalency Table that Would Result from a Future Systematic Study of the Effects of Tensile Geometry and Machining Damage. ....	66

## LIST OF FIGURES

Figure 2.1.	Cylindrical tensile specimen geometry used for the nonbanded U-5.6Nb and U-7.7Nb studies for both model fitting and for validation. ....	67
Figure 2.2.	Cylindrical tensile specimen geometry used for the banded U-6Nb validation experiments. ....	67
Figure 3.1.	Total elongation at 100°C for U-5.6Nb. ....	68
Figure 3.2.	Predicted TE and lifetime at 40°C for U-5.6Nb. ....	68
Figure 4.1.	Universal plot of U-5.6Nb TE data (points) and model fit to data (solid line). ....	69
Figure 4.2.	Universal plot of U-7.7Nb TE data (points) and model fit to data (solid line). ....	69
Figure 4.3.	Universal plot of U-5.6Nb UE data (points) and model fit to data (solid line). ....	70
Figure 4.4.	Universal plot of U-7.7Nb UE data (points) and model fit to data (solid line). ....	70
Figure 4.5.	Universal plot of U-5.6Nb 1YS data (points) and model fit to data (solid line). ....	71
Figure 4.6.	Universal plot of U-7.7Nb 1YS data (points) and model fit to data (solid line). ....	71
Figure 4.7.	Universal plot of U-5.6Nb 1YM data (points) and model fit to data (solid line). ....	72
Figure 4.8.	Universal plot of U-7.7Nb 1YM data (points) and model fit to data (solid line). ....	72
Figure 4.9.	Universal plot of U-5.6Nb 2YS data (points) and model fit to data (solid line). ....	73
Figure 4.10.	Universal plot of U-7.7Nb 2YS data (points) and model fit to data (solid line). ....	73
Figure 4.11.	Universal plot of U-5.6Nb UTS data (points) and model fit to data (solid line). ....	74
Figure 4.12.	Universal plot of U-7.7Nb UTS data (points) and model fit to data (solid line). ....	74
Figure 4.13.	Universal plot of U-5.6Nb HV data (points) and model fit to data (solid line). ....	75

Figure 4.14.	Universal plot of U-7.7Nb HV data (points) and model fit to data (solid line).....	75
Figure 4.15.	Consolidated aging response model fits at 200°C for (a) U-5.6Nb and (b) U-7.7Nb.....	76
Figure 4.16.	Consolidated aging response predictions at 40°C for (a) U-5.6Nb and (b) U-7.7Nb.....	77
Figure 4.17.	U-5.6Nb TE data, model fits to data, and low-temperature model predictions..	78
Figure 4.18.	U-7.7Nb TE data, model fits to data, and low-temperature model predictions.....	79
Figure 4.19.	U-5.6Nb UE data, model fits to data, and low-temperature model predictions.....	80
Figure 4.20.	U-7.7Nb UE data, model fits to data, and low-temperature model predictions.....	81
Figure 4.21.	U-5.6Nb 1YS data, model fits to data, and low-temperature model predictions...	82
Figure 4.22.	U-7.7Nb 1YS data, model fits to data, and low-temperature model predictions...	83
Figure 4.23.	U-5.6Nb 1YM data, model fits to data, and low-temperature model predictions.	84
Figure 4.24.	U-7.7Nb 1YM data, model fits to data, and low-temperature model predictions.	85
Figure 4.25.	U-5.6Nb 2YS data, model fits to data, and low-temperature model predictions...	86
Figure 4.26.	U-7.7Nb 2YS data, model fits to data, and low-temperature model predictions...	87
Figure 4.27.	U-5.6Nb UTS data, model fits to data, and low-temperature model predictions ..	88
Figure 4.28.	U-7.7Nb UTS data, model fits to data, and low-temperature model predictions. .	89
Figure 4.29.	U-5.6Nb HV data, model fits to data, and low-temperature model predictions. ...	90
Figure 4.30.	U-7.7Nb HV data, model fits to data, and low-temperature model predictions ...	91
Figure 4.31.	U-5.6Nb validation HV data and model predictions .....	92
Figure 4.32.	U-7.7Nb validation TE data and model predictions .....	93
Figure 4.33.	U-7.7Nb validation UE data and model predictions .....	93
Figure 4.34.	U-7.7Nb validation 1YS data and model predictions .....	94
Figure 4.35.	U-7.7Nb validation 1YM data and model predictions.....	94
Figure 4.36.	U-7.7Nb validation 2YS data and model predictions .....	95
Figure 4.37.	U-7.7Nb validation UTS data and model predictions.....	95
Figure 4.38.	U-7.7Nb validation HV data and model predictions .....	96
Figure 4.39.	U-6Nb validation TE data and model predictions .....	97
Figure 4.40.	U-6Nb validation UE data and model predictions.....	97
Figure 4.41.	U-6Nb validation 1YS data and model predictions .....	98
Figure 4.42.	U-6Nb validation 1YM data and model predictions.....	98
Figure 4.43.	U-6Nb validation 2YS data and model predictions .....	99
Figure 4.44.	U-6Nb validation UTS data and model predictions.....	99
Figure 4.45.	U-6Nb validation HV data and model predictions. ....	100

## LIST OF ACRONYMS AND SYMBOLS

$\alpha$	Equilibrium orthorhombic phase found in pure and alloyed uranium
$\alpha''$	Monoclinic phase found in alloyed uranium
$\gamma$	Body-centered cubic phase found in pure and alloyed uranium
$\gamma_2$	Equilibrium body-centered cubic phase containing approximately 75 at.% Nb
$\gamma^o$	Tetragonal phase found in uranium alloys, a distorted form of $\gamma$
%RA	Percent reduction in area
03K-422	LANL/MST-6 foundry identification number for the U-7.7Nb plate
03K-425	LANL/MST-6 foundry identification number for the U-5.6Nb plate
1YS	First-yield strength
1YM	First-yield modulus
2YS	Second-yield strength
$A$	Adjustable parameter for various nonlinear models
AM	Annealed-then-machined condition; also referred to as “as-machined”
AQ	As quenched, same as stating “time = 0, MA condition”
$A_s$	Austenite start temperature
at. %	Atomic percent
$B$	Adjustable parameter for various nonlinear models
BCC	Body-centered cubic
$CI$	Confidence interval
$df$	Degrees of freedom
$dx$	Adjustable parameter for the Boltzmann model
$f$	Fractional property change referred to $P(start)$
$f'$	Fractional property change referred to $P(t = 0)$
HV	Vickers Microhardness
LANL	Los Alamos National Laboratory (Los Alamos, NM)
MA	Machined-then-annealed condition; also referred to as “as-annealed”
$n$	Number of replicate data points
$nv$	Number of validation data points
$p$	Number of adjustable parameters
$P$	Generic age-sensitive property; also a $3 \times 1$ vector containing the first partial derivatives for the estimates of $Q$ , $A$ , and $B$ (Appendix 4 only)
$P(peak)$	P at the end of the age-hardening regime, at peak age

$P(start)$	P at the start of the age-hardening regime
$P(t = 0)$	P at aging time = 0, evaluated condition (AM vs MA) unspecified
$P(t = 0, AM)$	P at aging time = 0 evaluated in the as-machined condition
$P(t = 0, MA)$	P at aging time = 0 evaluated in the as-annealed condition, same as $P(AQ)$
$PI$	Prediction interval
$pred_i$	Predicted mean value for the time $i$
$Q$	Apparent activation energy for an aging or other physical process
$Q_{diff}$	Activation energy for diffusion
QMU	Quantification of margins and uncertainties
$R$	Universal gas constant
RFP	Rocky Flats Plant
$RSE$	Residual standard error
$RSS$	Residual sum-of-squares
$SD$	Standard Deviation
$se.fit_i$	Standard error of a fitted value at time $i$
$t$	Time; also a generic t-statistic
$t(n, df)$	t-statistic for a $100 \times n$ % confidence interval with $df$ degrees of freedom
$T$	Temperature
TE	total (plastic) elongation (engineering strain) to tensile failure
UE	uniform (plastic) elongation (engineering strain) to tensile failure
UTS	Ultimate tensile strength
VAR	Vacuum arc remelt(ed)
wt%	Weight percent
$x$	$\log_{10}(\text{time in minutes})$
$x'$	$\log_{10}(\text{equivalent time in minutes at a reference temperature } T_2)$
$x_o$	Adjustable parameter for the Boltzmann model
$y$	Generic response variable
Y-12	Oak Ridge Y-12 Plant (Oak Ridge, TN)

# Property and Lifetime Prediction in Aged U-Nb Alloys: A Statistical Assessment

by

Robert E. Hackenberg and GERALYN M. Hemphill

## ABSTRACT

This study was undertaken to better model the aging response of U-Nb alloys, particularly to predict properties and their scatter bands, from which lifetimes and their uncertainties can be evaluated. Predictive models of the aging time- and temperature-dependencies of seven age-sensitive properties were developed for nonbanded U-5.6 wt% Nb and U-7.7 wt% Nb alloys. These properties were total and uniform plastic tensile elongation to failure; first-yield, second-yield, and ultimate tensile strengths; first-yield elastic modulus; and Vickers microhardness. A more systematic and statistically aware kinetics modeling approach than employed previously gave reasonable models fits to accelerated aging property data in nonbanded U-5.6Nb and U-7.7Nb, and useful predictions for most of the properties studied. With minor modifications, the U-5.6Nb model was extended to banded U-6Nb. This modeling approach shared many of the key assumptions of the previous approach, including the assumption of Arrhenius behavior and the use of three adjustable parameters. Initial data returns from long-term aging experiments were used to validate the fitted models, a new feature to this study. The apparent activation energies of aging for the property of greatest interest, total elongation, were 32 kcal/mol for U-5.6Nb and 39 kcal/mol for U-7.7Nb, respectively; those for the other properties spanned 14–51 kcal/mol. Comparing the goodness of the model fits for the seven properties, the best fits were obtained for second-yield strength and hardness, the first-yield modulus fit the least well, and the other properties' fits were in between. The U-5.6Nb models are more robust and therefore are expected to have better predictive power than those of U-7.7Nb, especially at the lower aging temperatures of interest. Model extrapolations to longer times (up to 5 years) and lower temperatures (as low as 40°C) than those used for the model fitting agreed well with most of the validation data gathered for both nonbanded alloys, as well as banded U-6Nb, giving provisional validation of the fitted models. Property predictions for planned or already pending validation experiments are also provided. With a view towards enabling future modeling efforts, this report tabulates all replicate tensile properties and complete hardness scan data used for both model fitting and validation. For surveillance purposes, the properties most practically amenable to detecting the onset of aging at the earliest times are first-yield strength and second-yield strength. Even at aging temperatures as high as 60°C, the minimum lifetimes from this present study are beyond 100 years, giving no cause for concern, if the previously developed failure criterion based on uniaxial tensile elongation (with its caveats) is accepted.

**This document must be reproduced in COLOR  
to ensure accuracy of the figures.**

## 1. INTRODUCTION

There is concern that aging during long-term stockpile storage of U-6 wt% Nb alloy components will change the material in ways that will adversely affect their performance. In this context, “aging” is a generic term that can encompass a variety of specific physical mechanisms by which the microstructure and properties evolve as a function of time for a given temperature and local environment. U-6Nb<sup>1</sup> is a complex material because of its gross compositional inhomogeneity (its chemical banding spans 4–8 wt%), its metastable starting microstructure, and the fact that a variety of external factors such as temperature, stress, and gaseous species can cause aging through multiple mechanisms. In principle, such mechanisms can operate in overlapping time-temperature domains, at different rates, and with different signs and magnitudes of resulting property changes. These aging mechanisms have an aggregate effect on the properties (usually adversely) and ultimately the performance, but their deconvolution is not simple.

A previous report [2007hac2] assessed several different aging mechanisms and concluded that the most significant of these was the phase separation into Nb-rich and Nb-lean regions as the initially metastable, Nb-supersaturated  $\alpha''$  microstructure evolves toward the equilibrium two-phase mixture of  $\alpha + \gamma_2$ . These processes give rise to *age hardening*, phenomenologically defined as increasing hardness and strength and decreasing ductility observed as a function of increasing aging time-at-temperature. There continues to be uncertainty as to the specific physical mechanism of age hardening at temperatures relevant to U-6Nb material processing ( $\leq 200^\circ\text{C}$ ) and stockpile storage ( $\leq 60^\circ\text{C}$ ) [2008cla]. There is also uncertainty regarding the nature and magnitude of the failure criterion. These limitations make the most desirable approach of property response and lifetime prediction—that based on fundamental physics—unattainable at the present time.

Therefore, the next best approach, a semi-empirical one, was taken to model the phenomenological property evolution during aging, which enabled lifetime estimates to be made from an assumed failure criterion couched in terms of one or more of these age-sensitive properties. It should be noted that the predictions of age-sensitive properties are useful not just for lifetime prediction, but also as a tool that can be applied to U-6Nb component surveillance studies and also to “what-if” analyses. Drawing upon a large body of artificial aging data obtained from nonbanded U-5.6Nb and U-7.7Nb material [2007hac1], an earlier report [2007hac2] determined the aging (property evolution) kinetics as a function of time and temperature in terms of an Arrhenius model [1976eck, 2002eck], and used this to make a first prediction of banded U-6Nb component lifetimes.

The main purpose of this study was to provide a more statistically aware quantification of these property and lifetime predictions and uncertainties using the same body of model-fitting data. A secondary end was to expand the number of age-sensitive properties (from one to seven) that could be predicted with an aging model, which has relevance for the types of surveillance on U-6Nb components that might be contemplated. Finally, this report serves the tertiary purpose of archiving, in tabular format, all replicate tensile properties and complete hardness scan data used for both model fitting and validation. Aware that new aging data and scientific insights will likely become available in the future (e.g., from planned or already pending long-term validation experiments), this archiving is done with a view toward supporting future reanalyses of an expanded body of data.

---

<sup>1</sup> Alloy and phase compositions in this report are given in weight percent (wt%) unless otherwise specified.

The basic assumptions underlying this present analysis are the same as those of the previous study, particularly with regards to the fundamental axes by which aging is measured and analyzed:

1. Time-axis:  $\log(\text{aging time})$  is the relevant time unit of aging.
2. Temperature-axis: the Arrhenius formalism was used to compare the kinetics at different aging temperatures, for both model fitting and interpolation/extrapolation.
3. Property-axis: age-related property changes were normalized to a fractional property change spanning  $0 \leq f \leq 1$ , using a linear transformation of the property  $P$  to the fractional change  $f$ .

Early in this study, these three assumptions were compared against credible alternative time-, temperature- and property-scalings, with the result that the original assumptions yielded the most satisfactory results. Aging time, aging temperature, and alloy composition (Nb content) were the independent variables in this study, and the various property responses were the dependent variables.

It should be noted at the outset that, although considerable uncertainty exists with respect to the quantitative magnitude of the failure criterion (and even its conceptual validity), no attempt was made to quantify the uncertainty in the failure criterion; the failure criterion was accepted simply “as is.” In this light, it should be kept in mind that this study is meant only to quantify property predictions, lifetime predictions, and their statistical uncertainties. Given the doubt surrounding the magnitude and conceptual validity of the failure criterion, a further analysis involving property/performance *margin* calculations (as would be done in a bona fide Quantification of Margins and Uncertainties (QMU) study) could not be justified, and therefore was not undertaken in this study, although the information contained in this report is sufficient for such calculations, provided they are appropriately hedged by these caveats.

## **2. EXPERIMENTAL DATA SETS**

### **2.1. Model Fitting**

The data set used for aging kinetics model fitting was from the nonbanded U-5.6Nb (plate ID 03K-425) and U-7.7Nb (plate ID 03K-422) material, whose synthesis was described in [2007hac1]. These two nonbanded materials, which are compositionally homogeneous with respect to Nb, were used to represent the average (U~5.8Nb) and upper limit (U~8Nb) of compositions present on 100–200 micron length scales in the banded U-6Nb material. The high-Nb alloy was selected for study because it is considered to age faster than the mean (U~5.8Nb) or lower limit (U~4Nb) compositions of the banded U-6Nb [2002eck]. Therefore, there was concern that the high-Nb bands would degrade faster and cross the failure threshold sooner than the mean or lower-Nb bands, which on a conservative performance assessment would mean that the high-Nb band behavior would be the life-limiting factor for banded U-6Nb.

Tensile and microhardness specimens were machined from the U-5.6Nb and U-7.7Nb plates, solution heat treated 30 minutes in the  $\gamma$ -bcc single-phase field (800°C and 850°C, respectively) and water quenched in order to erase any memory of previous aging or machining damage. This is referred to as the “time = 0, machined-then-annealed ( $t = 0$ , MA),” “as-annealed,” or “as-quenched (AQ)” condition, a material state that allows the aging behavior to be observed without complications from machining damage [2007hac2]. Figure 2.1 provides the tensile specimen

geometry. The strain was measured with an extensometer of 0.5" length. About six tensiles were tested in the AQ condition within six hours of the quenching operation to minimize any effects of ambient-temperature aging (effects of which are expected to be insignificant in any event). The remainder of the specimens were subsequently aged at 100°C, 200°C, 250°C, and 300°C for various times, up to 140 days. In this context, age is defined as time-at-temperature, e.g., 100°C for 1,000 minutes.

The same data set as that used for the previous report [2007hac2] was analyzed in this present study. Unlike the previous report, Tables 2.1–2.4 provide all of the *replicate* data, not just averages and standard deviations for each aging condition. For any given age, the number of tensile specimens (= number of replicate measurements *n*) varied from 2–4. For any given age, a single metallographic coupon was used for Vickers microhardness (HV) evaluation; 7–15 measurements were taken from each coupon. In the HV data (Tables 2.2 and 2.4), note that the linescan used was actually a zig-zag trace to ensure proper separation between neighboring indents, especially in the majority of instances where a 500-gram load was used.

Data from all ages were used in the model fitting of both the previous and current studies except for those from ages suspected to be overaged. A softening in one or more properties (i.e., increasing elongation and/or decreasing hardness, strength, or modulus) beyond the age-hardening regime constituted *indirect* evidence of overaging. Microstructural evaluation of these aged specimens failed to reveal *direct* signs of classical overaging in U-Nb alloys—cellular decomposition products consuming the matrix phase [1976eck, 1984eck]—therefore, the apparent softening could be merely the result of scatter in the data or a “pause” in the hardening reaction, for example, arising from the dissolution of solute clusters or metastable precipitates. To err on the conservative side, indirect evidence of overaging was deemed sufficient to warrant exclusion from model fitting. Such ages include the following:

1. U-5.6Nb: 100,000 minutes at both 250°C and 300°C, and
2. U-7.7Nb: 10,000 minutes and 100,000 minutes at 300°C.

These overaged data are included in Tables 2.1 to 2.4 for the sake of completeness, with this caveat noted. It should be noted that no data points potentially associated with an initial *softening* transient at short times and low temperatures (before the onset of bona fide age *hardening*; see Section 3.2) were excluded from model fitting because the nature and extent of such a prehardening transient was not clearly enough defined, given the paucity of data and their large error bars.

## **2.2. Model Validation**

Long-term aging experiments were initiated to test the predictive power of the improved aging model description developed in this study. These validation aging experiments probed longer times ( $\geq 221$  days) and (in some instances) lower temperatures ( $\leq 100^\circ\text{C}$ ) than the aging data used to fit the aging kinetics model ( $\leq 140$  days and  $\geq 100^\circ\text{C}$ , respectively), therefore providing a more rigorous test of the model's extrapolative power. The initial data return from these experiments is presented here; more complete reports are planned in the next year or two to document more of this data that will soon become available, and in more detail (e.g., with complete stress-strain curves and microstructural and other characterization.) These validation studies are divided into two parts.

### **2.2.1. Nonbanded U-5.6Nb and U-7.7Nb**

The first set of validation data is from the same nonbanded U-5.6Nb and U-7.7Nb material that was employed previously for model fitting (Section 2.1.) Specimens were aged for 221 days (exactly 5,300 hours) at 100°C, 200°C, and 300°C. Even longer ages still in progress are anticipated to provide two-year and six-year aging data at these temperatures. These aging treatments were done in an identical manner to those documented in Section 2.1, namely, in the MA state and under encapsulation protection with an inert-gas (Ar) backfill. Because of specimen limitations, only a select number of the 221 day ages will have tensile data (Table 2.5), though hardness data were collected for all these aging conditions (Tables 2.6 and 2.7). Tensile data were collected in the same manner as in Section 2.1, with the specimen geometry of Figure 2.1 and an extensometer of 0.5" length.

### **2.2.2. Banded U-6Nb**

The second set of validation data is from banded U-6Nb of Rocky Flats Plant (RFP) pedigree. The material was twice vacuum arc remelted (VAR) and then hot worked (in the gamma-phase region) as follows: upset forged 50% and subsequently rolled ~90% over a number of passes while changing the rolling direction between each pass, according to a standard schedule. Portions of this plate 4" × 3" × 0.5" in size were solutionized 800°C for two hours in a furnace with inert atmosphere and then oil quenched.<sup>2</sup> Separate plates were then aged at 40°C, 65°C, and 90°C in air furnaces with no atmosphere control. Chemical analysis results (Table 2.8) indicate no significant changes in the metal or light-element content in 5-year-aged material (vs unaged), indicating that aging in air at these low temperatures is not detrimental to the material from an environmental degradation point of view. In particular, note the statistically indistinguishable oxygen contents, and also the low hydrogen contents for all conditions, which are too low to alter the age-sensitive properties of interest to this study. Finally, we note that the bulk Nb content was measured to be 6.3 wt%, which is at the upper end of the bulk (mean) Nb composition range expected in banded U-6Nb material, though not out of bounds. (No chemical analysis information was available from RFP.) Lacking significant aging data for alloys with 6.3 wt% Nb, the kinetic description (of fractional property change) generated from 5.6 wt% Nb aging data will be used to predict the response of this banded U-6Nb material (6.3 wt% measured composition). The only modification to the analysis as a result of the actual differences in Nb content will be a minor adjustment of the starting property values to those measured for the specific alloy (to be described later, and documented in Table 3.1).

After aging for a prescribed time, the plate was pulled from the furnace, and specimens for tensile testing (3 replicates), hardness testing, and chemical analysis were machined out of a 2"-long portion of the initially 4"-long plate (the other half was returned to the furnace for continued aging). Data from 5-year-aged specimens were available for comparison at the time of this study; other ages still in progress are anticipated to provide 0.625-, 1.25-, 2.5-, 10-, 20-, and 40-year aging data at these temperatures. Note that the tensile specimen size (Figure 2.2) is larger in all dimensions than that used for the nonbanded U-5.6Nb and U-7.7Nb specimens (Figure 2.1), though both are round. Particularly, the gage length and diameter are 1.25" and 0.25" for this larger specimen vs 0.70" and 0.10", respectively, for the smaller specimen. The larger size specimen has the advantage of having less variability in measured tensile properties

---

<sup>2</sup> An oil quench is sufficiently rapid [1984eck] to obtain the same metastable  $\alpha'$  starting microstructure and properties as those obtained from a water quench used for the other U-Nb compositions.

between otherwise identically treated replicates compared to the smaller size. The factor-of-six larger gage cross-section ( $0.0491 \text{ in.}^2$  vs  $0.0079 \text{ in.}^2$ ) also minimizes the magnitude of the machining damage effect [2007hac2]. This is an important point because these U-6Nb tensiles will be examined in the annealed-then-machined (AM) condition, different from the machined-then-annealed (MA) condition of all other tensile data. On the view that machining damage strengthens material residing a small, fixed distance from the machined surface, a larger cross-section lowers the fraction of material hardened due to machining damage, which on a “rule-of-mixtures” approach amounts to a lowering of the total increment of machine-damage “hardening” versus a specimen with a smaller cross section. For practical reasons, the tensile tests were run approximately 90 days after the tensile specimens underwent final machining, such a time interval could have allowed some relief of machining damage. The tensile data are listed in Table 2.9; these include data from unaged control specimens that were otherwise identically handled. The strain was measured with an extensometer of 0.5" length.

In spite of the differences in tensile geometry and machining damage condition between these banded U-6Nb tensile specimens and all the nonbanded U-5.6Nb and U-7.7Nb tensile specimens, the assumption was made that these two effects on property values because of these factors were small in relation to the effect on property values because of the intrinsic aging response. This is a debatable assumption, but was made in view of the paucity of data that would provide a direct conversion of any given tensile property value (e.g., first-yield strength) from one tensile geometry to another. A study of property equivalencies among different tensile geometries (and with machining damage condition as an added variable) is recommended for the future.

The hardness data from the 40°C, 65°C, and 90°C aged material are listed in Table 2.10; these include data from unaged control specimens that were otherwise identically handled. Significantly more hardness measurements were taken than in the nonbanded material to better average out the point-to-point changes in local hardness because of the Nb banding in this material; the scans were run through the entire 0.5" cross section of the metallographic coupon.

### **3. STATISTICAL EVALUATION METHOD**

#### **3.1. Sources and Magnitudes of Scatter**

Only the scatter arising from the intrinsic material variability, model (curve) fitting, and model fidelity to the physical aging mechanism(s) were accounted for in the current analysis method (Section 3.3). Other experimental errors deemed to be less significant were not explicitly accounted for. For completeness, the origins and estimated magnitudes of all the known or expected sources of scatter are detailed in Appendix 1.

The scatter in the experimental data could be accounted for in the fitting methods in two different ways:

1. Fitting the average of the replicate points weighted by the standard deviation. This was used for the previous analysis method [2007hac2].
2. Fitting all the replicate data points, each replicate weighted equally. This was used in the current analysis method.

A replicate is defined as an individual measurement from a particular specimen of a given alloy and given aging condition (e.g., U-5.6Nb, 200°C, 1,000 minutes, tensile specimen #1). In the

context of method 2 (above), the definition of what constitutes a replicate is important for weighting data during model fitting and determining prediction error bounds. In this work, it was assumed that a tensile replicate corresponded to the outcome from an individual tensile specimen; there were typically 2–4 replicates per aging condition.

Defining the entity that constitutes a hardness replicate was less clear-cut, because multiple measurements (tens to perhaps even hundreds) can be taken from the same coupon. Two definitions were considered. One definition is that the average of numerous hardness measurements on an individual coupon constitutes a single replicate point. The alternate definition is that each indent from an individual hardness measurement is a replicate point, potentially giving tens or even hundreds of replicate points per coupon. The previous and present study assume the former; but Appendix 2 documents an alternative analysis assuming the latter.

### **3.2. Previous Analysis Method**

#### **3.2.1. Modeling Approach**

The previous analysis method is documented in [2007hac2]. For the benefit of the reader, this methodology will be summarized. The aging response was tracked in U-5.6Nb and U-7.7Nb indirectly through the observed time-dependent changes in various mechanical properties generically referred to as  $P(\text{time})$ . These following age-sensitive properties were measured at ambient temperature following artificial ages at 100°C, 200°C, 250°C, and 300°C:

1. Total (Plastic) Elongation (TE)
2. Uniform (Plastic) Elongation (UE)
3. First-Yield Strength (1YS)
4. First-Yield Modulus (1YM)
5. Second-Yield Strength (2YS)
6. Ultimate Tensile Strength (UTS)
7. Vickers Hardness (HV)
8. Percent Reduction in Area (%RA)

The specific task common to both the previous and present study was to determine a best-fit analytical description of  $P$  as a function of both aging time and aging temperature. In this earlier study, fitting of  $P$  with respect to time was done *before* (upstream of) the fitting with respect to temperature.

Each of these eight properties was normalized with respect to the initial and peak-age property values pertinent to the age-hardening regime; these are termed  $P(\text{start})$  and  $P(\text{peak})$ , respectively, and were assumed to be independent of aging temperature.<sup>3</sup> They are listed in Table 3.1. The fractional property change (or fraction transformed) as a function of some time variable, at constant temperature, is defined as

---

<sup>3</sup> Note that  $P(\text{start})$  corresponds to the start of the *hardening* reaction and is not necessarily equal to the as-quenched value  $P(t = 0)$ , for example, when there is an initial transient softening effect before the onset of hardening. This distinction will be further elaborated later in this section.

$$f(\text{time}) = \frac{P(\text{time}) - P(\text{start})}{P(\text{peak}) - P(\text{start})} . \quad \text{Eq. 3.1}$$

This equation can be rearranged to the form where  $P(\text{time})$  can be evaluated, given knowledge of  $f(\text{time})$ :

$$P(\text{time}) = P(\text{start}) + f(\text{time}) \cdot (P(\text{peak}) - P(\text{start})) . \quad \text{Eq. 3.2}$$

As is customary for the analyses of aging kinetics in metals and alloys, the aging time is assessed on a logarithmic scale, i.e.,

$$x = \log_{10}(\text{aging time in minutes}) = \log(\text{time}) \quad \text{Eq. 3.3}$$

The fraction transformed  $f$  was fit to the time series data averages at each temperature using the following normalized (2-parameter) Boltzmann function:

$$f(x) = 1 - \frac{1}{1 + \exp\left(\frac{(x - x_o)}{dx}\right)} . \quad \text{Eq. 3.4}$$

The Boltzmann function in this format has two adjustable parameters  $x_o$  and  $dx$ <sup>4</sup>; these were adjusted by a commercially available software routine to optimize the fit for each log(time)-series. The Boltzmann function has the following properties:  $x = x_o$  is the log(time) at which  $f = 0.5$ ;  $dx$  is related to the maximum slope of the curve:  $df/dx$  (at  $x = x_o$ ) =  $1/(4dx)$ .

Reasonable  $f(x)$  fits were obtained for the TE and 2YS properties, which were subjected to further analysis. Although the HV provided relatively poor fits for U-5.6Nb, it was further analyzed to enable comparison with other data sets [2002eck]—comparisons that are outside of the scope of this study. The remaining properties—1YS, 1YM, UTS, UE, and %RA—had less-than-desirable fits and/or marginal utility in connection with a failure criterion and were not analyzed further.

The time-series fitting of the UE and TE at 100°C and 200°C was problematic because the UE and TE changed little (in relation to its own apparent scatter) over the time range studied, potentially introducing considerable errors into the fitting, which would flow downstream to errors in the apparent activation energy  $Q$ . At this point, the analyst intervened with an empirical solution where the time-series fit was nudged in the seemingly correct direction with the addition of a fictitious long-time data point where the UE and TE were expected to reach zero (equivalent to  $f = 1$ ). An example of this is given in Figure 3.1, located at  $x = 10.4$ . Although such an intervention was not satisfying from the standpoint of avoiding bias, it was justified by the avoidance of much more significant errors downstream of this (in  $Q$  and the lifetime predictions), which were uncovered during trial attempts to fit the model without such an intervention.

The log(time)-series fits of the TE, 2YS, and HV were fed into an Arrhenius analysis to determine the temperature-dependencies of  $f(x)$  by determining the scaling factor  $Q$ , the apparent activation energy of age-hardening. The determination of  $Q$  is as follows: the log(time) values to

---

<sup>4</sup>  $x_o$  and  $dx$  are referred to as  $A$  and  $B$ , respectively, in [2007hac2]; be aware that  $A$  and  $B$  from the previous report were defined differently from the  $A$  and  $B$  in the present analysis (Section 3.3).

reach a fixed value of  $f$  are plotted against the reciprocal of the absolute temperature, and the best-fit line has a slope linearly related to the apparent activation energy  $Q$ :

$$\text{slope} = \frac{Q \cdot \log(e)}{R} \approx \frac{0.43429Q}{R}, \quad \text{Eq. 3.5}$$

where  $e$  is the base of the natural logarithm ( $\approx 2.71828...$ ) and  $R$  is the universal gas constant. In the previous study, the  $Q$  used for lifetime assessment was evaluated at the  $\log(\text{time})$  to reach  $f = 0.25$ , with the understanding that somewhat different  $Q$  values are obtained when it is evaluated at other values of  $f$ . This is a consequence of (1) the reaction not being strictly isokinetic (where  $Q$  would be independent of  $f$ ), combined with (2) the decision to fit  $dx$  independently for each temperature (as opposed to forcing a common  $dx$  value for all temperatures).

Tables 3.2 and 3.3 provide the best-fit values of  $dx$ ,  $x_o$ , and  $Q$ .

Once  $Q$  is determined, one can calculate the kinetically equivalent time to reach a given  $f$  at some temperature  $T_2$  if the time to reach that same value of  $f$  is known at a reference temperature  $T_1$ :

$$\log(\text{time at } T_2) = \log(\text{time at } T_1) + \frac{Q \cdot \log(e)}{R} \left[ \frac{1}{T_2} - \frac{1}{T_1} \right]. \quad \text{Eq. 3.6}$$

In Eq. 3.6, the temperatures  $T_1$  and  $T_2$  must be absolute (e.g., Kelvin). If  $f(x)$  is completely defined for a reference temperature  $T_1$ , then the kinetic response  $f(x)$  at some temperature  $T_2$  is also completely defined through a mapping of the times using Eq. 3.6. In effect, the  $f(x)$  curves will have identical shapes for all temperatures (provided that they use the same  $dx$  value) when plotted on an  $x = \log(\text{time})$  abscissa. The curves are merely offset from one another along the abscissa by the additive factor, proportional to  $Q$ , the last term in Eq. 3.6. For the particular case of the Boltzmann model, this mapping is readily done by inserting the parameters  $x_o(T_2)$  and  $x_o(T_1)$  into Eq. 3.6, giving

$$x_o(T_2) = x_o(T_1) + \frac{Q \cdot \log(e)}{R} \left[ \frac{1}{T_2} - \frac{1}{T_1} \right]. \quad \text{Eq. 3.7}$$

Note that the Arrhenius temperature-scaling of the Boltzmann function in Eq. 3.7 only shifts  $x_o$ ; there is no rescaling of  $dx$ , resulting in identically shaped curves offset only along the abscissa.

### 3.2.2. Failure Criterion and Lifetime Prediction

The quasi-static, uniaxial loading failure criterion [2007hac2], from which the lifetime is determined, is defined in terms of the property change relative to the time = 0 condition  $P(t = 0)$ ,

$$f'(t) = \frac{P(\text{time}) - P(t = 0)}{P(\text{peak}) - P(t = 0)}. \quad \text{Eq. 3.8}$$

Failure is defined as taking place when this fractional change reaches a critical threshold:

$$f'(t = \text{lifetime}) = f'_{crit}. \quad \text{Eq. 3.9}$$

A value of 0.25 was assigned to  $f'_{crit}$ , which means that failure occurs when the property has changed by 25% relative to the  $t = 0$  condition. This can be equivalently stated as

$$P(t = \text{lifetime}) = P_{crit} = P(t = 0) + f'_{crit} (P(\text{peak}) - P(t = 0)) . \quad \text{Eq. 3.10}$$

It should be noted that for the instance of historically manufactured components  $P(t = 0)$  would be  $P(t = 0, AM)$ , while for the study here, it would be  $P(t = 0, MA)$ . Regardless of whether the  $t = 0$  condition is MA or AM, the  $P(t = 0)$  value is in general not the same as the  $P(\text{start})$  value, so  $f'(t)$  is not equivalent to  $f(t)$ . This complication arises from the observation of an apparent initial transient of softening, before the onset of hardening in the UE and TE. (It was much less noticeable in the HV, 1YM, 1YS, 2YS, UTS, and %RA.) This softening is most noticeable in the 100°C and 200°C for both U-5.6Nb and U-7.7Nb, and can be perceived in Figure 3.1 as an initial upward deviation of the TE data points relative to the  $P(t = 0)$  line. The origin of this softening is unclear, though one plausible explanation is that thermally-induced relaxation of quenching stresses (MA condition) or machining stresses (AM condition) were imparted to the soft, easily strained martensitic microstructure at  $t = 0$ .

The most straightforward evaluation of the lifetime from this failure criterion would be to model  $f'(\text{time})$ . However, no attempt was made to model  $f'(\text{time})$  of either U-Nb alloy, because this would ideally require explicit deconvolution of the softening portion of the aging curves vis-a-vis the hardening portion. At a minimum, a phenomenological fitting of the entire (nonmonotonic) aging curve without explicit consideration of the differences between softening and hardening regimes would require a more complex model with additional fitting parameters. Such an approach is not justified in view of the paucity of softening data. Instead, lifetime prediction was done by avoiding any explicit model of the softening part of the curve (apart from the  $P(\text{start})$  that results from softening) and simply determining the equivalent value of  $f_{crit}$  that corresponds to  $f'_{crit}$ . The value of  $f_{crit}$  is uniquely determined by the values of  $P(\text{start})$ ,  $P(t = 0)$ ,  $P(\text{peak})$ , and  $f'_{crit}$ , according to the following relationship:

$$P_{crit} = P(t = 0) + f'_{crit} [P(\text{peak}) - P(t = 0)] = P(\text{start}) + f_{crit} [P(\text{peak}) - P(\text{start})]. \quad \text{Eq. 3.11}$$

Rearranging to solve for  $f_{crit}$ :

$$f_{crit} = \frac{[P(t = 0) - P(\text{start})] + f'_{crit} [P(\text{peak}) - P(t = 0)]}{[P(\text{peak}) - P(\text{start})]} . \quad \text{Eq. 3.12}$$

For the special case of a property, such as TE, for which  $P(\text{peak}) = 0$ , this simplifies to

$$f_{crit} = 1 - \frac{(1 - f'_{crit})P(t = 0)}{P(\text{start})} . \quad \text{Eq. 3.13}$$

Rearranging further,

$$(1 - f_{crit})P(\text{start}) = (1 - f'_{crit})P(t = 0) . \quad \text{Eq. 3.14}$$

The equality in Eq. 3.14 is graphically depicted in Figure 3.2, which shows the TE for U-5.6Nb. On the basis of Eq. 3.13, the calculated values of  $f_{crit}$  for TE are 0.3866 and 0.3404 for U-5.6Nb and U-7.7Nb, respectively. The corresponding  $P_{crit}$  values were 0.1590 and 0.2572, respectively. The failure criterion and threshold value  $f'_{crit} = 0.25$ , as described here, were accepted unchanged for the current analysis method described in Section 3.3.

For the lifetime determination,  $T_2$  is the storage temperature of interest (e.g., 40°C), whereas  $T_1$  is the artificial aging temperature for which a Boltzmann time-series fit was determined (100°C, 200°C, 250°C, or 300°C). Thus, four lifetime values were generated from the four values of  $T_1$

and their fitted Boltzmann parameters, all of which used the common value of  $Q$  for a given alloy. In the previous report, the spread of lifetimes (minimum-to-maximum) were listed. Given this scatter, it was decided that the conservative lifetime estimate to be reported should be the minimum of these four lifetime values. Table 3.4 provides all four calculated lifetimes (minimum one in bold), evaluated for the  $f' \geq 0.25$  failure criterion of TE.

Model fitting (parameter optimization) was carried out on Origin Pro software using its nonlinear least-squares fitting routine. No quantitative error assessment was made of this lifetime estimate or the contributing and propagating errors.

At the time of the previous report [2007hac2], no data independent of the data set used for the fitting of this Boltzmann-Arrhenius model were available for model validation; therefore this was not done.

### 3.3. Current Analysis Method

#### 3.3.1. Statistical Modeling Overview

Seven of the eight age-sensitive properties listed in Section 3.2 were analyzed (all except %RA) and fitted to an aging model in the current study; lifetimes continued to be estimated only on the basis of TE, as before. Table 3.5 lists the similarities and differences between the previous and current analysis methods. Given the statistical focus of the current analysis method, some background on the formalism and approach will now be provided.

The first goal of this statistical modeling is to describe the “population” of all possible outcomes (mechanical properties in this instance) of aged U-Nb. The second goal is to use this description to make predictions of future observations, which requires the use of a model. The population is described on the basis of a “sample” taken, preferably at random, from that population. It is the sample we observe, but the population that we seek to know. Because an infinite number of specimens cannot be aged and measured, the population will never be known in a perfectly precise fashion. The degree to which we can describe the population is derived from a characterization of scatter of the sample, which here is referred to as the model-fitting data.

The general form of a regression model is as follows:

$$y_i = f(\mathbf{X}_i; \boldsymbol{\theta}) + \varepsilon_i; \quad \text{Eq. 3.15}$$

where  $y_i$  represents the response variable,  $\mathbf{X}_i$  represents a vector of explanatory variables, and  $\varepsilon_i$  represents the error term at the  $i$ th replicate data point,  $i = (1, 2, \dots, n)$ . The term  $f(\mathbf{X}; \boldsymbol{\theta})$  describes a function of the explanatory (independent) variables, represented by the vector  $\mathbf{X}$ , and the parameters to be fitted, represented by the vector  $\boldsymbol{\theta}$ . For the U-5.6Nb and U-7.7Nb data, the response (dependent) variables are the following properties: TE, UE, 1YS, 1YM, 2YS, UTS, and HV, as well as the fractional property change for each of these properties. The explanatory variables are artificial aging time and temperature.

In situations where there aren't first-principles models for complex physical mechanisms, such as those occurring in the materials studied in this report, the standard approach in statistical modeling is to develop empirical predictive models that fit the data well and provide a reasonable manner for both interpolation and extrapolation. As a result, various functional forms and different parameterizations for  $f(\mathbf{X}; \boldsymbol{\theta})$  were considered. In previous studies [1976eck, 2002eck, 2007hac2], the use of an Avrami-Arrhenius model and a Boltzmann-Arrhenius model

were explored. In this subsequent analysis, models similar in form to these, as well as a few other models, were examined.

Start and peak-age values for each property were the same as those used in the previous study [2007hac2], see Table 3.1. These upper and lower bounds are incorporated into the models considered in this report. For example, for fractional property change, the lower bound is 0 and the upper bound is 1. Most of the models are presented in the form of a function where the property value increases as the explanatory variable, time, increases. For the properties UE and TE, this relationship is reversed: the property value decreases with time.

### 3.3.2. Model Evaluation

Several models for the time-series response  $y_i(\text{time})$  or  $y_i(x)$  at a constant temperature were examined and will presently be described.

The following model, similar in form to the Avrami model from the previous report, was considered:

$$y_i = 1 - \exp(-At_i^B) + \varepsilon_i ; \quad \text{Eq. 3.16}$$

where  $t$  is linear time. Eq. 3.8 has an alternate parameterization of the form

$$y_i = 1 - \exp(-\exp(A - Bt_i)) + \varepsilon_i . \quad \text{Eq. 3.17}$$

In both Equations. 3.16 and 3.17,  $y_i$  represents the fractional property change  $f$ , as it varies from zero to one.

The general form of a Logistic model that was considered, similar to the Boltzmann model in the previous report (Eq. 3.4), is as follows:

$$y_i = 1 - \frac{1}{[1 + \exp(A - Bx_i)]} + \varepsilon_i ; \quad \text{Eq. 3.18}$$

where the time-variable  $x$  is defined in Eq. 3.3. Eq. 3.18 has alternate parameterizations of the form

$$y_i = 1 - \frac{1}{[1 + \exp(A(x_i - B))]} + \varepsilon_i ; \quad \text{Eq. 3.19}$$

and

$$y_i = \frac{U}{[1 + \exp(A(x_i - B))]} + \varepsilon_i ; \quad \text{Eq. 3.20}$$

where  $U$  is a predetermined upper bound. In Eqs. 3.18 and 3.19,  $y_i$  represents the fractional property change  $f$ , whereas it represents the absolute property value  $P$  in Eq. 3.20, where  $U$  has the same units as the property of interest, for example, MPa when the property is 1YS.

Another useful nonlinear model that was considered, the Gompertz model, is of the form

$$y_i = 1 - \exp(-\exp(A - Bx_i)) + \varepsilon_i ; \quad \text{Eq. 3.21}$$

with an alternate parameterization of the form

$$y_i = U \cdot \exp(-\exp(A - Bx_i)) + \varepsilon_i ; \quad \text{Eq. 3.22}$$

where  $U$  is a predetermined upper bound. In Eq. 3.21,  $y_i$  represents the fractional property change  $f(x)$ , whereas it represents the absolute property value  $P$  in Eq. 3.22, where  $U$  has the same units as the property of interest.

Changing the parameterization of a model is simply a way of improving the fitting and predictive behavior of the nonlinear model. Better behaved models produce better parameter estimates. For more information on various forms of nonlinear models and their parameterizations, see Ratkowsky [1990rat]. Note that in this context, alternate parameterizations are those belonging to a particular class of model, and are not necessarily symbolically equivalent, in the sense that a simple substitution of variables will transform one equation to its alternate. The special case of true symbolic equivalency does occur, however, between Eqs. 3.4 (Boltzmann), 3.18 (Logistic), and 3.19 (Logistic).

Model fitting (parameter optimization) and related statistical analyses were carried out on S-Plus software licensed by Insightful Corp. See Venables and Ripley [1994ven] for details on the software code. The primary function for fitting a nonlinear regression model in S-plus is *nls*. The inputs provided to this routine include a nonlinear model formula expressing the model, an optional data frame as the reference point for the variables in the model, a list of starting values for the parameters to be estimated, an optional argument allowing control of some features of the iterative procedure, an optional argument specifying the iterative procedure, and an argument allowing trace information to be printed.

Given the general form of a nonlinear regression model as in Eq. 3.15, the following provides a general outline of the fitting algorithm:

1. Near an initial point, the solution locus is approximated by its tangent plane.
2. The observation vector  $\mathbf{y}$  is projected onto the tangent to give a new coefficient vector,  $\tilde{\boldsymbol{\theta}}$ .
3. The tangent plane is calculated at the new coefficient vector,  $\boldsymbol{\theta}$ , and the procedure continues until convergence occurs.

Trial fits with the three models and their various parameterizations (Eqs. 3.16–3.22) were carried out. The residual standard errors (*RSEs*) for the various fits were compared. This summary statistic represents the variation of the actual data points around the mean fitted values from the model. Plots of residuals from the model were used to look for a constant variance, independence of successive noise terms, and also assess model adequacy. If the model provides an adequate fit to the data, then the residuals from the model plotted against the quartiles of a standard normal distribution should fall along a straight line. Normal probability plots of the residuals are provided in Appendix 3, along with profile plots of the residual sum-of-squares (*RSS*) function to check for linearity in the parameters. The goodness of fit of a nonlinear model can be assessed by the degree of linearity of the parameter estimates (i.e., linearity implies that the model is stable with respect to perturbations in  $A$ ,  $B$ , and  $Q$ ).

Based on various statistical tests of goodness of fit as well as practicality and understanding of the model, it was determined that the best fit to the data was provided by the Logistic model using the second parameterization (Eq. 3.19). This is the model that will be presented and discussed in the rest of the report. Note that this is equivalent to the Boltzmann model (Eq. 3.4)

with the following substitutions:  $A = 1/dx$  and  $B = x_o$ . Therefore, the Logistic model can be considered as a symbolically equivalent parameterization of the Boltzmann model.

To summarize, the outcome of this initial survey of empirical models and variables recommended the following for further use, which were employed for the remainder of this study:

1. Logistic model, second parameterization (Eq. 3.19) for time-series fits.
2.  $x = \log(\text{time})$  (Eq. 3.3) as the independent variable for the Logistic model.
3. Fractional transformed  $f$  (Eq. 3.1) as the dependent variable for the Logistic model.
4. Arrhenius model (Eq. 3.6) for temperature-series fits.

This Logistic-Arrhenius model can be considered semiempirical (instead of purely empirical) because it retains the Arrhenius temperature dependence, which can in some instances, provide scientific insight, from the value of  $Q$ , into the physical aging mechanism(s).

### 3.3.3. Model Fitting

The initial parameter-fitting approach was similar to that used in the previous study: the time-series data for the four aging temperatures were fit independent of one another and before (upstream of) fitting these as a temperature series. From these four time-series fits (one for each temperature), the point  $x$  where each of the curves crossed a predetermined threshold line,  $f = 0.25$ , was obtained, and a straight line was fit to these points when plotted against  $1/T$ . Eq. 3.5 then was used to provide an estimate of the activation energy,  $Q$ . This regression involved one data point with high leverage (the point from the fit to the 100°C data that had the most variability). In order to find a model that would be less sensitive to the influence of one data point, an alternate method for fitting the parameters and estimating  $Q$  was sought.

In this alternate method, the data from all four accelerated aging temperatures were combined into one data set for analysis by collapsing the data from separate temperatures onto a universal aging-response plot. To do this, the nonlinear Logistic model (Eq. 3.19) for fractional property change (Eq. 3.1) is couched in terms of a modified, universal time variable  $x'$ ;

$$f = 1 - \frac{1}{[1 + \exp(A(x' - B))]} + \varepsilon \quad \text{Eq. 3.23}$$

The times from various aging temperatures  $T_1$  were rescaled to equivalent  $\log(\text{times})$   $x'$  at a reference temperature  $T_2$  through the Arrhenius relationship, where the temperatures are in Kelvin:

$$x' = \log(\text{time at } T_2) = \log(\text{time at } T_1) + \frac{Q \cdot \log(e)}{R} \left[ \frac{1}{T_2} - \frac{1}{T_1} \right] \quad \text{Eq. 3.24}$$

The analysis is independent of the specific choice of  $T_2$ ; for convenience,  $T_2$  was set at 300°C = 573.15 K. The error term,  $\varepsilon$ , is distributed as a Normal random variable, with mean, 0, and variance, 1, written as  $\varepsilon \sim N(0,1)$ .

Note that the Eq. 3.24 comes from the assumption of Arrhenius extrapolation that serves to shift the entire aging-response, fraction-transformed curve from one temperature to another while preserving the shape of the curve on a log time scale.

With all of the data collapsed onto a single universal aging-response plot (through Eqs. 3.23 and 3.24), the effects of both time and temperature could be assessed simultaneously rather than sequentially, resulting in improved estimates for the Logistic time-series model parameters  $A$  and  $B$ , and for the activation energy,  $Q$ . The nonlinear least-squares fitting of  $A$ ,  $B$ , and  $Q$  was subjected to the following constraints. The parameter  $A$  had the same value for all temperatures, in effect ensuring shape similarity among fitted and predicted curves for different temperatures. This constraint allowed the data to be collapsed onto the universal plot, and in effect forced an isokinetic description (where  $Q$  is independent of the  $f$  at which it is evaluated). Furthermore,  $A$ ,  $B$ , and  $Q$  were further constrained to conform to a “perfect-Arrhenius” description, where any best-fit line on an Arrhenius plot passes through the model-fitted point for each temperature exactly, making it a “perfect-fit” line.

The parameter estimates for each property are given in Tables 3.6–3.19.

### 3.3.4. Model Predictions and Statistical Intervals

Combining Eqs. 3.23 and 3.24 allows the fraction-transformed time-response for any given property to be calculated as follows:

$$f(x) = 1 - \frac{1}{[1 + \exp(A(x + \frac{Q \cdot \log(e)}{R} [\frac{1}{573.15K} - \frac{1}{T}] - B))] + \varepsilon_i} . \quad \text{Eq. 3.25}$$

To compute predicted  $f(x)$ , replace the parameters  $A$ ,  $B$ , and  $Q$  in Eq. 3.17 with their estimates, replace the  $x$  with the log(time in minutes), and replace  $T$  with the temperature in Kelvin. For a given property and alloy, the estimated parameters for the  $f(x)$  and  $P(x)$  models are the same, because fractional property change is a linear transformation of the property value:

$$P(x) = P(\text{start}) + f(x) \cdot (P(\text{peak}) - P(\text{start})) . \quad \text{Eq. 3.26}$$

The property response at any given aging time and temperature can be computed by substituting Eq. 3.25 into 3.26. The method for computing approximate confidence intervals ( $CI$ s) and prediction intervals ( $PI$ s) [1982mee, 1991hah] are described in Appendix 4. A  $CI$  indicates the probabilistic degree of scatter (for example, at the 95% level) of the true predicted value (the population mean) on the basis of the scatter in the data— $n$  observations—used in model-fitting (“the sample,” a subset of the population). The  $CI$ , by accounting for the uncertainty in the fitted model parameters  $A$ ,  $B$ , and  $Q$ , will contain the mean of the sampled population, in the long run, at the specified level of confidence. The  $CI$  is compared against the  $n$  data points used to fit the model.

A  $PI$ , by contrast, indicates the degree of scatter expected for  $nv$  future<sup>5</sup> replicate measurements (or, on a slightly modified formula, their average) given the model fit from the  $n$  observations. In this report,  $nv$  refers to the number of validation specimens, because data from such specimens are what will be compared with the  $PI$ ; standard reference works on this topic call this “ $k$ ” [1982mee, 1991hah] or “ $m$ ” [1974net]. The  $PI$  will contain the value(s) of these  $nv$  future observations, in the long run, at the specified level of confidence. The  $PI$  is by definition wider than a  $CI$  at a given value of  $x = \log(\text{time})$ , because it includes the  $CI$ ’s scatter in the mean value

<sup>5</sup> The computation of a  $PI$  is the same regardless of whether the  $x = \log(\text{time})$  of the future age being evaluated lies inside or outside the time-temperature bounds of the model-fitting data.

position plus an additional source of scatter, that of the random variation in the future result about the mean. Figure 3.4 in Neter and Wasserman demonstrates this point [1974net].

The lifetime for each alloy at a variety of aging (storage) temperatures was evaluated with the same  $f' \geq f'_{crit} = 0.25$  criterion for TE as described in Section 3.2; see particularly Eqs. 3.8–3.14. Because of the “perfect-Arrhenius” constraint placed on the fitting of  $A$ ,  $B$ , and  $Q$ , only a single mean value of the predicted lifetime resulted. The error assessment associated with this fitting provided 95% confidence intervals about this mean value.

## 4. RESULTS AND DISCUSSION

### 4.1. Model Fitting—General Comments

#### 4.1.1. Quality of Fitting

Seven age-sensitive properties were fitted to the same three-parameter ( $A$ ,  $B$ , and  $Q$ ) Logistic-Arrhenius model. The optimized (fitted) models will be evaluated on the basis of three criteria: goodnesses of fit, robustness of fit, and symmetry of fit. These three evaluations of fitting quality will be preceded by several remarks about the generation of universal aging response plots that are useful for these evaluations.

Universal aging response plots for all model fits are shown in Figures 4.1–4.14. The experimental data and fitted curve for all temperatures are collapsed onto the same time axis by scaling them to a common reference temperature, according to Eqs. 3.23–3.25. For these plots, 300°C was chosen as the reference temperature, though this choice is done only for convenience: any temperature can be selected. This is essentially the same “view” that the current model-fitting routine had, where it adjusted the  $A$ ,  $B$ , and  $Q$  parameters to give the best fit Logistic curve to the data thus displayed. It is helpful at this point to recall the geometric meanings of the parameters and their specific influences on the Logistic-Arrhenius model curve shapes:

- $A$  is equal to four times the slope at  $x = B$  (and also where  $f = 0.5$ ); a higher value of  $A$  results in a more steeply sloped fitted curve.
- $B$  is the  $x$ -value at which  $f = 0.5$ ; a higher value of  $B$  uniformly shifts the fitted curve to the right.
- $Q$  scales the aging times at the actual aging temperature to equivalent aging times at the reference temperature. Data points from each temperature shift as a bloc when  $Q$  is changed; furthermore, the shifts of all temperature blocs are correlated, being uniquely determined by the value of  $Q$ .

Note that the 40°C, 65°C, and 90°C data points in the U-5.6Nb universal plots are from the banded U-6Nb, not the nonbanded U-5.6Nb; they can be plotted on the same axes when the y-axis is  $f$  because they use the same  $A$ ,  $B$ , and  $Q$  parameters. Data from U-5.6Nb and U-6Nb cannot, however, be plotted on the same axes when the y-axis is the absolute property because their values of  $P(start)$  and  $P(peak)$  can differ (Table 3.1.)

The shifting (offsetting) of the time axis for the data points from other temperatures is not shown (as it is, for example, in Eckelmeyer’s universal curve of U-Ti aging—Figure 7 of [1976eck]), but can be conceptually understood as follows. The simplest way is to take advantage of the fact the earliest-time replicate point for each temperature series is at 10 minutes. Find the  $x = 1$  (i.e., the 10 minute) point for 300°C. Now shift (without distorting) the visible log(time) axis for

300°C to the left until that point lines up over the 10-minute data point for the (lower) temperature of interest. The axis shifted accurately represents all the data points of this other temperature. (The vertical axis,  $f$ , required no rescaling.)

Specific comments will now be made on the three quality-of-fitting metrics: goodnesses of fit, robustness of fit, and symmetry of fit. This information is summarized in Tables 4.1 and 4.2.

The first evaluation of the model, the goodness of model fit with respect to the experimental data, is best quantified by a scalar value, the *RSE*, which represents the variation of the observed values around the predicted values<sup>6</sup> from the model. Indeed, the “best-fit” or optimized model parameters are defined as those that give the minimum *RSE* value. The *RSE* is defined as

$$RSE = \sqrt{\frac{\sum_{i=1}^n (y_i - pred_i)^2}{(n - p)}} . \quad \text{Eq. 4.1}$$

In Eq. 4.1,  $y_i$  represents an observed measurement,  $pred_i$  represents a predicted value from the nonlinear model for the  $i$ th replicate data point; these can be either absolute property values or their normalized value,  $f$ . The total number of replicate points used in the fitting process is  $n$ , and  $p$  is the number of parameters in the model (for this model  $p$  is always 3:  $A$ ,  $B$ , and  $Q$ ). The difference  $n-p$  is called the degrees of freedom ( $df$ ) of the fit.

A lower value of the *RSE* indicates a better fit of the model to the data. Values of the *RSE* and ancillary quantities are provided in Table 4.3. The following trends are observed when comparing the fractional *RSE* values:

1. 2YS and HV showed the best fits in both alloys. For 2YS, this is a similar outcome as the previous study [2007hac2]. For HV, this outcome is an improvement, especially for U-5.6Nb.
2. 1YM fit the least well in both alloys.
3. TE and UE fit moderately well in both alloys.
4. 1YS fit very well in U-5.6Nb but fit only moderately well in U-7.7Nb.
5. UTS fit very well in U-7.7Nb but fit only moderately well in U-5.6Nb.

The second evaluation, robustness of fitting of the individual parameters ( $A$ ,  $B$ , and  $Q$ ), is done by *RSS* testing, the details of which are in Appendix 3. Relatively low robustness in one or more parameters were identified for 1YM in U-5.6Nb and TE, UE, 1YM, and HV for U-7.7Nb. Note that poor *RSS* test results do not necessarily correlate to the poor (i.e., high) *RSE* value, or vice-versa; however, a poor showing in either metric casts greater doubt on the validity of the model for the particular property in question.

The third evaluation, symmetry of fitting, refers to how evenly the data points from specific aging temperatures are distributed about the fitted curve. A markedly uneven distribution among the points for a given temperature (or span of time) is a statistical sign that the model may not be applicable to this temperature (or span of time). Focusing on the 100°C data points in the universal plots (Figures 4.1–4.14) reveals an important difference between the two alloys. For all of the properties, most of the observed 100°C data points for U-7.7Nb alloy consistently lie

---

<sup>6</sup> In this report, the terms “predicted values,” “mean fitted values,” and “model predictions” are used interchangeably.

above the predicted curve; however, this trend does not occur for the U-5.6Nb alloy data points, which are distributed more evenly. Essentially, what this implies is that there is an underlying physical consistency in the relationship between the curves at all of the accelerated aging temperatures for the U-5.6Nb alloy data, but not for the U-7.7Nb alloy data. For the U-7.7Nb, there is only consistency between the 200°C, 250°C, and 300°C curves and below 200°C there is a change, perhaps attributable to a change in the physical aging mechanism. By contrast, the results of this study provide no statistical evidence that there is a change in aging mechanism at lower temperatures for U-5.6Nb.

To summarize, both alloys show reasonable goodnesses of fit, which vary from property to property. However, the U-5.6Nb models are more robust and symmetric, and therefore are expected to have better predictive power than those of U-7.7Nb, especially at the lower aging temperatures (<100°C) of interest.

#### **4.1.2. Comparison of Parameters and Aging Responses**

The values of fitted parameters from the models for all properties and alloys are summarized in Tables 4.4 ( $Q$ ), 4.5 ( $A$ ), and 4.6 ( $B$ ). The values from the present study can be compared with those of the previous study for the TE, 2YS, and HV properties. For the most important property, TE, the new values of the activation energy  $Q$  are both higher than the old values: 10% higher (to 32 kcal/mol) for U-5.6Nb and 50% higher (to 39 kcal/mol) for U-7.7Nb. The old and new  $A$  and  $B$  values for TE are almost identical for U-5.6Nb, though they differ significantly for U-7.7Nb. This finding suggests that the old and new lifetimes will be similar for U-5.6Nb and less similar for U-7.7Nb. The differences between the old and new modeling approaches come into greater relief when comparing their values for 2YS in U-7.7Nb and HV for both alloys. In particular, the old and new HV values for U-5.6Nb are dramatically different, going from 116 kcal/mol to 28 kcal/mol, and while at the same time shifting  $B$  (the log(time) at which  $f = 0.5$ ) forward in time by six orders of magnitude (in linear time), from 9.4 to 3.4. This extreme example highlights the influence that points of high leverage (100°C data in this instance) have when examined through two different analysis methods.

Turning now to a comparison only among the parameters fitted for this study, the following generalizations can be made. The activation energy  $Q$  will be examined first, as follows:

1.  $Q(\text{TE})$  in both alloys is close to that for Nb volume diffusion in  $\gamma\text{-U}$ ,  $Q_{\text{diff}} = 32.6$  kcal/mol, marginally so for U-7.7Nb, which is 20% higher. The similarities between  $Q(\text{TE})$  and  $Q_{\text{diff}}$  are not inconsistent with previous studies [1976eck, 2002eck, 2007hac2]. In light of the most recent atom probe experiments [2008cla] (which indicate that Nb diffusion is not even relevant at 200°C and below) we note that the apparent agreement between any measured  $Q$  and  $Q_{\text{diff}}$  could merely be coincidental.
2.  $Q(\text{TE})$  for U-7.7Nb is higher than that of U-5.6Nb, which is opposite the trend of previous studies [2002eck, 2007hac2]. However,  $Q(\text{HV})$  for U-7.7Nb is lower than that of U-5.6Nb, which is the same trend observed before.
3. 1YS and 1YM, have consistently low  $Q$ , roughly one-third to two-thirds that of TE.
4.  $Q(\text{UE})$  and  $Q(\text{TE})$  are nearly identical for U-5.6Nb, and differ by 20% for U-7.7Nb. Such similarities are consistent with the fact that UE is usually the major contributor to the TE, especially at lesser degrees of aging when reasonably high ductility obtains.

5.  $Q(\text{UTS})$  values for both alloys are within 10% of one another.

In summary, activation energies for the properties spanned 14–52 kcal/mol. Given the aforementioned difficulties interpreting the  $Q$  values for TE (point #1), further comment on specific physical mechanisms responsible for the  $Q$  values from other properties is not warranted at this time.

Comparison of the impact of differing  $A$  and  $B$  values among the seven properties is best done graphically. The variation in the aging response of the seven properties is highlighted in Figures 4.15 and 4.16. The fractional property change is used to enable direct comparison among the properties. Two representative temperatures are plotted; 200°C is a typical accelerated aging temperature, and 40°C is a representative storage temperature.

At 200°C (Figure 4.15), the seven property responses are more tightly grouped with respect to  $\log(\text{time})$  in U-5.6Nb than in U-7.7Nb. This is consistent with the smaller range of  $B$  parameter values (Table 4.6) in U-5.6Nb (+0.9955 to +2.5672) relative to those corresponding to U-7.7Nb (-0.6659 to +4.1543). The maximum slope of the curve, proportional to parameter  $A$  (Table 4.5), shows less scatter in U-5.6Nb than in U-7.7Nb. For both alloys, TE, UE, and 2YS respond earlier in time at 200°C, but the UTS response lags in time.

The differences between properties and alloys become much more pronounced when comparing the predictions at 40°C (Figure 4.16), where the differences in the activation energy  $Q$  (Table 4.4) are the most significant contributors to the splitting of the curves relative to higher temperatures, such as 200°C (Figure 4.15). Eight to nine orders of magnitude time difference separate the response of the earliest-changing property (1YM) from the latest-developing one (UTS). The properties in both alloys (except for the UE, as will be noted) can be grouped into three categories:

1. Early-time responders at 40°C: 1YM and 1YS
2. Middle-time responders at 40°C: TE, HV, 2YS, and UE (U-5.6Nb only)
3. Late-time responders at 40°C: UTS and UE (U-7.7Nb only)

Of all seven properties examined, one should trust the 1YM predictions the least because they had the poorest model fits (i.e., with the highest  $RSE$ , Table 4.3) for both alloys. The diverging behavior of the UE between the two alloys is somewhat puzzling. In general, one would expect UE and TE to follow the same pattern, because UE is a major component of TE. The superficial cause of the UE lagging so far behind in U-7.7Nb is its very high activation energy, 52 kcal/mol (the highest of any  $Q$  fitted in this study), since curves for a given property will be spread out more at lower temperatures with a higher value of  $Q$  than a lower value (Eqs. 3.6 and 3.7). A more fundamental physical explanation for why the data for U-7.7Nb resulted in such a high value of  $Q(\text{UE})$  was not readily apparent.

#### **4.1.3. Modeling Assumptions**

The previous and current modeling process (summarized in Table 3.5) gave similar outcomes for all three parameters for TE and 2YS in U-5.6Nb, and for none of the TE parameters for U-7.7Nb. This provides added assurance in the robustness of the TE and 2YS models in U-5.6Nb, while casting some doubt on the robustness of the TE model in U-7.7Nb. This finding is consistent with the  $RSS$  analysis in Appendix 3. Vastly different results were obtained from the two approaches for the case of the least well-behaved property, HV in U-5.6Nb, highlighting the

sensitivity of the modeling approach for property responses that appear to be poorly behaved, especially with regards to high-leverage data (i.e., 100°C).

The validity of each of the models depends on the following assumptions:

1. The model is able to explain or represent all of the reactions or processes taking place within the experiment.
2. Related to #1 is the further assumption that such aging-related property changes, which are *indirect* measures of aging, bear a meaningful, if not unique correlation with the time progression of the underlying physical processes (e.g., diffusional nucleation and growth of precipitates) that are ultimately responsible for such property changes.
3. The estimated start value and peak value for each property are accurate and are valid for all aging and storage temperatures (Table 3.1).
4. The dominant source of error in the measured properties is due to the intrinsic material variability, and all other sources of error are either negligible or are incorporated in the measure of intrinsic material variability (Appendix 1).
5. There are no gross systematic errors present in the measurements. A systematic error is a type of error that remains constant over a series of experiments and would result in an offset, or bias, between the estimated measurements and the “true” measurement values (Appendix 1).
6. The shape of the response curve is the same at each of the accelerated aging temperatures. In terms of the Logistic (Boltzmann) model, this means that  $A (= 1/dx)$  is the same for all aging temperatures.
7. A linear relationship, on a log(time) scale, exists between the curves at different temperatures, defined by the Arrhenius formalism developed for describing the kinetics of thermally activated processes.
8. The reactions and processes taking place at each of the accelerated aging temperatures are the same and are representative of the temperatures of interest (i.e., near-ambient storage temperatures).
9. Aging in banded U-6Nb (6.3 wt% Nb measured composition) can be represented by the same  $A$ ,  $B$ , and  $Q$  parameters fitted to the nonbanded U-5.6Nb data.

Assumptions 1 and 2 are the most critical, and the most subject to uncertainty given the current lack of maturity regarding the fundamental scientific understanding and the related paucity of predictive power of aging models in general, and U-Nb alloys in particular. Such concerns were reiterated in a recent study of aging mechanisms in U-5.6Nb [2008cla]. Significantly more fundamental mechanistic studies would be required to critically evaluate these assumptions in a more satisfactory manner.

Assumption 3 was accepted as-is in this study, e.g., no error bars were assigned to the  $P(start)$  and  $P(peak)$  values. Adding error bars and/or refining these values are recommended for examination in future studies, especially with regard to the initial softening transient that is observed before the onset of phenomenological age-hardening in U-Nb alloys. Assumptions 4 and 5 were examined and deemed to be reasonably valid. Assumptions 6 and 7 were implicitly

tested through the examination of the goodness of fits in Sections 4.2 through 4.8, with results that varied from good to poor, depending on the property and alloy.

Assumptions 8 and 9 were tested with the banded U-6Nb validation data at 40°C, 65°C, and 90°C and fared well, as will be described in Section 4.3. However, the fitting symmetry considerations in Section 4.1.1 call into question the validity of Assumption 8 to U-7.7Nb, because its behavior for all properties at 100°C (and possibly lower temperatures still) appears to be different than at 200°C, 250°C, and 300°C.

## **4.2. Model Fitting—Specific Properties**

Sections 4.2.1–4.2.7 describe the model *fitting* results specific to each of the properties. Note that every replicate data point is plotted on the graphs. Both  $f(x)$  and  $P(x)$  graphs are given for each property and alloy; these are linearly-scaled (along the y-axis) versions of each other according to Eqs. 3.1 and 3.2. These sections also provide property-response curves with 95% confidence interval bounds at three representative temperatures of stockpile interest: 30°C, 40°C, and 50°C.

### **4.2.1. Total Elongation**

Figures 4.17 and 4.18 show the fitted model results for TE. For both alloys, the predicted curves at 300°C don't seem to be steep enough to fit the points at the largest age. As observed for the other properties, it appears that the data points for U-5.6Nb at 100°C are scattered fairly evenly about the predicted curve, but for the U-7.7Nb data, most of the points lie above the predicted curve (when  $f$  is the y-axis). Examination of the universal aging curves (Figures 4.1 and 4.2) highlights the considerable scatter of the 100°C data in both alloys.

### **4.2.2. Uniform Elongation**

Figures 4.19 and 4.20 show the fitted model results for UE. The predicted curves seem to fit reasonably well for the U-5.6Nb data, given that there is a lot of scatter in the data. But for the U-7.7Nb data, all of the 100°C data points lie above the predicted curve (when  $f$  is the y-axis), indicating that the relationship between the curves, as defined by the activation energy, may not be valid at temperatures lower than 200°C. In fact, the UE for U-7.7Nb yielded the highest  $Q$ , 52 kcal/mol, of any of the property-alloy combinations in this study. Given the skewed scatter of the points noted previously, it may be that two (or possibly more) aging regimes transpire: one with  $Q > 52$  kcal/mol over 200°C–300°C, and the other with  $Q < 52$  kcal/mol at <200°C. Examination of the universal aging curves (Figures 4.3 and 4.4) highlights the considerable scatter of the 100°C data in both alloys, though the magnitude of scatter is somewhat less than for TE, an observation consistent with the contribution of stochastic necking-and-failure processes to TE, but not UE.

### **4.2.3. First-Yield Strength**

Figures 4.21 and 4.22 show the fitted model results for 1YS. For this property, the slopes of the predicted curves are steeper than for most of the other properties, and the curves at the different aging temperatures are closer together, indicative of relatively low activation energies for this property compared to that of the other properties. The model appears to provide a better fit to the U-5.6Nb alloy data than to the U-7.7Nb alloy data, where the data points in the latter at both 300°C and 100°C don't seem to fall along their representative curves. Examination of the universal aging curves (Figures 4.5 and 4.6) highlights the relative lack scatter among all data in both alloys.

#### **4.2.4. First-Yield Modulus**

Figures 4.23 and 4.24 show the fitted model results for 1YM. The estimated activation energies are the smallest of all the properties for both U-5.6Nb and U-7.7Nb. In addition, the scatter in the data points at all temperatures is relatively large (see also the universal aging curves in Figures 4.7 and 4.8), making it appear that the predicted curves don't adequately fit the data.

#### **4.2.5. Second-Yield Strength**

Figures 4.25 and 4.26 show the fitted model results for 2YS. The predicted curves at the aging temperatures appear to fit better for the U-5.6Nb alloy data than for the U-7.7Nb alloy data. The fits for both alloys are marginal at 100°C: for U-5.6Nb, most of the data points fall below the curve; therefore, for the U-7.7Nb data, all of the points fall above the curve. Statistical models are expected to fit data in an unbiased way. It is expected that the data points would be randomly scattered about the fitted curve. In other words, approximately half of the data points would be expected to lie above a population-wide model fit, and the other half expected to lie below. The fact that most of the points at 100°C lie on one side of the predicted curve could be an indication that there is a fundamental difference between the reactions at the higher temperatures and the reactions at 100°C that is not adequately captured by a single value of the activation energy over 100°C–300°C. In other words, an Arrhenius relationship with a single value of  $Q$  obtained over 200°C–300°C may not hold when applied to curves at temperatures below 200°C. Examination of the universal aging curves (Figures 4.9 and 4.10) highlights the relative lack scatter among all data in both alloys.

#### **4.2.6. Ultimate Tensile Strength**

Figures 4.27 and 4.28 show the fitted model results for UTS. For the U-7.7Nb data, all the predicted curves seem to fit at the three higher temperatures, but at 100°C, all of the data falls above the curve. According to the estimated value for  $Q$ , it is expected that these measured values would be smaller than they actually are. In effect, the data all falling above the predicted curve at 100°C could indicate that there is something different about the experiment at 100°C that is not accounted for in the model. For the U-5.6Nb data, the curves seem to fit the average trend reasonably well, partly because of the large scatter among the data points. Examination of the universal aging curves (Figures 4.11 and 4.12) highlights the relatively high scatter in U-5.6Nb and the relatively low scatter in U-7.7Nb.

#### **4.2.7. Vickers Hardness**

Figures 4.29 and 4.30 show the fitted model results for HV. For the U-5.6Nb alloy, the predicted curves seem to fit well at all of the temperatures except for 200°C, where all of the points fall above the predicted curve. For the U-7.7Nb alloy, all of the points fall above the predicted curve at 100°C. Examination of the universal aging curves (Figures 4.13 and 4.14) highlights the relative lack scatter among all data in both alloys.

### **4.3. Model Validation**

Validation data and predictions from the models are listed in Tables 4.7–4.13. The entire validation aging matrix is represented; data for only a few of the ages were available at the time these predictions were made; the ages without experimental data values are either planned or already pending. All of the validation ages require extrapolation of the aging model. Extrapolations outside of the time-temperature domain of the model fitting provides a more severe test of the model than validation experiments that would involve model interpolations. In

the case of U-5.6Nb and U-7.7Nb, only extrapolation to longer times is done, because the aging temperatures are a subset (100°C, 200°C, and 300°C) of those used for model fitting. In the case of banded U-6Nb, combined extrapolation to both longer times and lower temperatures is required with respect to the times and temperatures employed for model fitting, providing the more stringent validation test.

Validation plots for U-5.6Nb, U-7.7Nb, and U-6Nb are provided in Figures 4.31, 4.32–4.38, and 4.39–4.45, respectively. The validation data are also plotted in the universal aging response plots (Figures 4.1–4.14), which aid in the visualization of the validation data in the context of the overall model fit. All seven properties were measured in U-7.7Nb and U-6Nb, while only hardness was measured in U-5.6Nb because of specimen limitations for the ages documented in this study (tensile data for U-5.6Nb are planned for longer ages, though).

The model predictions listed in Tables 4.7–4.13 include mean values, 95% *CI*, and 95% prediction interval (*PI*) bounds. The *PI* bounds define the relevant scatter band of the model predictions for the validation plots. Appendix 4 explains the definition and computation of confidence interval (*CI*) and *PI* bounds; they are also briefly described in Section 3.3.4. If a validation data point were to fall outside of the prediction interval bounds, then one could conclude either that the sample is different from the population from which the model was obtained, or that the model does not adequately represent the population. The validation data points for all the tensile properties are the averages of more than one measurement:  $nv = 2$  in the case of U-7.7Nb and  $nv = 3$  in the case of U-6Nb. (Recall that data points from HV scans from a given aged coupon are considered to be a single replicate, so  $nv = 1$  for hardness in all alloys.) The *PI* bounds were calculated on the assumption that they will be compared with these averages, given their associated  $nv$  value.<sup>7</sup>

The HV validation points in U-5.6Nb (Figure 4.31) show good agreement with prediction. The 100°C and 200°C points lie very close to the predicted mean. The 300°C point is potentially overaged (based on microstructural evidence of a partial cellular transformation<sup>8</sup>), though it nonetheless lies within the *PI* bounds.

The U-7.7Nb validation data (Figures 4.32–4.38) are in good agreement with predicted mean values for TE, 1YS, and 2YS, with marginal agreement for UE and 1YM. Poor agreement obtained for UTS, whose 200°C point lies outside of the *PI* bounds. For the HV, good agreement was obtained for 100°C and 200°C, but the 300°C point fell outside of the *PI* bounds. The 300°C point cannot be excluded on the grounds that overaging had begun, because no microstructural evidence for overaging (i.e., cellular decomposition products) was observed.

The banded U-6Nb validation data (Figures 4.39–4.45) were more difficult to compare with prediction because the extent of aging is much less after 5 years at 40°C, 65°C, and (to a lesser extent) 90°C than it is after ~0.6 years at 100°C, 200°C, and 300°C. The TE and UE are difficult to compare with prediction because they are larger than the *P(start)* value assigned to this alloy

---

<sup>7</sup> The *PI* bounds could also have been calculated on the assumption that they will be compared with individual replicate points (not their average), though this was not done in this study.

<sup>8</sup> HV indent readings made in or near the cellular products were deliberately excluded from this data average; only those indents in the presumably unaffected matrix were considered. In this light, the 300°C–318,000 minute HV point in U-5.6Nb can be considered physically legitimate if the typical assumption is made that a cellular transformation, one not governed by diffusion of an interstitial solute, does not affect the aging processes in the untransformed matrix removed a modest distance from the cellular-matrix growth front (say, >10 times the interlamellar spacing.)

in Table 3.1. This is not surprising, because an extended time duration of initial softening might be expected to occur at these lower temperatures, longer in duration (given the lower temperature) than that seen at 100°C in U-5.6Nb (Figures 3.1 and 3.2) and U-7.7Nb. Until more validation data are available at 40°C, 65°C, and 90°C for banded U-6Nb that better define a more accurate  $P(start)$  value, comparison of TE and UE with prediction is not recommended. However, the negative result that little or no downward change occurred in the TE and UE after five years at these temperatures is not inconsistent with expectation; therefore, it is interpreted as a favorable sign. Among all the other properties (which did not show an initial softening at 100°C), all lie within the  $PI$  bounds, with good-to-modest agreement with predicted mean values; the best agreement was obtained for 1YS and 2YS. The changes in UTS (both actual and predicted) were so small as to preclude meaningful comment, though at face value the agreement was quite good.

It is noted that the agreement between prediction and experiment for banded U-6Nb is good considering potential complications from (1) using the  $f(x)$  model developed for nonbanded U-5.6Nb—a material of different chemical homogeneity and lower bulk Nb content, and (2) using a larger tensile geometry, which in addition (3) was tested in the AM condition. The tensile size and machining damage issues were expected to be partially factored out by assigning  $P(start)$  and  $P(peak)$  values specific for the banded U-6Nb in Table 3.1, and it appears as if this strategy was successful.

Overall, it is gratifying to observe that the vast majority of validation data agreed well with the model predictions, especially given the fact that these required extrapolations of the model, a more severe test of model fidelity and robustness than interpolations. This indicates that the validation specimens are largely from the same population as that from which the model was obtained, and the model does adequately represent the population. It gives added assurance that the property prediction models can be used with confidence. Upcoming validation points will provide a better test and give a better idea about just how much confidence can be placed in any given property model. The most important property, TE, was well-validated with U-7.7Nb, but the lack of any TE data for U-5.6Nb at the present time and expected interference from initial softening in banded U-6Nb necessitate a suspension of judgment on TE until further validation data become available.

Tables 4.7–4.13 lay out predicted values and associated  $PI$ s for all expected ages in both planned and already ongoing validation studies. At some point in the future, the available validation data can be used to update the model fits and predictions for future validation. In principle, this should be done as each validation point is gathered, though for practical reasons, this process will likely be done only when larger batches of new validation data are in hand.

#### **4.4. Lifetime Predictions**

Tables 4.14 and 4.15 provide the lifetime predictions for U-5.6Nb and U-7.7Nb, respectively. For ease of comparison with the lifetimes from the previous study (Table 3.4) and between alloys, an arbitrarily selected aging temperature, 40°C will be used; the relative comparisons are valid for all other temperatures. Compared with the previous study, the U-5.6Nb lower-bound lifetime decreased by a factor of ~4 from 7,759 to 1,828 years, whereas that of U-7.7Nb increased by a factor of ~60 from 95 to 5,466 years. The larger change in the U-7.7Nb relative to that of U-5.6Nb is certainly consistent with U-7.7Nb's greater nonlinearity in  $RSS$  (Appendix 3); therefore, its lower robustness of fit, relative to that of U-5.6Nb for TE. Even at aging

temperatures as high as 60°C, the minimum lifetimes from this present study are beyond 100 years, giving no cause for concern, if this failure criterion is accepted. It is reiterated that this failure criterion is considered overly simplistic; more detailed elaboration of this caveat can be found in the previous report [2007hac2].

#### 4.5. Evaluation of Age-Sensitive Properties for Surveillance

A larger number of fitted properties was analyzed (relative to the previous study) to provide predictive models to support U-6Nb component surveillance studies and help address “what-if” questions that involve various aging (time-at-temperature) scenarios, for example, the impact of a transient thermal excursion above the normal storage temperature. The foregoing analysis (Section 4.1.2) indicated that 1YM and 1YS are the most age-sensitive properties from the standpoint of being the first to respond to age. From an engineering and surveillance point of view, the determination of the most age-sensitive property should also take into account the likely experimental errors, which show up in the form of scatter (e.g., standard deviation) of measurements carried out on replicate specimens. The practical threshold of ages that are most likely to give a statistically significant experimentally observable property change relative to the time = 0 condition can be evaluated from knowledge of the scatter of the  $P(t = 0)$  point and the scatter of the short-time age points. This critical fraction transformed was defined as the point at which

$$P(t) - P(t = 0) > SD(t) + SD(t = 0) \quad \text{Eq. 4.2}$$

Here the scatter is quantified in terms of the standard deviation ( $SD$ ) of the experimental measurements at time = 0 and at low- $f$  ages. The  $SD$ s of the latter were defined as average  $SD$  values for the 100°C aging data for U-5.6Nb and U-7.7Nb, and the 5-year ages at 40°C, 65°C, and 90°C for banded U-6Nb. The threshold  $P$  values resulting from Eq. 4.2, and their corresponding threshold  $f$  values, appear in Tables 4.16–4.18. In all three alloys, 1YS and HV show consistently low thresholds, while TE and 1YM have consistently high thresholds. Thresholds for UE, 2YS, and UTS vary from alloy to alloy.

The aging time needed to exceed these thresholds can be evaluated from Eq. 3.25. This was done for a representative aging temperature of 40°C, with results given in Tables 4.16, 4.17, and 4.18. The properties 1YS and 1YM show the earliest aging response (typically, on a timescale of weeks) in all three alloys; therefore, these are the most sensitive tripwires. The relatively high thresholds ( $0.13 \leq f \leq 0.22$ ) for 1YM were more than offset by its low values of  $Q$  (Table 4.4) to give this early-time response (in comparison to those of other properties). It is also noted that 2YS and HV can show an early response, but only in U-7.7Nb.

The engineering interest of this threshold calculation lies in banded U-6Nb (Table 4.16), where changes in 1YS and 1YM could be observable in weeks or possibly days after the solutionize-and-quench processing step. This remarkably rapid response has the following caveat. The data are from one lot of RFP material, which may give a lower-than-normal  $\Delta P$ , at least for 1YS (8.1 MPa). Banded U-6Nb of Y-12 origin is known to have time = 0, AM condition values of 1YS ranging over 100–200 MPa. An alternative calculation of the times it takes to progress from a representative time = 0 value of 157.3 MPa to 200 MPa gave times of 251 days, 3 years, and 196 years for the lower bound, mean, and upper bound aging times at 40°C, respectively. (This row is denoted by the asterisk in Table 4.16) This shows that 1YS in Y-12 pedigree material is still expected to change on timescales of surveillance interest, though on a scale of years, not a scale of months as is the case for RFP pedigree material. Similar differences,

between Y-12 and RFP pedigrees, in the threshold response of other properties may also occur, though at the present time there is scant data that would facilitate a quantitative evaluation like that done for 1YS.

The differences between the banded U-6Nb and the nonbanded U-5.6Nb and U-7.7Nb are quite pronounced when comparing the threshold values in Tables 4.16 with those of Tables 4.17 and 4.18. The threshold of  $f$  in U-6Nb is comparable or lower than that of the nonbanded alloys in all instances.<sup>9</sup> This leads to the conclusion that the much higher degree of redundant hot work experienced by banded U-6Nb and/or the larger tensile specimen size employed (both of which lower the scatter) far outweighs the expected increase in mechanical response scatter because of its higher chemical inhomogeneity vis-a-vis the nonbanded alloys that had less hot work and were tested with smaller tensile specimens.

In summary, the most sensitive tripwires to detect an aging process in U-Nb alloys—which are defined by a combination of early-time aging responses and relatively low experimental scatter—were determined to be 1YM, 1YS, and in some instances, HV. This finding is consistent with long-standing observations of rapid changes in 1YS with age relative to other properties, particularly TE and UTS, for example in U-4.6Nb and U-6.4Nb [1967jac], U-4.2Nb [1971jac], and U-4.5Nb [1976jac].

#### **4.6. Recommendations for Future Work**

Any future reexaminations of U-Nb aging with goals similar to those that motivated this study might benefit from improvements prompted mainly by the examination of the assumptions outlined in Section 4.1.3 and the acquisition of more data. To this end, the following recommendations are made:

1. An analysis identical to that taken in this study can be carried out with the benefit of a larger model-fitting data set. The validation data used in this study are obvious examples. Additionally, the potentially overaged data points excluded at the outset of this study can now be released for legitimate use in model fitting in view of microstructural evidence (Section 2.1) and theoretical considerations (see footnote in Section 4.3) that came to light during the course of this work.
2. The models can be improved by additional data that will reduce the residual errors and the *CI* and *PI* bounds, assuming the models are basically sound. Any additional data should concentrate on the domain of sub-200°C aging temperatures. The top three recommended temperatures are 125°C, 150°C, and 175°C. Such data will help shed light on whether the aging mechanism truly changes (at least in a phenomenological sense), and if so, define more precisely the temperature that the mechanisms cross from one to another. Recall the instances of high uncertainty caused by “high-leverage” 100°C data points (Section 4.1.2) identified in both nonbanded alloys examined in this study.<sup>10</sup> This addresses assumption #8.

---

<sup>9</sup> The one exception to this trend, HV, is likely due to the fact that the microhardness traces will capture the local spatial variations in Nb content in the microstructure (whereas these are averaged out in a tensile specimen), which are much larger in the banded U-6Nb than for the nonbanded U-5.6Nb and U-7.7Nb.

<sup>10</sup> High leverage arising from outlying 100°C data was also revealed in a similar analysis of microhardness data (shown in Figure 3.5 in [2007hac2]) obtained from banded Y-12 U-6Nb that was aged at similar times and temperatures as the nonbanded alloys in this study.

3. The functional forms of model fitting at any given temperature could be reexamined, especially if additional data become available. Specific topics in this regard include, in order of increasing complexity:
  - a. Re-examine (and modify as needed) the assumption (#3) that  $P(\text{start})$  and  $P(\text{peak})$  are independent of aging temperature. At a minimum, error bars can be placed on these parameters and the errors propagated through the model fitting process. Also update  $P(\text{peak})$  for the 1YS, 2YS, and UTS—further consideration indicated that the 1,200 MPa value for U-5.6Nb is probably too low, and would be set at 1,400 MPa or at an updated value for U-7.7Nb (say, 1,500 MPa), whichever is higher.
  - b. Further study of the phenomenology and time-temperature dependence of the apparent age-softening transient that precedes the age-hardening mechanism is desirable. A better understanding of this will result in an improved value of  $P(\text{start})$ .
  - c. Reexamine, and modify as needed, the relationship of  $P$  to  $f$ . In this study, it was assumed to be a simple linear transformation (Eq. 3.1). Other aging models, backed up by more physical insight, have proposed different functional forms [1994rob, 2002guo1, 2002guo2].
  - d. The time-series model-fitting equation could be reexamined (assumption #6). After the probatation of various functional forms (Section 3.3), the Logistic-cum-Boltzmann function (Eq. 3.18) was deemed the most appropriate to fit the data at hand, but additional data may prompt an exploration of other functional forms of the time-series equation.
  - e. A reexamination of the temperature-series function, the Arrhenius one (Eq. 3.6, assumption #7), is *not* recommended in the absence of a physically plausible alternative—too few alternative models are available at the present time.
4. A systematic study should be undertaken of the effects of tensile geometry and machining damage state (AM vs MA) on the various properties on material of otherwise identical pedigree and heat treatment. One could envision that a property equivalency table would result from such a study, along the lines of that shown in Table 4.19. This would address (and provide quantitative correction for) the provisional assumption, made in this study, that the validation tensile data from banded U-6Nb could be directly compared with the model prediction data in spite of differences in both geometry and machining damage state. It would also give more confidence to the first recommendation of using existing validation data as model-fitting data. This addresses assumption #9.
5. Develop an improved understanding of the physical aging mechanism(s), to address assumptions 1 and 2. Recent 3D atom probe results effectively ruled out Nb-diffusion-controlled phase separation mechanisms at 200°C and presumably lower-still aging temperatures [2008cla]. The finding of this study that the 1YM is the earliest-changing property might suggest certain alternative avenues of investigation, for example, those involving internal friction or resonant ultrasound spectroscopy measurements.
6. The failure criterion should be critically reexamined with input from the relevant stakeholders. As mentioned at the outset, uncertainty in the nature and magnitude of the failure criterion for U-6Nb components is expected to be the most significant contributor to uncertainty in the lifetime evaluation.

## 5. CONCLUSIONS

A more systematic and statistically aware kinetics modeling approach than employed previously gave reasonable model fits to accelerated aging property data in U-5.6Nb and U-7.7Nb, and useful age-sensitive property predictions for most of the properties studied, including TE, UE, 1YS, 2YS, and HV. This approach shared all of the fitting data, and many of the key assumptions of the previous approach, including the assumption of Arrhenius behavior. The key findings of this work include the following:

1. The activation energies for TE were 32 kcal/mol for U-5.6Nb, in line with the previous study, but 39 kcal/mol for U-7.7Nb, 50% higher than the  $Q$  value in the previous study. In light of recent atom probe studies, the closeness of these values to that for Nb diffusion in uranium, 32.6 kcal/mol, may merely be coincidental.
2. The models generally showed more or less reasonable goodnesses of fit for both U-5.6Nb and U-7.7Nb, which vary from property to property. The best model fits were obtained for 2YS and HV, 1YM fit the least well, and the other properties' fits were in-between.
3. The U-5.6Nb models are more robust and symmetric, and therefore are expected to have better predictive power than those of U-7.7Nb, especially at the lower aging temperatures of interest.
4. Model extrapolations to longer times, and in some cases, lower temperatures than used for the model fitting agreed well with most of the validation data gathered, giving provisional validation of the fitted models.
5. The consistency of the banded U-6Nb validation data with the model predictions ratified the choice of using the model parameters fitted from nonbanded U-5.6Nb data, in the face of potential complexities owing to the materials' different bulk Nb contents, Nb homogeneity, tensile specimen size, and state of machining damage.
6. Even at aging temperatures as high as 60°C, the minimum lifetimes from this present study are beyond 100 years, giving no cause for concern, if the failure criterion based on uniaxial tensile elongation is accepted, along with its serious caveats.
7. For surveillance purposes, 1YM, 1YS, and to a lesser extent, HV are the properties most amenable to the early detection of the onset of aging.
8. The models can be improved by additional data that will test the various assumptions and, if the models are basically sound, reduce the residual errors and the  $CI$  and  $PI$  bounds. The additional data deemed of highest priority should concentrate on the domain of sub-200°C aging temperatures.

## ACKNOWLEDGEMENTS

Robert Aikin, Jason Cooley, Paul Dunn, Duncan Hammon, Larry Hults, Dan Thoma, Phil Tubesing, and Chastity Vigil are thanked for their roles in planning and establishing the long-term aging experiments and associated apparatus within MST-6. David Alexander, John Balog, Tim Beard, Robert Forsyth, Denny Guidry, Ann Kelly, Martin Koby, Kathy Lao, Mike Lopez, Manny Lovato, Pallas Papin, Amanda Smith and Tim Tucker are thanked for assistance with specimen machining, heat treatment, testing, characterization, and analyses for the validation aging experiments. We also acknowledge useful discussions with Mike Hamada, Aparna Huzurbazar, Jennifer Lillard, Richard Picard, David Teter, and Alyson Wilson.

## REFERENCES

- 1967jac R.J. Jackson, R.P. Brugger, and D.V. Miley, "Tensile Properties of Gamma Quenched and Aged Uranium-Rich Niobium Alloys," Rocky Flats Plant, report RFP-933 (June 2, 1967).
- 1971jac R.J. Jackson and J.F. Boland, "Mechanical Properties of Uranium-Base Niobium Alloys," Rocky Flats Plant, report RFP-1703 (June 17, 1971).
- 1974net J. Neter and W. Wasserman, *Applied Linear Statistical Models*, (Richard D. Irwin, Inc., Homewood, IL, 1974).
- 1976eck K.H. Eckelmeyer, "Aging Phenomena in Dilute Uranium Alloys," in *Physical Metallurgy of Uranium Alloys*, J.J. Burke, D.A. Colling, A.E. Gorum, and J. Greenspan, ed. (Brook Hill, Chestnut Hill, MA, 1976), pp. 463–509.
- 1976jac R.J. Jackson, "Elastic, Plastic and Strength Properties of U-Nb and U-Nb-Zr Alloys," in *Physical Metallurgy of Uranium Alloys*, J.J. Burke, D.A. Colling, A.E. Gorum, and J. Greenspan, ed. (Brook Hill, Chestnut Hill, MA, 1976), pp. 611–656.
- 1978kle D. Kleinbaum and L. Kupper, *Applied Regression Analysis and Other Multivariable Methods*. (Duxbury Press, North Scituate, MA, 1978).
- 1978sny1 W.B. Snyder, "Homogenization of Arc-Melted Uranium-6 Weight Percent Niobium Alloy Ingots," Oak Ridge Y-12 Plant, report Y-2102 (January 31, 1978).
- 1978sny2 W.B. Snyder, "Fabrication and Characterization of Uranium-6 Niobium Alloy Plate with Improved Homogeneity," Oak Ridge Y-12 Plant, report Y-2135 (October 31, 1978).
- 1981dra N.R. Draper and H. Smith, *Applied Regression Analysis*, 2nd ed. (Wiley, New York, 1981).
- 1982mee W.Q. Meeker and G.J. Hahn, "Sample sizes for prediction intervals," *Journal of Quality Technology* **14**, 201–206 (1982).
- 1983rat D.A. Ratkowsky, *Nonlinear Regression Modeling*. (Marcel Dekker, New York, 1983).
- 1984eck K.H. Eckelmeyer, A.D. Romig, Jr., and L.J. Weirick, "The Effect of Quench Rate on the Microstructure, Mechanical Properties, and Corrosion Behavior of U-6 Wt Pct Nb," *Metallurgical Transactions A* **15A**, 1319–1330 (1984).

- 1988bat D.M. Bates and D.G. Watts, *Nonlinear Regression Analysis and Its Applications*. (Wiley, New York, 1988).
- 1990rat D.A. Ratkowsky, *Handbook of Nonlinear Regression Models*. (Marcel Dekker, New York, 1990).
- 1991hah G.J. Hahn and W.Q. Meeker, *Statistical Intervals*. (Wiley, New York, 1991).
- 1994rob C.V. Robino, M.J. Cieslak, P.W. Hochanadel, and G.R. Edwards, "Heat Treatment of Investment Cast PH 13-8 Mo Stainless Steel 2: Isothermal Aging Kinetics," *Metallurgical Transactions A* **25A**, 697–704 (1994).
- 1994ven W.N. Venables, and B.D. Ripley, *Modern Applied Statistics with S-Plus*. (Springer-Verlag, New York, 1994).
- 2002eck K.H. Eckelmeyer and D.J. Thoma, "Age Hardening of U-6wt%Nb: Kinetic Analysis of Existing Heat Treatment Data and Prediction of Property Changes During Long Term Storage," Los Alamos National Laboratory report LA-UR-02-7188 (June 2002).
- 2002guo1 Z. Guo, W. Sha, and E.A. Wilson, "Modeling of Precipitation Kinetics and Age Hardening of Fe-12Ni-6Mn Maraging Type Alloy," *Materials Science and Technology* **18**, 377–382 (2002).
- 2002guo2 Z. Guo and E.A. Wilson, "Quantification of Precipitation Kinetics and Age Hardening of Fe-12Ni-6Mn Alloy during Overaging," *Materials Science and Technology* **18**, 529–533 (2002).
- 2007hac1 R.E. Hackenberg, R.M. Aikin, Jr., J.A. Balog, B.L. Bingham, R. Casey, A. Casteel, I. Cordova, R. Forsyth, F.G. Garcia, D. Guidry, D.L. Hammon, W.L. Hulst, D.R. Korzekwa, A.M. Kelly, M.W. Koby, K.A. Lao, J.C. Lashley, M.F. Lopez, R. McCabe, D.E. Nye, P.A. Papin, S.W. Quintana, J.L. Smith, D.F. Teter, D.J. Thoma, T. Tucker, P.K. Tubesing, R.R. Trujillo, C.J. Vigil, and H.M. Volz, "Synthesis and Characterization of Nonbanded U-Nb Plate Material," Los Alamos National Laboratory report LA-14316 (January 2007).
- 2007hac2 R.E. Hackenberg, D.W. Brown, A.J. Clarke, L.B. Dauelsberg, R.D. Field, W.L. Hulst, A.M. Kelly, M.F. Lopez, D.F. Teter, D.J. Thoma, T.J. Tucker, C.J. Vigil, and H.M. Volz, "U-Nb Aging Final Report," Los Alamos National Laboratory report LA-14327 (May 2007).
- 2008ale D.J. Alexander, private communication to REH, February 2008.
- 2008cla A.J. Clarke, R.D. Field, R.E. Hackenberg, D.J. Thoma, D.W. Brown, D.F. Teter, M.K. Miller, K.F. Russell, D.V. Edmonds, and G. Beverini, "Low Temperature Age-Hardening in U-13at.%Nb: An Atom Probe Study," *J. Nuclear Materials*, submitted (2008). Also available as LANL Report LA-UR-08-05743 (2008).

**Table 2.1. Tensile Data from Each Replicate of Nonbanded U-5.6Nb. Elongations are dimensionless; strengths and moduli are in MPa.**

Aging Temp. (C)	Aging Time (min.)	Rep. #	Engineering Stress-Strain Curve Parameters									Notes
			1YS stress	1YS slope	2YS stress	2YS slope	UTS stress	Plastic Elongation			% RA	
								Uniform	Non-Uniform	Total		
23	<360	1	107	37000	501	16673	715	0.2186	0.0269	0.2456	42.37	AQ
23	<360	2	148	70000	618	9803	873	0.1896	0.0063	0.1959	17.16	AQ
23	<360	3	112	57000	507	13711	747	0.2039	0.0084	0.2122	22.13	AQ
23	<360	4	132	80000	553	10667	819	0.1969	0.0055	0.2025	24.12	AQ
23	<360	6	128	75000	547	10804	806	0.1938	0.0084	0.2022	34.33	AQ
100	10	1	124	60000	530	11446	745	0.1630	0.0063	0.1693	18.59	
100	10	2	121	55000	519	12527	791	0.2149	0.0077	0.2227	24.83	
100	100	1	114	62000	512	16489	742	0.2331	0.0343	0.2673	32.26	
100	100	2	136	90000	536	11002	808	0.2100	0.0101	0.2202	33.64	
100	165	1	139	52000	517	14321	771	0.2396	0.0629	0.3025	37.20	
100	165	2	142	90000	544	11127	755	0.1555	0.0119	0.1674	17.05	
100	215	1	178	55000	640	9949	902	0.2138	0.0040	0.2178	15.43	
100	215	2	149	54000	534	10768	820	0.2491	0.0515	0.3006	28.22	
100	1000	1	160	67000	531	11233	814	0.2478	0.0413	0.2890	32.05	
100	1000	3	167	55000	508	16736	700	0.2247	0.0148	0.2395	24.09	
100	10000	1	164	68000	563	15480	817	0.2338	0.0294	0.2632	31.47	
100	10000	2	169	70000	570	15395	821	0.2202	0.0158	0.2360	28.69	
100	100000	1	225	66000	542	15051	757	0.2179	0.0108	0.2286	23.41	
100	100000	2	223	86000	595	13409	845	0.2144	0.0069	0.2214	18.57	
200	10	1	240	55000	595	12857	807	0.2049	0.0059	0.2108	21.88	
200	10	3	208	50000	581	11809	811	0.2044	0.0046	0.2091	19.15	
200	100	1	368	85000	640	8577	852	0.2228	0.0100	0.2328	22.47	
200	100	2	202	38000	625	15516	758	0.2097	0.0257	0.2354	38.56	
200	100	3	365	73000	641	7668	872	0.2498	0.0290	0.2788	27.85	
200	1000	1	494	81000	788	7510	868	0.0797	0.0071	0.0868	8.55	
200	1000	2	284	60000	720	11261	805	0.1881	0.0088	0.1969	19.89	
200	1000	3	474	70000	737	5857	810	0.1324	0.0079	0.1403	13.86	
200	10000	1	670	105000	880	2242	905	0.1092	0.0137	0.1229	10.23	
200	10000	3	668	115000	857	3664	914	0.1125	0.0061	0.1186	13.16	
200	100000	1	906	114000	1022	2847	1029	0.0670	0.0058	0.0728	17.69	
200	100000	2	922	94000	978		978	0.0021	0.0026	0.0046	9.07	2
200	100000	3	762	75000	917	2756	924	0.0539	0.0055	0.0594	10.41	
200	100000	4	960	95000	960		1005	0.0045	0.0038	0.0083	12.73	1

**Notes**

AQ) Unaged "as-quenched" condition.

- 1) 2YS stress set equal to 1YS stress because they aren't distinguishable; 2YS slope indeterminate.
- 2) UTS stress set equal to 2YS stress because they aren't distinguishable; 2YS slope indeterminate.
- 3) Potentially overaged condition; not used in model fitting.

**Table 2.1 (continued). Tensile Data from Each Replicate of Nonbanded U-5.6Nb.**  
**Elongations are dimensionless; strengths and moduli are in MPa.**

Aging Temp. (C)	Aging Time (min.)	Rep. #	Engineering Stress-Strain Curve Parameters									Notes
			1YS stress	1YS slope	2YS stress	2YS slope	UTS stress	Plastic Elongation			% RA	
								Uniform	Non-Uniform	Total		
250	10	1	387	110000	778	6916	920	0.1451	0.0039	0.1490	19.19	
250	10	2	178	55000	630	12935	759	0.1307	0.0017	0.1324	17.06	
250	100	1	227	62000	716	12186	875	0.2044	0.0483	0.2526	30.53	
250	100	2	299	75000	749	10391	858	0.1233	0.0041	0.1274	14.60	
250	100	3	443	65000	801	4490	885	0.1256	0.0065	0.1322	12.46	
250	1000	1	392	65000	842	9774	923	0.1342	0.0044	0.1386	19.88	
250	1000	2	413	70000	845	9206	932	0.1275	0.0040	0.1315	11.98	
250	10000	1	925	87000	998		998	0.0047	0.0005	0.0052	3.86	2
250	10000	2	1058	121000	1177		1177	0.0071	0.0009	0.0080	5.12	2
250	100000	1	1039	100000	1145		1145	0.0048	0.0008	0.0056	1.78	2,3
250	100000	2	890	110000	890		890	0.0000	0.0000	0.0000	0.82	1,2,3
300	10	1	296	60000	837	10661	1000	0.1617	0.0067	0.1684	17.38	
300	10	2	255	60000	806	12597	904	0.0653	0.0007	0.0660	11.43	
300	100	1	539	74000	980	9834	1041	0.0596	0.0032	0.0627	5.64	
300	100	2	494	84000	957	9005	1025	0.0718	0.0030	0.0748	9.47	
300	1000	1	927	80000	1013		1013	0.0027	0.0002	0.0029	0.14	2
300	1000	2	799	120000	1067		1067	0.0064	0.0006	0.0070	2.27	2
300	10000	1	1039	115000	1039		1039	0.0000	0.0000	0.0000	2.98	1,2
300	10000	2	1249	113000	1249		1249	0.0000	0.0000	0.0000	2.51	1,2
300	100000	1	966	124000	966		966	0.0000	0.0000	0.0000	0.60	1,2,3
300	100000	2	942	160000	942		942	0.0000	0.0000	0.0000	2.17	1,2,3

Notes

AQ) Unaged "as-quenched" condition.

1) 2YS stress set equal to 1YS stress because they aren't distinguishable; 2YS slope indeterminate.

2) UTS stress set equal to 2YS stress because they aren't distinguishable; 2YS slope indeterminate.

3) Potentially overaged condition; not used in model fitting.

**Table 2.2. Vickers Microhardness Linescan Data from Nonbanded U-5.6Nb.**

Aging temp. (C)		23	100	100	100	100	100	100
Aging time (min.)		<360	10	100	165	215	1000	100000
Notes		AQ						
Indenter force (g)		500	500	500	500	500	500	500
Spacing (micron)		250	210	210	210	210	210	210
HV	Average	147.2	147.1	153.1	156.0	160.7	163.1	163.4
	SD	7.9	13.0	9.8	6.3	6.3	8.2	8.0
	Individual Data Points	164	173	168	166	168	173	165
		144	166	160	148	172	164	168
		155	152	153	159	165	167	149
		146	147	144	154	165	176	150
		143	145	143	145	158	158	162
		147	145	135	160	157	157	169
		146	139	157	163	161	158	162
		151	147	146	154	155	158	156
		139	143	161	151	152	165	164
		137	127	156	153	155	146	175
			151	164	158	155	165	159
			130	150	161	165	170	176
								164
								168

Aging temp. (C)		200	200	200	200	200
Aging time (min.)		10	100	1000	10000	100000
Notes						
Indenter force (g)		500	500	50	500	500
Spacing (micron)		200	210	200	170	210
HV	Average	177.8	194.5	246.2	284.6	331.9
	SD	8.2	6.0	9.3	7.1	6.9
	Individual Data Points	171	210	248	288	331
		176	194	240	281	334
		163	199	265	282	330
		176	189	243	274	337
		172	190	243	282	337
		178	192	233	280	317
		173	194	243	274	327
		183	187	235	282	322
		188	192	238	284	338
		180	195	248	285	338
		194	194	256	282	333
		180	198	256	291	339
				253	301	
					289	
					294	

**Notes**

AQ) Unaged "as-quenched" condition.

1) Potentially overaged condition.

**Table 2.2 (continued). Vickers Microhardness Linescan Data from Nonbanded U-5.6Nb.**

Aging temp. (C)		250	250	250	250	250
Aging time (min.)		10	100	1000	10000	100000
Notes						1
Indenter force (g)		500	50	500	500	500
Spacing (micron)		210	200	210	175	210
HV	Average	189.4	252.2	265.6	316.8	407.8
	SD	7.6	21.1	14.7	8.0	9.2
	Individual Data Points	191	265	274	320	407
		188	268	277	315	409
		195	308	247	324	416
		180	245	250	317	422
		182	265	249	327	416
		185	243	261	298	411
		182	253	261	306	406
		182	245	260	315	399
		192	223	258	320	399
		193	240	272	317	413
		204	248	284	322	407
		199	235	294	321	388
			240		308	
					325	

Aging temp. (C)		300	300	300	300	300
Aging time (min.)		10	100	1000	10000	100000
Notes						1
Indenter force (g)		500	500	500	500	500
Spacing (micron)		175	175	175	175	210
HV	Average	217.4	273.9	357.1	427.4	468.10
	SD	15.8	8.1	11.0	13.4	14.40
	Individual Data Points	195	277	356	433	480
		228	274	362	439	458
		210	279	360	434	491
		202	265	349	426	468
		208	261	366	407	480
		211	264	362	435	475
		199	264	337	415	458
		214	277	349	445	458
		214	271	341	431	445
		223	271	369	413	449
		234	279	369	429	473
		239	284	346	445	482
		217	281	371	430	
		250	287	363	402	

Notes

AQ) Unaged "as-quenched" condition.

1) Potentially overaged condition.

**Table 2.3. Tensile Data from Each Replicate of Nonbanded U-7.7Nb. Elongations are dimensionless; strengths and moduli are in MPa.**

Aging Temp. (C)	Aging Time (min.)	Rep. #	Engineering Stress-Strain Curve Parameters									Notes
			1YS stress	1YS slope	2YS stress	2YS slope	UTS stress	Plastic Elongation			% RA	
								Uniform	Non-Uniform	Total		
23	<360	1	110	27000	546	16800	729	0.2885	0.0507	0.3391	53.94	AQ
23	<360	2	100	32000	507	19013	719	0.2862	0.1952	0.4814	49.71	AQ
23	<360	3	95	25000	522	17658	686	0.1985	0.0084	0.2069	25.98	AQ
23	<360	4	94	32000	500	19334	694	0.2349	0.0096	0.2445	26.25	AQ
23	<360	5	96	26000	496	16601	684	0.2829	0.1508	0.4337	50.15	AQ
23	<360	6	84	52000	495	16771	672	0.2733	0.0316	0.3050	30.29	AQ
23	<360	7	98	40000	499	17559	709	0.2683	0.1186	0.3869	58.16	AQ
100	10	1	113	43000	556	19256	720	0.2847	0.0725	0.3572	49.99	
100	10	2	136	28000	590	17722	726	0.2833	0.1389	0.4222	57.82	
100	100	1	215	33000	606	17071	733	0.2770	0.1068	0.3837	58.37	
100	100	2	188	29000	586	16891	726	0.2644	0.0412	0.3055	29.82	
100	1000	1	300	43000	632	14833	739	0.2652	0.0735	0.3387	63.18	
100	1000	2	330	48000	648	14940	747	0.2312	0.0442	0.2754	50.57	
100	10000	1	546	42000	617	9660	744	0.2163	0.1319	0.3482	56.78	
100	10000	2	476	46000	638	3158	725	0.2349	0.0920	0.3269	58.85	
100	230385	1	589	53000	762	4638	784	0.2290	0.0412	0.2703	51.68	
100	230385	2	534	55000	710	6449	785	0.2726	0.1095	0.3822	43.85	
200	10	1	269	31000	656	16067	742	0.2118	0.0777	0.2895	56.02	
200	10	2	155	31000	630	18299	733	0.2459	0.0481	0.2940	57.91	
200	100	1	153	37000	630	16409	759	0.2638	0.0216	0.2854	26.45	
200	100	2	318	29000	702	14943	760	0.2184	0.0363	0.2548	27.77	
200	1000	1	296	55000	730	13419	811	0.2346	0.0345	0.2691	42.41	
200	1000	2	284	45000	770	11621	796	0.2058	0.0789	0.2847	44.92	
200	10000	1	611	52000	855	6540	874	0.1347	0.0648	0.1994	25.80	
200	10000	2	576	56000	868	6466	880	0.0549	0.0460	0.1009	39.46	
200	10000	3	404	30000	768	5220	793	0.1096	0.0259	0.1355	14.50	
200	100000	1	763	65000	979	2482	987	0.0501	0.1061	0.1562	27.08	
200	100000	2	806	60000	982	1597	986	0.0471	0.0466	0.0937	24.78	

Notes

AQ) Unaged "as-quenched" condition.

1) 2YS stress set equal to 1YS stress because they aren't distinguishable; 2YS slope indeterminate.

2) UTS stress set equal to 2YS stress because they aren't distinguishable; 2YS slope indeterminate.

3) Potentially overaged condition; not used in model fitting.

**Table 2.3 (continued). Tensile Data from Each Replicate of Nonbanded U-7.7Nb.**  
**Elongations are dimensionless; strengths and moduli are in MPa.**

Aging Temp. (C)	Aging Time (min.)	Rep. #	Engineering Stress-Strain Curve Parameters									Notes
			1YS stress	1YS slope	2YS stress	2YS slope	UTS stress	Plastic Elongation			% RA	
								Uniform	Non-Uniform	Total		
250	10	1	146	45000	746	19173	794	0.2065	0.0323	0.2388	47.94	
250	10	2	170	38000	774	20382	809	0.1274	0.0605	0.1880	50.31	
250	100	1	187	41000	861	20791	894	0.0277	0.0370	0.0647	42.66	
250	100	2	191	40000	855	21047	870	0.0264	0.0064	0.0328	46.97	
250	1000	1	412	51000	1018	14571	1046	0.0305	0.0164	0.0469	30.31	
250	1000	2	522	50000	1017	12998	1047	0.0335	0.0106	0.0441	31.18	
250	10000	1	988	73000	988		1058	0.0058	0.0008	0.0066	0.89	1
250	10000	2	961	73000	1166	2780	1169	0.0427	0.0096	0.0523	17.99	
250	10000	3	728	78000	1105	5697	1116	0.0416	0.0207	0.0623	21.86	
250	10000	4	775	72000	1118	5580	1123	0.0374	0.0094	0.0468	21.89	
250	100000	1	1216	75000	1216		1225	0.0022	0.0015	0.0037	11.19	1
250	100000	2	1176	98000	1176		1229	0.0066	0.0023	0.0089	9.58	1
300	10	1	232	37000	856	21375	900	0.1189	0.1541	0.2731	38.21	
300	10	2	242	40000	871	21171	908	0.0309	0.1239	0.1548	36.97	
300	100	1	378	38000	1041	19672	1096	0.0338	0.0329	0.0667	23.28	
300	100	2	394	34000	1045	17869	1095	0.0352	0.0216	0.0568	19.22	
300	1000	1	1177	68000	1177		1261	0.0131	0.0000	0.0131	0.36	1
300	1000	2	1124	63000	1124		1234	0.0063	0.0027	0.0091	1.54	1
300	10000	1	1340	77000	1340		1340	0.0000	0.0000	0.0000	1.10	1,2,3
300	10000	2	1268	76000	1268		1268	0.0000	0.0000	0.0000	0.92	1,2,3
300	100000	1	1137	76000	1137		1137	0.0000	0.0000	0.0000	1.33	1,2,3
300	100000	2	1213	81000	1213		1213	0.0000	0.0000	0.0000	2.68	1,2,3

Notes

AQ) Unaged "as-quenched" condition.

1) 2YS stress set equal to 1YS stress because they aren't distinguishable; 2YS slope indeterminate.

2) UTS stress set equal to 2YS stress because they aren't distinguishable; 2YS slope indeterminate.

3) Potentially overaged condition; not used in model fitting.

**Table 2.4. Vickers Microhardness Linescan Data from Nonbanded U-7.7Nb.**

Aging temp. (C)		23	100	100	100	100	100
Aging time (min.)		<360	10	100	1000	10000	230385
Notes		AQ					
Indenter force (g)		500	500	500	500	500	500
Spacing (micron)		194	234	235	233	236	250
HV	Average	115.2	145.6	158.5	157.2	192.6	214.8
	SD	2.2	5.2	6.4	7.6	4.9	3.5
	Individual Data Points	116	139	171	139	185	214
		120	135	164	156	196	221
		112	145	156	153	198	210
		113	146	149	165	190	212
		115	149	161	162	191	217
		114	145	159	159	198	214
		115	149	151	167	192	215
		117	143	155	158	185	215
		115	147	154	161	196	219
		115	151	161	157	195	211
			153	163	152		

Aging temp. (C)		200	200	200	200	200
Aging time (min.)		10	100	1000	10000	100000
Notes						
Indenter force (g)		500	500	500	500	500
Spacing (micron)		315	293	335	335	261
HV	Average	147.9	179.0	204.8	229.4	272.6
	SD	6.7	7.1	10.8	8.8	7.3
	Individual Data Points	155	172	195	215	275
		149	189	194	227	275
		151	175	195	229	273
		145	176	199	239	269
		151	183	204	243	282
		148	184	220	227	273
		151	188	218	232	262
		133	170	213	223	282
			174			262

Notes

AQ) Unaged "as-quenched" condition.

1) Potentially overaged condition.

**Table 2.4 (continued). Vickers Microhardness Linescan Data from Nonbanded U-7.7Nb.**

Aging temp. (C)		250	250	250	250	250
Aging time (min.)		10	100	1000	10000	100000
Notes						
Indenter force (g)		500	500	500	500	500
Spacing (micron)		373	350	350	350	275
HV	Average	172.7	183.3	230.6	321.4	372.6
	SD	2.6	4.6	4.0	8.2	11.7
	Individual Data Points	175	175	225	316	356
		172	189	230	315	380
		175	184	225	334	369
		171	182	234	324	380
		173	187	233	325	392
		175	181	233	310	374
		168	185	234	326	359
						371

Aging temp. (C)		300	300	300	300	300
Aging time (min.)		10	100	1000	10000	100000
Notes					1	1
Indenter force (g)		500	500	500	500	500
Spacing (micron)		325	293	329	275	217
HV	Average	181.5	234.4	365.9	416.0	488.8
	SD	6.5	5.8	10.4	8.7	8.0
	Individual Data Points	192	233	353	409	487
		181	247	374	404	482
		183	228	355	426	489
		180	238	380	422	491
		185	228	374	415	477
		185	236	365	433	496
		171	232	371	416	484
		175	236	355	413	489
			232		409	501
					413	501
						480

Notes

AQ) Unaged "as-quenched" condition.

1) Potentially overaged condition.

**Table 2.5. Tensile Validation Data for Nonbanded U-7.7Nb. Elongations are dimensionless; strengths and moduli are in MPa.**

Aging Temp. (C)	Aging Time (min.)	Rep. #	Engineering Stress-Strain Curve Parameters								
			1YS stress	1YS slope	2YS stress	2YS slope	UTS stress	Plastic Elongation			% RA
								Uniform	Total	Non-Uniform	
100	318000	1	546	64000	703	4698	754	0.2624	0.3628	0.1004	48.87
100	318000	2	451	65000	655	8822	763	0.2352	0.3096	0.0744	56.78
200	318000	1	978	84000	1084	1034	1084	0.0450	0.0732	0.0282	18.37
200	318000	2	997	79000	1119	1466	1121	0.0440	0.0833	0.0394	15.36

**Table 2.6. Vickers Hardness Validation Data for Nonbanded U-5.6Nb. The individual HV data point lists are split into two columns, running top-to-bottom, then left-to-right. Blank spaces indicate the locations of points that gave invalid HV readings because of inclusion or edge effects.**

Aging temp. (C)		100		200		300	
Aging time (min.)		318000		318000		318000	
Replicate		1		1		1	
Notes						1	
Indenter force (g)		50		50		50	
Spacing (micron)		50		50		50	
HV	Average	188.7		366.5		529.6	
	SD	7.9		12.8		24.0	
	Individual Data Points		182	373	378	564	546
		214	192	363	359	529	520
		200	196	383	363	537	546
		198	192	363	368	529	520
		192	190	349	373	537	504
		187	182	388	328	504	489
		200	189	388	363	546	504
		192	202	378	349	555	512
		194	200	378	363	520	504
		198	198	363	349	564	529
		192	189	373	359	529	537
		189	175	368	368	537	529
		187	183	373	373		546
		182	182	368	368	546	537
		202	185	368	363	546	497
		185	183	368	363	546	529
		192	187	388	354	555	555
			177	378		546	564
		189	178		373	546	555
		185	177	388	349	546	
		180	185	378	378	546	
			177	373		546	497
		187	183	368	363	482	482
		187	196	354	368	537	467
		187	190	373	345	546	497
		187	183	378	341	529	482
		183	177	373	345	546	529
		194		359		546	

Notes

1) Potentially overaged condition.

**Table 2.7. Vickers Hardness Validation Data for Nonbanded U-7.7Nb. The individual HV data point lists are split into two columns, running top-to-bottom, then left-to-right. Blank spaces indicate the locations of points that gave invalid HV readings because of inclusion or edge effects. For the two ages having more than one replicate (200°C and 300°C), only replicate #2 data were used for the validation; replicate #1 is listed for information only.**

Aging temp. (C)		100		200		200		300		300	
Aging time (min.)		318000		318000		318000		318000		318000	
Replicate		1		1		2		1		2	
Notes		2		2				1,2		1	
Indenter force (g)		50		50		50		50		50	
Spacing (micron)		50		50		50		50		50	
HV	Average	190.9		306.8		320.9		518.5		526.6	
	SD	5.8		13.9		20.4		26.3		24.7	
Individual Data Points		198	198	328	301	349	316	520	489	564	537
		189	185	308	290	312	324	537	482	573	520
		198	190	312	308	336	332	529	537	537	497
		196	202	324	294	332	328	529	512	546	497
		189	190	316	332	345	308	537	489	537	489
		187	190	320	336	332	320	564	489	546	489
		189	200	308		328	308	537	520	564	489
		190	190	308	328	336	297	546	504	564	497
		189	196	320	320	316	297	520	475	573	504
		189	194	308	320	363	301	434	504	573	489
		178	192	312	316	359	290	537	497	555	504
		185	189	312	297	359	294	564	489		520
		185	192	287	312	354	328	497	489	546	512
		190	189	297	308	345	305	537	512	546	489
		187	198	320			301	555	546	520	546
		182	192	297	284	312	297	520	537	537	504
		182	206		301	312	297	537	520	537	489
		177	196	287	287	336	312	537	512	529	504
		180	192	290	305	308	336	529	537	520	537
		192	194	312	290	312	308	537	529	512	555
		187	198	332	280	332	280	497	537	512	520
		190	196	297	305	328	294	489	555		520
		189	190	305	294	305	316	512	555	504	520
		194		297		316	312			512	529
		196		320		316	324			520	564
		192		308		336	294	497		546	529
		189		297		363		497		529	537
		189		294		345		497		520	

Notes

- 1) Potentially overaged condition.
- 2) This replicate specimen may be less chemically homogeneous than typical specimens of this alloy.

**Table 2.8. Chemical Analysis Results of Banded U-6Nb from the Validation Experiments.** The units are in wppm; the SD is from multiple replicate measurements. The elements H, C, N, O, and S were analyzed as described in [2007hac1]. The remaining elements were analyzed by inductively coupled plasma-optical emission spectroscopy (regular font) or by inductively coupled plasma-mass spectroscopy (bold font), with the aliquot preparation technique as described in [2007hac1], with the exception that aqua regia was used for initial specimen dissolution. Less than (<) indicates the method detection limit.

Element	Unaged		40C-5 years		65C-5 years		90C-5 years	
	Average	SD	Average	SD	Average	SD	Average	SD
H	0.05	0.08	0.04	0.03	0.09	0.09	0.17	0.05
B	<25.50		<25.50		<25.50		<25.50	
C	60.50	15.66	58.71	9.41	51.12	8.34	55.66	10.70
N	5.02	1.15	4.68	1.06	7.93	1.15	5.15	1.07
O	55.57	6.89	60.07	5.34	59.83	7.04	53.58	6.18
Na	<19.10		<19.10		<19.10		<19.10	
Mg	<3.20		<3.20		<3.20		<3.20	
Al	<22.30		<22.30		<22.30		<22.30	
Si	<79.70		<79.70		<79.70		<79.70	
P	<510.00		<510.00		<510.00		<510.00	
S	<4.10		<4.10		<4.10		<4.10	
K	<25.50		<25.50		<25.50		<25.50	
Ca	<31.90		<31.90		<31.90		<31.90	
Ti	<b>3.84</b>	<b>0.83</b>	<b>3.23</b>	<b>0.25</b>	<b>2.90</b>	<b>0.10</b>	<b>1.90</b>	<b>1.39</b>
V	<22.30		<22.30		<22.30		<22.30	
Cr	<19.10		<19.10		<19.10		<19.10	
Mn	<b>5.89</b>	<b>0.97</b>	4.83	0.25	<b>4.40</b>	<b>0.00</b>	<b>4.50</b>	<b>0.10</b>
Fe	<22.30		<22.30		<22.30		<22.30	
Co	<19.10		<19.10		<19.10		<19.10	
Ni	<b>5.41</b>	<b>1.49</b>	<b>3.73</b>	<b>0.38</b>	<b>3.07</b>	<b>0.25</b>	<b>2.97</b>	<b>0.06</b>
Cu	<b>7.05</b>	<b>1.92</b>						
Zn	<b>4.25</b>	<b>4.60</b>						
Ga	<37.30		<37.30		<37.30		<37.30	
Ge	<210.00		<210.00		<210.00		<210.00	
As	<234.00		<234.00		<234.00		<234.00	
Y	<3.20		<3.20		<3.20		<3.20	
Zr	<b>&lt;0.23</b>		<b>6.80</b>	<b>0.30</b>	<b>6.33</b>	<b>0.15</b>	<b>5.97</b>	<b>0.15</b>
Nb	62628.57	969.04	63300.00	793.73	64000.00	1609.35	63600.00	1178.98
Mo	<35.10		<35.10		<35.10		<35.10	
Ru	<b>&lt;0.07</b>		<b>&lt;0.07</b>		<b>&lt;0.07</b>		<b>&lt;0.07</b>	
Cd	<9.60		<9.60		<9.60		<9.60	
In	<166.00		<166.00		<166.00		<166.00	
Sb	<134.00		<134.00		<134.00		<134.00	
Ba	<b>2.26</b>	<b>0.98</b>	<b>2.37</b>	<b>0.40</b>	<b>2.20</b>	<b>0.10</b>	<b>1.50</b>	<b>0.95</b>
Hf	<b>&lt;0.05</b>		<b>&lt;0.05</b>		<b>&lt;0.05</b>		<b>&lt;0.05</b>	
Ta	<b>43.27</b>	<b>1.99</b>	<b>45.13</b>	<b>1.06</b>	<b>45.70</b>	<b>0.95</b>	<b>44.93</b>	<b>0.95</b>
W	<b>2.84</b>	<b>0.08</b>	<b>2.83</b>	<b>0.12</b>	<b>3.13</b>	<b>0.12</b>	<b>3.03</b>	<b>0.12</b>
Re	<54.20		<54.20		<54.20		<54.20	
Pb	<89.30		<89.30		<89.30		<89.30	

<3.20: Li, Be, Sc, Sr

<0.12: Sn, Ir

<0.04: Cs, Pt

<0.02: Rh, Pd, Ag, La, Tm, Tl, Th

ICP-OES normal

ICP-MS bold

**Table 2.9. Tensile Validation Data for Banded U-6Nb.**

Aging Temp. (C)	Aging Time (min.)	Rep. #	Engineering Stress-Strain Curve Parameters										Notes
			1YS stress	1YS slope	2YS stress	2YS slope	UTS stress	Plastic Elongation			% RA		
								Uniform	Total	Non-Uniform			
23	<135000	1	159	60000	657	20602	821	0.2354	0.3930	0.1576	38.49		
23	<135000	2	161	50000	658	21047	819	0.2337	0.3490	0.1153	34.92		
23	<135000	3	152	50000	650	20315	816	0.2453	0.4339	0.1886	43.91		
40	2629440	1	196	66000	674	19484	826	0.2476	0.3792	0.1316	38.93		
40	2629440	2	197	70000	664	20580	823	0.2542	0.4110	0.1568	40.31		
40	2629440	3	191	69000	663	20119	821	0.2458	0.3568	0.1110	39.63		
65	2629440	1	269	69000	680	17500	829	0.2508	0.4001	0.1494	37.92		
65	2629440	2	268	72000	678	17607	835	0.2500	0.3606	0.1106	35.23		
65	2629440	3	261	72000	673	17361	824	0.2598	0.3808	0.1209	32.82		
90	2629440	1	399	82000	726	13129	832	0.2556	0.4140	0.1583	34.30		
90	2629440	2	396	88000	722	13954	827	0.2550	0.4142	0.1592	39.81		
90	2629440	3	394	79000	716	14187	828	0.2528	0.3879	0.1352	37.88		

**Table 2.10. Vickers Hardness Validation Data for Banded U-6Nb. The individual HV data point lists are split into five columns, running top-to-bottom, then left-to-right. Blank spaces indicate the locations of points that gave invalid HV readings because of inclusion or edge effects.**

Aging temp. (C)		23				
Aging time (min.)		<135000				
Replicate		1				
Notes						
Indenter force (g)		50				
Spacing (micron)		75				
HV	Average	166.7				
	SD	11.8				
	Individual Data Points	163	172	145	180	178
		164	194		178	175
		163	196	161	185	167
		173	160	155	175	200
		190	178	175	167	
		148	156	169	159	
		151	161	164	182	
		155	164	185	173	
			178	134	164	
		152	167	160	156	
		177	164	143	190	
		173	167	167	160	
		189	146	161	177	
			160	161	161	
			138	167	177	
		175	166	173	159	
		170	164	175	159	
		166	178	160		
		167	169	163	164	
		164	173	182		
			170	151	164	
		172	167	148	167	
		177	167	175	170	
		167	159	172	161	
		182	155	163	163	
		177	152	164	152	
		159	149	169	169	
		170	169	157	173	
		156	156	167	156	
		155	178	177	166	
		169	163	167	151	
		169	164	166	169	
		172	161	167	170	
		153	196	173	159	
		178	142	160	196	

**Table 2.10 (continued). Vickers Hardness Validation Data for Banded U-6Nb. The individual HV data point lists are split into five columns, running top-to-bottom, then left-to-right. Blank spaces indicate the locations of points that gave invalid HV readings because of inclusion or edge effects.**

Aging temp. (C)		40				
Aging time (min.)		2629440				
Replicate		1				
Notes						
Indenter force (g)		50				
Spacing (micron)		65				
HV	Average	170.7				
	SD	11.9				
	Individual Data Points	180	152	152	163	178
		169	153	172	177	178
		187	167	169	172	170
		161	160	192	172	161
		160	177	185	170	170
		160	185	196	169	178
		163	164	147	167	157
		169	163	148	177	190
		167	155	160	160	157
		170	170	159	166	157
		185	160	175	177	155
			160	160	172	164
		172	172	161	178	175
		210	163	169	170	173
		178	178	164	146	
		164	173	169	177	175
		170	155	194	175	163
		173	149	175	180	175
		161	161	160	178	166
		194		167	172	170
		159	177	170	166	170
		182	164	185	160	153
		163	166	167	170	196
		144	172	190	169	182
		175	167	183	175	183
		163		190	173	182
		166	173	163	192	
		173	156	160	159	
		178	173	187	180	
			180	166	167	
		177	190	172	182	
		152	182	159	177	
		190	177	152	182	
		167	182	160	214	
		170	163	166	189	

**Table 2.10 (continued). Vickers Hardness Validation Data for Banded U-6Nb. The individual HV data point lists are split into five columns, running top-to-bottom, then left-to-right. Blank spaces indicate the locations of points that gave invalid HV readings because of inclusion or edge effects.**

Aging temp. (C)		65				
Aging time (min.)		2629440				
Replicate		1				
Notes						
Indenter force (g)		50				
Spacing (micron)		65				
HV	Average	181.5				
	SD	13.2				
	Individual Data Points	172	163	194	198	169
		192	190	185	177	169
		172	178	182	188	187
			167	190	175	164
		187	187	172	183	160
		185	177	204	170	159
		169	183	210	190	167
		185	185	185	182	189
		167	182	183	196	155
		166	175	196	182	
		177	194	169	169	194
		170	187	183	190	192
		170	177	185	212	192
		167	185	204	182	177
		161		208	190	172
		173	178	177	166	164
		163	202	163	166	169
		172	167	190	173	177
		187	163	182	204	173
		178	180	192	187	200
			178	178	182	175
		177	183	200	190	157
		183	169	192	187	172
		175	187		225	172
		194	189	182	237	216
		192	182	178	216	177
		189	175	189	178	196
		172	180	175	183	187
		187	183	180	173	167
		183	185	172		
		208	177	183	173	
		200	177	178	169	
		185	182	177	172	
		164	189	180	166	
		157	189	182	178	

**Table 2.10 (continued). Vickers Hardness Validation Data for Banded U-6Nb. The individual HV data point lists are split into five columns, running top-to-bottom, then left-to-right. Blank spaces indicate the locations of points that gave invalid HV readings because of inclusion or edge effects.**

Aging temp. (C)		90				
Aging time (min.)		2629440				
Replicate		1				
Notes						
Indenter force (g)		50				
Spacing (micron)		65				
HV	Average	201.3				
	SD	9.7				
	Individual Data Points	204	194	208	200	202
		204	196	182		206
		198	192	221	208	196
		200	196	206	202	196
		196	208	196	194	194
		182	208	200	206	206
		178	214	196	202	202
		173	202	192	185	210
		183	206	196	212	202
		204	190	196	196	212
		200	198	187		235
		200	200	202	223	210
		216	210	202	206	210
		210	208	190	218	206
		212	190	198	216	206
		196	206	196	204	210
		189	194	208	216	204
		192	200	204	218	214
		182	208	189	200	223
		204	202	185	187	188
		214	200	192	198	194
		190	192	185	194	202
		208	192	182	194	198
		196	210	196	200	196
		196	206	206	194	218
		208	198	196	210	
		206	194	200	206	
		198	208	214	208	
		187	204	204	202	
		202	198	190	198	
		192	218	210	208	
		185	208	202	216	
		200	204	216	200	
		202	202	202	208	
		212	208	206	200	

**Table 3.1. Property Values at the Start and End (Peak) of Age-Hardening. The same values for U-5.6Nb and U-7.7Nb used in the previous study [2007hac2] were also used in the present work.**

Property		U-5.6Nb	U-7.7Nb	Banded U-6Nb
HV	$P(start)$	147.2	115.2	166.7
	$P(peak)$	600.0	600.0	600.0
1YS (MPa)	$P(start)$	125.4	96.7	157.3
	$P(peak)$	1,200.0	1,400.0	1,200.0
2YS (MPa)	$P(start)$	545.2	509.0	655.0
	$P(peak)$	1,200.0	1,400.0	1,200.0
UTS (MPa)	$P(start)$	792.0	699.0	818.7
	$P(peak)$	1,200.0	1,400.0	1,200.0
UE	$P(start)$	0.2314	0.2840	0.2382
	$P(peak)$	0.0000	0.0000	0.0000
TE	$P(start)$	0.2592	0.3900	0.3920
	$P(peak)$	0.0000	0.0000	0.0000
% RA	$P(start)$	32.95	56.97	39.11
	$P(peak)$	0.00	0.00	0.00
1YM (MPa)	$P(start)$	52,500	31,000	53,333
	$P(peak)$	120,000	85,000	120,000

**Table 3.2. Kinetic Parameters for U-5.6Nb Obtained from the Previous Study [2007hac2]. The  $Q$  values were fit at  $f = 0.25$  using data from all 4 temperatures.**

$P$	$Q$ (kcal/mol)	$x_o$ value at the indicated temperature				$dx$ value at the indicated temperature			
		100°C	200°C	250°C	300°C	100°C	200°C	250°C	300°C
HV	115.922	33.2797	5.6516	4.6900	3.3261	8.2681	1.9506	1.7056	1.5891
2YS	29.069	6.8210	4.1863	3.2708	1.3850	0.7923	1.2408	1.9511	1.2687
TE	29.030	6.8129	3.5431	2.2016	0.8536	0.9853	0.9450	1.4430	0.8303

**Table 3.3. Kinetic Parameters for U-7.7Nb Obtained from the Previous Study [2007hac2]. The  $Q$  values were fit at  $f = 0.25$  using data from all 4 temperatures.**

$P$	$Q$ (kcal/mol)	$x_o$ value at the indicated temperature				$dx$ value at the indicated temperature			
		100°C	200°C	250°C	300°C	100°C	200°C	250°C	300°C
HV	20.650	9.7186	6.7170	4.7351	3.3211	3.2504	2.3486	1.7270	1.3380
2YS	30.532	10.4549	5.1036	2.6139	1.5471	3.9061	2.0877	1.6372	1.3549
TE	25.216	6.6042	3.5201	1.0653	1.1052	1.1993	1.5680	0.6342	0.5359

**Table 3.4. Lifetimes for U-5.6Nb and U-7.7Nb Obtained from the Previous Study [2007hac2], on the Basis of the  $f' \geq 0.25$  Failure Criterion for TE. The minimum lifetime values for each alloy and storage temperature of the four values calculated are highlighted in bold.**

Storage Temp.	U-5.6Nb lifetime (years) extrapolated from the column-heading temperature				U-7.7Nb lifetime (years) extrapolated from the column-heading temperature			
	100°C	200°C	250°C	300°C	100°C	200°C	250°C	300°C
30°C	<b>36,071</b>	78,400	40,035	39,270	3,132	1,927	<b>362</b>	3,815
40°C	<b>7,759</b>	16,863	8,611	8,447	824	507	<b>95</b>	1,004
50°C	<b>1,835</b>	3,989	2,037	1,998	236	145	<b>27</b>	287

**Table 3.5. Analytic Method Comparison between the Previous and Present Studies.**

Topic	Characteristic	Previous Study	Present Study
Experimental data set	For model fitting	Nonbanded U-5.6Nb and U-7.7Nb aged 100°C, 200°C, 250°C, 300°C up to 140 days.	Same
	For validation	None	1) Nonbanded U-5.6Nb and U-7.7Nb aged 100°C, 200°C, 300°C for 221 days. 2) Banded U-6Nb aged 40°C, 65°C, 90°C for 5 years.
Fraction transformed	Formula	Eq. 3.1	Same
	Normalization values $P(start)$ and $P(peak)$	Table 3.1	Same
Model fitting	Data form and weighting	Averages, weighted by $SD$	All replicate data points, equally weighted
	Analyst interventions	Fictitious long-time points added to guide 100°C and 200°C time-series UE and TE	None
	Time-series function	Boltzmann; two adjustable parameters $x_o$ and $dx$	Logistic, two adjustable parameters $A$ ( $= 1/dx$ ) and $B$ ( $= x_o$ ); equivalent to Boltzmann
	Temperature-series function	Arrhenius	Same
	Fitting method	Sequential time, then temp.: 1) Time-series: Nonlinear least-squares fitting of $x_o$ and $dx$ . Both parameters were specific to each temperature and were unconstrained. 2) Arrhenius fitting for $Q$ from linear fit to $\log(\text{time to reach } f = 0.25)$ vs $1/T$ .	Simultaneous time and temp.: Nonlinear least-squares fitting of $A$ , $B$ , and $Q$ . $A$ was constrained to have the same value for all temperatures (making it isokinetic). $A$ , $B$ , and $Q$ were further forced to be “perfectly-Arrhenius.”
Lifetime prediction	Failure criterion	$f' \geq 0.25$ for TE; equivalently, $f \geq 0.3866$ (U-5.6Nb) or $f \geq 0.3404$ (U-7.7Nb)	Same
	Lifetime evaluation	Lifetime spread from minimum and maximum values from extrapolations from each of the four aging temperature fits.	Extrapolations from each of the four aging temperature fits resulted in a single value (from “perfect-Arrhenius” forcing). Lifetime spread from 95% $CIs$ .
Model validation		None	1a) U-5.6Nb: HV only 1b) U-7.7Nb: HV and tensile 2) U-6Nb: HV and tensile

**Table 3.6. Total Elongation Kinetic Parameters for U-5.6Nb. The  $t$  value used to compute the confidence interval is 2.018. The units of  $Q$  are kcal/mol;  $A$  and  $B$  were assessed on the basis of the time in minutes.**

U-5.6Nb TE				
Parameter	Estimate	Standard Error	95% Confidence Interval	
			Lower Bound	Upper Bound
$Q$	31.699	4.985	21.639	41.759
$A$	0.9666	0.1734	0.6167	1.3165
$B$	0.9955	0.3043	0.3814	1.6096

**Table 3.7. Total Elongation Kinetic Parameters for U-7.7Nb. The  $t$  value used to compute the confidence interval is 2.028. The units of  $Q$  are kcal/mol;  $A$  and  $B$  were assessed on the basis of the time in minutes.**

U-7.7Nb TE				
Parameter	Estimate	Standard Error	95% Confidence Interval	
			Lower Bound	Upper Bound
$Q$	39.286	6.285	26.540	52.032
$A$	0.6577	0.1225	0.4093	0.9061
$B$	-0.1346	0.4805	-1.1091	0.8399

**Table 3.8. Uniform Elongation Kinetic Parameters for U-5.6Nb. The  $t$  value used to compute the confidence interval is 2.018. The units of  $Q$  are kcal/mol;  $A$  and  $B$  were assessed on the basis of the time in minutes.**

U-5.6Nb UE				
Parameter	Estimate	Standard Error	95% Confidence Interval	
			Lower Bound	Upper Bound
$Q$	31.836	4.306	22.696	40.526
$A$	1.0612	0.1680	0.7222	1.4002
$B$	1.1163	0.2514	0.6090	1.6236

**Table 3.9. Uniform Elongation Kinetic Parameters for U-7.7Nb. The  $t$  value used to compute the confidence interval is 2.028. The units of  $Q$  are kcal/mol;  $A$  and  $B$  were assessed on the basis of the time in minutes.**

U-7.7Nb UE				
Parameter	Estimate	Standard Error	95% Confidence Interval	
			Lower Bound	Upper Bound
$Q$	51.741	6.415	38.731	64.751
$A$	0.9927	0.1637	0.6607	1.3247
$B$	-0.6659	0.4295	-1.5369	0.2051

**Table 3.10. First-Yield Strength Kinetic Parameters for U-5.6Nb. The  $t$  value used to compute the confidence interval is 2.018. The units of  $Q$  are kcal/mol;  $A$  and  $B$  were assessed on the basis of the time in minutes.**

U-5.6Nb 1YS				
Parameter	Estimate	Standard Error	95% Confidence Interval	
			Lower Bound	Upper Bound
$Q$	20.813	1.796	17.189	24.437
$A$	1.1425	0.0956	0.9496	1.3354
$B$	2.4264	0.1132	2.1980	2.6548

**Table 3.11. First-Yield Strength Kinetic Parameters for U-7.7Nb. The  $t$  value used to compute the confidence interval is 2.028. The units of  $Q$  are kcal/mol;  $A$  and  $B$  were assessed on the basis of the time in minutes.**

U-7.7Nb 1YS				
Parameter	Estimate	Standard Error	95% Confidence Interval	
			Lower Bound	Upper Bound
$Q$	15.243	2.204	10.773	19.713
$A$	0.9190	0.1252	0.6651	1.1729
$B$	3.0692	0.1783	2.7076	3.4308

**Table 3.12. First-Yield Modulus Kinetic Parameters for U-5.6Nb. The  $t$  value used to compute the confidence interval is 2.018. The units of  $Q$  are kcal/mol;  $A$  and  $B$  were assessed on the basis of the time in minutes.**

U-5.6Nb 1YM				
Parameter	Estimate	Standard Error	95% Confidence Interval	
			Lower Bound	Upper Bound
$Q$	14.259	4.084	6.017	22.501
$A$	0.7710	0.1823	0.4031	1.1389
$B$	2.5672	0.3672	1.8262	3.3082

**Table 3.13. First-Yield Modulus Kinetic Parameters for U-7.7Nb. The  $t$  value used to compute the confidence interval is 2.028. The units of  $Q$  are kcal/mol;  $A$  and  $B$  were assessed on the basis of the time in minutes.**

U-7.7Nb 1YM				
Parameter	Estimate	Standard Error	95% Confidence Interval	
			Lower Bound	Upper Bound
$Q$	13.655	2.312	8.966	18.344
$A$	1.0966	0.1890	0.7133	1.4799
$B$	2.8964	0.2051	2.4805	3.3123

**Table 3.14. Second-Yield Strength Kinetic Parameters for U-5.6Nb. The  $t$  value used to compute the confidence interval is 2.018. The units of  $Q$  are kcal/mol;  $A$  and  $B$  were assessed on the basis of the time in minutes.**

U-5.6Nb 2YS				
Parameter	Estimate	Standard Error	95% Confidence Interval	
			Lower Bound	Upper Bound
$Q$	34.178	2.570	28.992	39.364
$A$	0.8244	0.0690	0.6852	0.9636
$B$	1.4401	0.1444	1.1488	1.7315

**Table 3.15. Second-Yield Strength Kinetic Parameters for U-7.7Nb. The  $t$  value used to compute the confidence interval is 2.028. The units of  $Q$  are kcal/mol;  $A$  and  $B$  were assessed on the basis of the time in minutes.**

U-7.7Nb 2YS				
Parameter	Estimate	Standard Error	95% Confidence Interval	
			Lower Bound	Upper Bound
$Q$	33.927	3.038	27.766	40.088
$A$	0.4981	0.0458	0.4052	0.5910
$B$	1.6405	0.1751	1.2854	1.9956

**Table 3.16. Ultimate Tensile Strength Kinetic Parameters for U-5.6Nb. The  $t$  value used to compute the confidence interval is 2.018. The units of  $Q$  are kcal/mol;  $A$  and  $B$  were assessed on the basis of the time in minutes.**

U-5.6Nb UTS				
Parameter	Estimate	Standard Error	95% Confidence Interval	
			Lower Bound	Upper Bound
$Q$	41.365	4.984	31.307	51.423
$A$	0.8555	0.1444	0.5641	1.1469
$B$	1.8603	0.2418	1.3723	2.3483

**Table 3.17. Ultimate Tensile Strength Kinetic Parameters for U-7.7Nb. The  $t$  value used to compute the confidence interval is 2.028. The units of  $Q$  are kcal/mol;  $A$  and  $B$  were assessed on the basis of the time in minutes.**

U-7.7Nb UTS				
Parameter	Estimate	Standard Error	95% Confidence Interval	
			Lower Bound	Upper Bound
$Q$	46.146	2.593	40.887	51.405
$A$	0.7636	0.0538	0.6545	0.8727
$B$	1.7249	0.1116	1.4986	1.9512

**Table 3.18. Vickers Hardness Kinetic Parameters for U-5.6Nb. The  $t$  value used to compute the confidence interval is 2.110. The units of  $Q$  are kcal/mol;  $A$  and  $B$  were assessed on the basis of the time in minutes.**

U-5.6Nb HV				
Parameter	Estimate	Standard Error	95% Confidence Interval	
			Lower Bound	Upper Bound
$Q$	27.734	2.263	22.959	32.509
$A$	0.6136	0.0470	0.5144	0.7128
$B$	3.4006	0.1141	3.1598	3.6414

**Table 3.19. Vickers Hardness Kinetic Parameters for U-7.7Nb. The  $t$  value used to compute the confidence interval is 2.131. The units of  $Q$  are kcal/mol;  $A$  and  $B$  were assessed on the basis of the time in minutes.**

U-7.7Nb HV				
Parameter	Estimate	Standard Error	95% Confidence Interval	
			Lower Bound	Upper Bound
$Q$	22.538	4042	13.924	31.152
$A$	0.4763	0.0716	0.3237	0.6289
$B$	4.1543	0.3261	3.4594	4.8492

**Table 4.1. Results for Three Quality-of-Model-Fitting Metrics Evaluated for each Property in U-5.6Nb. The color coding is a redundant indicator of the text result in each box (green = good, yellow = fair, pink = questionable). The number in parentheses in the Goodness of Fit column is the *RSE* value. The parenthetical comments in the Symmetry of Fit column call out the temperatures where notable asymmetry was found.**

Property	Goodness of Fit (RSE, fractional basis)	Robustness of Fit (plot of RSS tau)	Symmetry of Fit (evenness of data point scatter about prediction)
TE	fair (0.1696)	fair	good
UE	fair (0.1517)	fair	good
1YS	good (0.0851)	good	good
1YM	questionable (0.2410)	questionable	good
2YS	good (0.0763)	good	fair (100C below line)
UTS	fair (0.1326)	fair	good
HV	good (0.0321)	fair	good

**Table 4.2. Results for Three Quality-of-Model-Fitting Metrics Evaluated for each Property in U-7.7Nb. The color coding is a redundant indicator of the text result in each box (green = good, yellow = fair, pink = questionable). The number in parentheses in the Goodness of Fit column is the *RSE* value. The parenthetical comments in the Symmetry of Fit column call out the temperatures where notable asymmetry was found.**

Property	Goodness of Fit (RSE, fractional basis)	Robustness of Fit (plot of RSS tau)	Symmetry of Fit (evenness of data point scatter about prediction)
TE	fair (0.1409)	questionable	questionable (100C, 250C above line)
UE	fair (0.1233)	questionable	questionable (100C above line)
1YS	fair (0.1210)	fair	questionable (100C above line, 200C below line)
1YM	fair (0.1631)	questionable	questionable (100C above line, 200C below line)
2YS	good (0.0657)	fair	questionable (100C above line, 200C below line)
UTS	good (0.0533)	good	questionable (100C above line)
HV	good (0.0614)	questionable	questionable (100C above line, 200C below line)

**Table 4.3. Residual Standard Errors and Ancillary Quantities. The *RSE* is quoted as an absolute value (MPa units for 1YS, 1YM, 2YS, and UTS) and on the basis of fractional property change. The difference quantity *n-p* is the degrees of freedom (*df*).**

Property	U-5.6Nb					U-7.7Nb				
	<i>RSE</i>		<i>n</i>	<i>p</i>	<i>n-p</i>	<i>RSE</i>		<i>n</i>	<i>p</i>	<i>n-p</i>
	fractional	absolute				fractional	absolute			
TE	0.1696	0.043964	45	3	42	0.1409	0.054955	39	3	36
UE	0.1517	0.035097	45	3	42	0.1233	0.035004	39	3	36
1YS	0.0851	91.4812	45	3	42	0.1210	157.638	39	3	36
1YM	0.2410	16271	45	3	42	0.1631	8808.38	39	3	36
2YS	0.0763	49.9509	45	3	42	0.0657	58.5185	39	3	36
UTS	0.1326	54.1052	45	3	42	0.0533	37.3853	39	3	36
HV	0.0321	14.5191	20	3	17	0.0614	29.7493	18	3	15

**Table 4.4. Summary of Activation Energies  $Q$  from Model Fitting of the Previous Study [2007hac2] and This Study.**

Property	Activation Energy $Q$ (kcal/mol)			
	U-5.6Nb		U-7.7Nb	
	Previous Study	This Study	Previous Study	This Study
TE	29.030	31.699	25.216	39.286
UE		31.836		51.741
1YS		20.813		15.243
1YM		14.259		13.655
2YS	29.069	34.178	30.532	33.927
UTS		41.365		46.146
HV	115.922	27.734	20.650	22.538

**Table 4.5. Summary of A Parameter ( $= 1/dx$ ) from Model Fitting of the Previous Study [2007hac2] and This Study. The value listed for the previous study is the arithmetically averaged value of the reciprocals of the 4 individual  $dx$  values provided in Tables 3.2 and 3.3.**

Property	A Parameter			
	U-5.6Nb		U-7.7Nb	
	Previous Study	This Study	Previous Study	This Study
TE	0.9926	0.9666	1.2285	0.6577
UE		1.0612		0.9927
1YS		1.1425		0.9190
1YM		0.7710		1.0966
2YS	0.8422	0.8244	0.5210	0.4981
UTS		0.8555		0.7636
HV	0.4623	0.6136	0.5150	0.4763

**Table 4.6. Summary of B Parameter ( $= x_0$  at 300°C) from Model Fitting of the Previous Study [2007hac2] and This Study. The value listed for the previous study is the arithmetically averaged value of the 4 individual values of  $x_0$ , provided in Tables 3.2 and 3.3, after rescaling to 300°C.**

Property	B Parameter			
	U-5.6Nb		U-7.7Nb	
	Previous Study	This Study	Previous Study	This Study
TE	1.0235	0.9955	1.0504	-0.1346
UE		1.1163		-0.6659
1YS		2.4264		3.0692
1YM		2.5672		2.8964
2YS	1.5865	1.4401	2.9066	1.6405
UTS		1.8603		1.7249
HV	9.4076	3.4006	4.0997	4.1543

**Table 4.7. Experimentally Measured and Predicted Mean TE Values for Various U-Nb Alloys for Current and Future Model Validation. The 95% prediction and confidence intervals are also given. The alloy identified as 6 wt% Nb is the RFP banded U-6Nb; the alloys identified as 5.6 wt% and 7.7 wt% are nonbanded. “NP” indicates that no data point is expected, because of material limitations.**

Alloy Wt.% Nb	Aging Temp. (C)	Aging Time		Total Plastic Elongation					
		(min.)	(years)	Experimental Mean	Prediction Interval		Prediction Mean	Confidence Interval	
					Lower	Upper		Lower	Upper
6	40	328320	0.625		0.3451	0.3920	0.3901	0.3850	0.3920
6	40	656640	1.25		0.3442	0.3920	0.3894	0.3828	0.3920
6	40	1311840	2.5		0.3430	0.3920	0.3886	0.3799	0.3920
6	40	2629440	5.0	0.3823	0.3413	0.3920	0.3874	0.3760	0.3920
6	40	5260320	10.0		0.3387	0.3920	0.3859	0.3709	0.3920
6	40	10519200	20.0		0.3350	0.3920	0.3839	0.3642	0.3920
6	40	21038400	40.0		0.3296	0.3920	0.3813	0.3555	0.3920
6	65	328320	0.625		0.3345	0.3920	0.3829	0.3644	0.3920
6	65	656640	1.25		0.3291	0.3920	0.3799	0.3559	0.3920
6	65	1311840	2.5		0.3215	0.3920	0.3760	0.3449	0.3920
6	65	2629440	5.0	0.3805	0.3108	0.3920	0.3709	0.3308	0.3920
6	65	5260320	10.0		0.2961	0.3920	0.3642	0.3128	0.3920
6	65	10519200	20.0		0.2766	0.3920	0.3557	0.2904	0.3920
6	65	21038400	40.0		0.2515	0.3920	0.3449	0.2629	0.3920
6	90	328320	0.625		0.2923	0.3920	0.3587	0.3096	0.3920
6	90	656640	1.25		0.2727	0.3920	0.3487	0.2872	0.3920
6	90	1311840	2.5		0.2480	0.3920	0.3362	0.2602	0.3920
6	90	2629440	5.0	0.4054	0.2180	0.3920	0.3207	0.2283	0.3920
6	90	5260320	10.0		0.1833	0.3920	0.3021	0.1921	0.3920
6	90	10519200	20.0		0.1450	0.3920	0.2804	0.1526	0.3920
6	90	21038400	40.0		0.1051	0.3920	0.2558	0.1119	0.3920
5.6	100	318000	0.6	NP			0.2254	0.1827	0.2592
5.6	100	1052400	2.0		0.1335	0.2592	0.2077	0.1482	0.2592
5.6	100	3153600	6.0		0.1043	0.2592	0.1861	0.1099	0.2592
5.6	200	318000	0.6	NP			0.0340	0.0082	0.0598
5.6	200	1052400	2.0	NP			0.0217	0.0011	0.0423
5.6	200	3153600	6.0	NP			0.0141	0.0000	0.0300
5.6	300	318000	0.6	NP			0.0033	0.0000	0.0081
5.6	300	1052400	2.0	NP			0.0020	0.0000	0.0053
5.6	300	3153600	6.0	NP			0.0013	0.0000	0.0035
7.7	100	318000	0.6	0.3362	0.2450	0.3900	0.3226	0.2686	0.3766
7.7	100	1052400	2.0		0.2137	0.3890	0.3014	0.2337	0.3690
7.7	100	3153600	6.0		0.1886	0.3676	0.2781	0.1967	0.3595
7.7	200	318000	0.6	0.0782	0.0000	0.1307	0.0640	0.0274	0.1006
7.7	200	1052400	2.0		0.0000	0.1128	0.0477	0.0142	0.0813
7.7	200	3153600	6.0		0.0000	0.0993	0.0361	0.0062	0.0659
7.7	300	318000	0.6	NP			0.0093	0.0000	0.0190
7.7	300	1052400	2.0	NP			0.0067	0.0000	0.0144
7.7	300	3153600	6.0	NP			0.0049	0.0000	0.0112

**Table 4.8. Experimentally Measured and Predicted Mean UE Values for Various U-Nb Alloys for Current and Future Model Validation. The 95% prediction and confidence intervals are also given. The alloy identified as 6 wt% Nb is the RFP banded U-6Nb; the alloys identified as 5.6 wt% and 7.7 wt% are nonbanded. “NP” indicates that no data point is expected, because of material limitations.**

Alloy Wt.% Nb	Aging Temp. (C)	Aging Time		Uniform Plastic Elongation					
		(min.)	(years)	Experimental Mean	Prediction Interval		Prediction Mean	Confidence Interval	
					Lower	Upper		Lower	Upper
6	40	328320	0.625		0.2133	0.2382	0.2376	0.2360	0.2382
6	40	656640	1.25		0.2130	0.2382	0.2374	0.2353	0.2382
6	40	1311840	2.5		0.2126	0.2382	0.2371	0.2342	0.2382
6	40	2629440	5.0	0.2101	0.2121	0.2382	0.2367	0.2328	0.2382
6	40	5260320	10.0		0.2113	0.2382	0.2361	0.2309	0.2382
6	40	10519200	20.0		0.2100	0.2382	0.2353	0.2283	0.2382
6	40	21038400	40.0		0.2082	0.2382	0.2343	0.2247	0.2382
6	65	328320	0.625		0.2097	0.2382	0.2349	0.2281	0.2382
6	65	656640	1.25		0.2077	0.2382	0.2337	0.2245	0.2382
6	65	1311840	2.5		0.2048	0.2382	0.2321	0.2198	0.2382
6	65	2629440	5.0	0.2535	0.2005	0.2382	0.2298	0.2135	0.2382
6	65	5260320	10.0		0.1943	0.2382	0.2268	0.2052	0.2382
6	65	10519200	20.0		0.1854	0.2382	0.2228	0.1944	0.2382
6	65	21038400	40.0		0.1732	0.2382	0.2175	0.1805	0.2382
6	90	328320	0.625		0.1917	0.2382	0.2241	0.2026	0.2382
6	90	656640	1.25		0.1822	0.2382	0.2193	0.1913	0.2382
6	90	1311840	2.5		0.1697	0.2382	0.2129	0.1771	0.2382
6	90	2629440	5.0	0.2545	0.1534	0.2382	0.2047	0.1595	0.2382
6	90	5260320	10.0		0.1335	0.2382	0.1944	0.1386	0.2382
6	90	10519200	20.0		0.1104	0.2382	0.1819	0.1146	0.2382
6	90	21038400	40.0		0.0850	0.2382	0.1670	0.0887	0.2382
5.6	100	318000	0.6	NP			0.2091	0.1797	0.2314
5.6	100	1052400	2.0		0.1391	0.2314	0.1953	0.1517	0.2314
5.6	100	3153600	6.0		0.1135	0.2314	0.1771	0.1180	0.2314
5.6	200	318000	0.6	NP			0.0292	0.0088	0.0496
5.6	200	1052400	2.0	NP			0.0178	0.0021	0.0334
5.6	200	3153600	6.0	NP			0.0110	0.0000	0.0226
5.6	300	318000	0.6	NP			0.0022	0.0000	0.0053
5.6	300	1052400	2.0	NP			0.0013	0.0000	0.0033
5.6	300	3153600	6.0	NP			0.0008	0.0000	0.0021
7.7	100	318000	0.6	0.2488	0.2443	0.2840	0.2804	0.2738	0.2840
7.7	100	1052400	2.0		0.2410	0.2840	0.2780	0.2676	0.2840
7.7	100	3153600	6.0		0.2460	0.2840	0.2746	0.2586	0.2840
7.7	200	318000	0.6	0.0445	0.0000	0.0769	0.0342	0.0104	0.0579
7.7	200	1052400	2.0		0.0000	0.0615	0.0214	0.0028	0.0401
7.7	200	3153600	6.0		0.0000	0.0520	0.0137	0.0000	0.0280
7.7	300	318000	0.6	NP			0.0006	0.0000	0.0017
7.7	300	1052400	2.0	NP			0.0004	0.0000	0.0011
7.7	300	3153600	6.0	NP			0.0002	0.0000	0.0007

**Table 4.9. Experimentally Measured and Predicted Mean 1YS Values for Various U-Nb Alloys for Current and Future Model Validation. The 95% prediction and confidence intervals are also given. The alloy identified as 6 wt% Nb is the RFP banded U-6Nb; the alloys identified as 5.6 wt% and 7.7 wt% are nonbanded. “NP” indicates that no data point is expected, because of material limitations.**

Alloy Wt.% Nb	Aging Temp. (C)	Aging Time		First Yield Strength (MPa)					
		(min.)	(years)	Experimental Mean	Prediction Interval		Prediction Mean	Confidence Interval	
					Lower	Upper		Lower	Upper
6	40	328320	0.625		157.3	239.9	176.3	157.3	198.1
6	40	656640	1.25		157.3	250.6	183.9	157.3	213.7
6	40	1311840	2.5		157.3	266.6	194.4	157.3	235.0
6	40	2629440	5.0	195	157.3	290.1	208.9	157.3	263.9
6	40	5260320	10.0		157.3	323.6	228.7	157.3	302.5
6	40	10519200	20.0		157.3	369.8	255.2	157.4	353.0
6	40	21038400	40.0		157.3	431.0	290.3	162.8	417.7
6	65	328320	0.625		157.3	299.7	219.2	165.3	273.1
6	65	656640	1.25		157.3	335.6	242.6	171.2	314.0
6	65	1311840	2.5		163.0	384.3	273.6	180.5	366.8
6	65	2629440	5.0	266	180.9	447.8	314.3	195.0	433.7
6	65	5260320	10.0		205.6	526.3	365.9	217.1	514.8
6	65	10519200	20.0		240.1	618.4	429.2	249.7	608.7
6	65	21038400	40.0		287.7	719.8	503.8	296.1	711.4
6	90	328320	0.625		202.6	432.6	317.6	219.3	415.9
6	90	656640	1.25		234.5	505.4	370.0	248.4	491.5
6	90	1311840	2.5		276.6	591.4	434.0	288.3	579.6
6	90	2629440	5.0	396	331.3	687.6	509.5	341.7	677.3
6	90	5260320	10.0		399.6	787.6	593.6	409.0	778.1
6	90	10519200	20.0		480.7	884.3	682.5	489.7	875.2
6	90	21038400	40.0		571.1	971.1	771.1	580.2	962.0
5.6	100	318000	0.6	NP			348.7	232.6	464.7
5.6	100	1052400	2.0		292.2	650.6	471.4	317.8	625.0
5.6	100	3153600	6.0		421.4	796.8	609.1	431.8	786.5
5.6	200	318000	0.6	NP			1019.6	960.8	1078.4
5.6	200	1052400	2.0	NP			1092.3	1045.9	1138.7
5.6	200	3153600	6.0	NP			1134.8	1100.3	1169.2
5.6	300	318000	0.6	NP			1168.9	1149.8	1188.0
5.6	300	1052400	2.0	NP			1182.6	1170.2	1195.0
5.6	300	3153600	6.0	NP			1189.8	1181.7	1198.0
7.7	100	318000	0.6	499	308.6	794.8	551.7	368.6	734.9
7.7	100	1052400	2.0		438.3	963.9	701.1	492.5	909.7
7.7	100	3153600	6.0		599.0	1087.2	843.1	623.5	1062.7
7.7	200	318000	0.6	988	879.0	1274.3	1076.6	960.4	1192.9
7.7	200	1052400	2.0		984.8	1372.4	1178.6	1069.0	1288.1
7.7	200	3153600	6.0		1061.9	1400.0	1247.9	1152.8	1343.1
7.7	300	318000	0.6	NP			1274.2	1191.5	1356.8
7.7	300	1052400	2.0	NP			1319.0	1254.6	1383.3
7.7	300	3153600	6.0	NP			1346.5	1297.3	1395.7

**Table 4.10. Experimentally Measured and Predicted Mean 1YM Values for Various U-Nb Alloys for Current and Future Model Validation. The 95% prediction and confidence intervals are also given. The alloy identified as 6 wt% Nb is the RFP banded U-6Nb; the alloys identified as 5.6 wt% and 7.7 wt% are nonbanded. “NP” indicates that no data point is expected, because of material limitations.**

Alloy Wt.% Nb	Aging Temp. (C)	Aging Time		First Yield Modulus (MPa)					
		(min.)	(years)	Experimental Mean	Prediction Interval		Prediction Mean	Confidence Interval	
					Lower	Upper		Lower	Upper
6	40	328320	0.625		53333	89866	68742	53333	86890
6	40	656640	1.25		53333	94825	71661	53333	92148
6	40	1311840	2.5		53333	100079	74895	53333	97641
6	40	2629440	5.0	68333	53333	105467	78421	53629	103213
6	40	5260320	10.0		53568	110720	82144	55692	108596
6	40	10519200	20.0		56352	115616	85984	58394	113574
6	40	21038400	40.0		59732	119953	89843	61740	117945
6	65	328320	0.625		54581	98256	76419	57444	95393
6	65	656640	1.25		56823	103245	80034	59494	100574
6	65	1311840	2.5		59477	108151	83814	62010	105618
6	65	2629440	5.0	71000	62580	112794	87687	65026	110348
6	65	5260320	10.0		66089	116956	91523	68501	114545
6	65	10519200	20.0		69945	120000	95229	72373	118085
6	65	21038400	40.0		74048	120000	98722	76542	120000
6	90	328320	0.625		63646	104798	84222	66714	101729
6	90	656640	1.25		66817	109353	88085	69769	106400
6	90	1311840	2.5		70246	113562	91904	73137	110672
6	90	2629440	5.0	83000	73907	117302	95605	76792	114417
6	90	5260320	10.0		77698	120000	99073	80633	117513
6	90	10519200	20.0		81526	120000	102253	84568	119938
6	90	21038400	40.0		85287	120000	105108	88494	120000
5.6	100	318000	0.6	NP			86578	69816	103340
5.6	100	1052400	2.0		69175	117301	93238	75646	110830
5.6	100	3153600	6.0		78365	119425	98895	81526	116264
5.6	200	318000	0.6	NP			106414	96596	116232
5.6	200	1052400	2.0	NP			110252	101246	119258
5.6	200	3153600	6.0	NP			112936	105065	120000
5.6	300	318000	0.6	NP			113640	106681	120000
5.6	300	1052400	2.0	NP			115603	109933	120000
5.6	300	3153600	6.0	NP			116893	112326	120000
7.7	100	318000	0.6	64500	41625	69039	55332	44935	65729
7.7	100	1052400	2.0		48921	77001	62961	52129	73793
7.7	100	3153600	6.0		57538	81120	69329	59152	79506
7.7	200	318000	0.6	81500	65929	85000	76320	71010	81629
7.7	200	1052400	2.0		69791	85000	79722	75380	84064
7.7	200	3153600	6.0		72211	85000	81741	78419	85000
7.7	300	318000	0.6	NP			82069	79007	85000
7.7	300	1052400	2.0	NP			83302	81183	85000
7.7	300	3153600	6.0	NP			83980	82519	85000

**Table 4.11. Experimentally Measured and Predicted Mean 2YS Values for Various U-Nb Alloys for Current and Future Model Validation. The 95% prediction and confidence intervals are also given. The alloy identified as 6 wt% Nb is the RFP banded U-6Nb; the alloys identified as 5.6 wt% and 7.7 wt% are nonbanded. “NP” indicates that no data point is expected, because of material limitations.**

Alloy Wt.% Nb	Aging Temp. (C)	Aging Time		Second Yield Strength (MPa)					
		(min.)	(years)	Experimental Mean	Prediction Interval		Prediction Mean	Confidence Interval	
					Lower	Upper		Lower	Upper
6	40	328320	0.625		655.0	685.2	657.1	655.0	659.7
6	40	656640	1.25		655.0	685.9	657.7	655.0	661.0
6	40	1311840	2.5		655.0	686.7	658.5	655.0	662.6
6	40	2629440	5.0	667	655.0	687.9	659.4	655.0	664.6
6	40	5260320	10.0		655.0	689.4	660.7	655.0	667.2
6	40	10519200	20.0		655.0	691.4	662.3	655.0	670.5
6	40	21038400	40.0		655.0	694.1	664.3	655.0	674.6
6	65	328320	0.625		655.0	693.2	663.9	655.4	672.4
6	65	656640	1.25		655.0	696.3	666.4	655.8	677.0
6	65	1311840	2.5		655.0	700.4	669.5	656.3	682.7
6	65	2629440	5.0	677	655.0	705.9	673.5	656.9	690.0
6	65	5260320	10.0		655.0	713.1	678.4	657.9	699.0
6	65	10519200	20.0		655.0	722.5	684.7	659.2	710.1
6	65	21038400	40.0		655.0	734.5	692.5	661.0	723.9
6	90	328320	0.625		655.0	720.1	685.0	663.7	706.2
6	90	656640	1.25		655.0	731.0	692.8	666.8	718.9
6	90	1311840	2.5		660.3	744.8	702.5	670.9	734.2
6	90	2629440	5.0	721	667.1	762.0	714.5	676.2	752.8
6	90	5260320	10.0		675.2	782.8	729.0	683.1	774.9
6	90	10519200	20.0		685.2	807.6	746.4	691.9	800.8
6	90	21038400	40.0		697.3	836.3	766.8	703.2	830.5
5.6	100	318000	0.6	NP			599.6	565.9	633.3
5.6	100	1052400	2.0		556.7	693.6	625.1	578.8	671.5
5.6	100	3153600	6.0		587.8	726.3	657.0	596.5	717.6
5.6	200	318000	0.6	NP			1034.2	995.9	1072.5
5.6	200	1052400	2.0	NP			1081.5	1045.8	1117.2
5.6	200	3153600	6.0	NP			1115.0	1083.5	1146.5
5.6	300	318000	0.6	NP			1177.8	1165.8	1189.8
5.6	300	1052400	2.0	NP			1185.4	1176.4	1194.3
5.6	300	3153600	6.0	NP			1190.0	1183.3	1196.8
7.7	100	318000	0.6	679	589.6	746.9	668.2	616.6	719.9
7.7	100	1052400	2.0		619.7	790.2	704.9	643.7	766.2
7.7	100	3153600	6.0		662.3	824.9	743.6	672.6	814.6
7.7	200	318000	0.6	1102	1001.2	1152.4	1076.8	1030.0	1123.7
7.7	200	1052400	2.0		1050.0	1206.1	1128.0	1077.4	1178.7
7.7	200	3153600	6.0		1091.6	1249.9	1170.7	1118.4	1223.1
7.7	300	318000	0.6	NP			1286.4	1253.3	1319.5
7.7	300	1052400	2.0	NP			1309.7	1279.1	1340.3
7.7	300	3153600	6.0	NP			1327.2	1299.4	1355.1

**Table 4.12. Experimentally Measured and Predicted Mean UTS Values for Various U-Nb Alloys for Current and Future Model Validation. The 95% prediction and confidence intervals are also given. The alloy identified as 6 wt% Nb is the RFP banded U-6Nb; the alloys identified as 5.6 wt% and 7.7 wt% are nonbanded. “NP” indicates that no data point is expected, because of material limitations.**

Alloy Wt.% Nb	Aging Temp. (C)	Aging Time		Ultimate Tensile Strength (MPa)					
		(min.)	(years)	Experimental Mean	Prediction Interval		Prediction Mean	Confidence Interval	
					Lower	Upper		Lower	Upper
6	40	328320	0.625		818.7	852.8	818.8	818.7	819.2
6	40	656640	1.25		818.7	852.9	818.9	818.7	819.3
6	40	1311840	2.5		818.7	852.9	818.9	818.7	819.4
6	40	2629440	5.0	823	818.7	853.0	819.0	818.7	819.6
6	40	5260320	10.0		818.7	853.1	819.0	818.7	819.9
6	40	10519200	20.0		818.7	853.2	819.1	818.7	820.2
6	40	21038400	40.0		818.7	853.3	819.3	818.7	820.7
6	65	328320	0.625		818.7	853.5	819.4	818.7	821.1
6	65	656640	1.25		818.7	853.7	819.7	818.7	821.7
6	65	1311840	2.5		818.7	854.1	819.9	818.7	822.5
6	65	2629440	5.0	829	818.7	854.5	820.3	818.7	823.6
6	65	5260320	10.0		818.7	855.0	820.8	818.7	824.9
6	65	10519200	20.0		818.7	855.8	821.4	818.7	826.6
6	65	21038400	40.0		818.7	856.8	822.2	818.7	828.8
6	90	328320	0.625		818.7	856.8	822.3	818.7	828.2
6	90	656640	1.25		818.7	858.1	823.3	818.7	830.8
6	90	1311840	2.5		818.7	859.9	824.6	818.7	834.0
6	90	2629440	5.0	829	818.7	862.3	826.3	818.7	838.1
6	90	5260320	10.0		818.7	865.6	828.5	818.7	843.2
6	90	10519200	20.0		818.7	870.0	831.3	818.7	849.7
6	90	21038400	40.0		818.7	875.9	834.9	818.7	857.8
5.6	100	318000	0.6	NP			798.6	792.0	808.5
5.6	100	1052400	2.0		792.0	858.7	802.2	792.0	816.6
5.6	100	3153600	6.0		792.0	848.9	807.2	792.0	827.5
5.6	200	318000	0.6	NP			1023.2	971.2	1075.2
5.6	200	1052400	2.0	NP			1065.8	1009.6	1122.0
5.6	200	3153600	6.0	NP			1099.7	1044.1	1155.2
5.6	300	318000	0.6	NP			1182.7	1164.5	1200.9
5.6	300	1052400	2.0	NP			1188.7	1175.1	1202.3
5.6	300	3153600	6.0	NP			1192.4	1182.2	1202.6
7.7	100	318000	0.6	759	699.0	746.7	708.3	702.2	714.4
7.7	100	1052400	2.0		699.0	751.7	712.8	704.1	721.5
7.7	100	3153600	6.0		699.0	746.6	718.7	706.7	730.7
7.7	200	318000	0.6	1103	1004.2	1111.9	1058.1	1019.8	1096.3
7.7	200	1052400	2.0		1069.7	1183.0	1126.3	1084.2	1168.5
7.7	200	3153600	6.0		1126.6	1241.7	1184.1	1140.8	1227.4
7.7	300	318000	0.6	NP			1362.9	1348.7	1377.1
7.7	300	1052400	2.0	NP			1374.6	1363.5	1385.8
7.7	300	3153600	6.0	NP			1382.2	1373.4	1390.9

**Table 4.13. Experimentally Measured and Predicted Mean HV Values for Various U-Nb Alloys for Current and Future Model Validation. The 95% prediction and confidence intervals are also given. The alloy identified as 6 wt% Nb is the RFP banded U-6Nb; the alloys identified as 5.6 wt% and 7.7 wt% are nonbanded. “NP” indicates that no data point is expected, because of material limitations.**

Alloy Wt.% Nb	Aging Temp. (C)	Aging Time		Vickers Microhardness					
		(min.)	(years)	Experimental	Prediction Int.		Prediction	Confidence Int.	
				Mean	lower	upper	Mean	lower	upper
6	40	328320	0.625		166.7	208.7	173.9	168.7	179.0
6	40	656640	1.25		166.7	210.3	175.3	169.2	181.4
6	40	1311840	2.5		166.7	212.2	177.0	169.8	184.3
6	40	2629440	5.0	171	166.7	214.6	179.1	170.5	187.7
6	40	5260320	10.0		166.7	217.4	181.5	171.3	191.7
6	40	10519200	20.0		166.7	220.9	184.4	172.2	196.5
6	40	21038400	40.0		166.7	225.1	187.8	173.4	202.2
6	65	328320	0.625		166.7	219.3	183.6	174.0	193.2
6	65	656640	1.25		166.7	223.1	186.9	175.6	198.2
6	65	1311840	2.5		166.7	227.6	190.7	177.4	204.0
6	65	2629440	5.0	182	166.7	233.1	195.3	179.6	210.9
6	65	5260320	10.0		166.7	239.7	200.6	182.2	219.0
6	65	10519200	20.0		166.7	247.5	206.9	185.3	228.4
6	65	21038400	40.0		171.5	256.8	214.1	189.0	239.3
6	90	328320	0.625		163.6	238.7	201.2	186.1	216.3
6	90	656640	1.25		168.8	246.1	207.5	189.9	225.1
6	90	1311840	2.5		174.8	254.9	214.8	194.4	235.3
6	90	2629440	5.0	201	181.6	265.2	223.4	199.6	247.1
6	90	5260320	10.0		189.1	277.1	233.1	205.7	260.5
6	90	10519200	20.0		197.5	290.8	244.2	212.7	275.6
6	90	21038400	40.0		206.9	306.3	256.6	220.8	292.4
5.6	100	318000	0.6	189	157.5	228.6	193.1	175.1	211.0
5.6	100	1052400	2.0		169.6	246.3	208.0	184.8	231.1
5.6	100	3153600	6.0		183.0	267.2	225.1	196.2	253.9
5.6	200	318000	0.6	367	325.1	404.0	364.6	339.7	389.5
5.6	200	1052400	2.0		358.3	442.8	400.5	371.5	429.6
5.6	200	3153600	6.0		388.3	476.5	432.4	400.7	464.1
5.6	300	318000	0.6	530	464.0	540.4	502.2	479.4	525.1
5.6	300	1052400	2.0		487.0	562.0	524.5	502.8	546.1
5.6	300	3153600	6.0		504.6	577.7	541.1	521.3	561.0
7.7	100	318000	0.6	191	123.9	276.4	200.2	157.8	242.5
7.7	100	1052400	2.0		138.2	299.7	218.9	169.0	268.9
7.7	100	3153600	6.0		152.8	324.5	238.6	180.8	296.5
7.7	200	318000	0.6	321	256.1	405.6	330.8	291.3	370.4
7.7	200	1052400	2.0		281.4	440.1	360.7	313.0	408.4
7.7	200	3153600	6.0		304.5	471.6	388.1	333.7	442.5
7.7	300	318000	0.6	527	350.5	515.2	432.9	380.3	485.4
7.7	300	1052400	2.0		375.1	542.6	458.8	404.1	513.6
7.7	300	3153600	6.0		396.4	564.4	480.4	425.4	535.5

**Table 4.14. Lifetime Predictions for U-5.6Nb.**

Aging Temperature (°C)	Lifetime (years)		
	Predicted Value	95% Confidence Interval	
		Lower Bound	Upper Bound
20	2,117,408	41,783	$3.2 \times 10^8$
25	851,245	18,296	$1.2 \times 10^8$
30	352,667	8,255	$4.4 \times 10^7$
35	150,344	3,832	$1.7 \times 10^7$
40	65,862	1,828	$6.7 \times 10^6$
45	29,611	895	$2.7 \times 10^6$
50	13,646	449	$1.1 \times 10^6$
55	6,439	231	$4.9 \times 10^5$
60	3,108	121	$2.1 \times 10^5$

**Table 4.15. Lifetime Predictions for U-7.7Nb.**

Aging Temperature (°C)	Lifetime (years)		
	Predicted Value	95% Confidence Interval	
		Lower Bound	Upper Bound
20	26,714,967	243,514	$3.3 \times 10^{10}$
25	8,635,443	89,812	$9.3 \times 10^9$
30	2,897,308	34,194	$2.7 \times 10^9$
35	1,007,151	13,413	$7.9 \times 10^8$
40	362,122	5,466	$2.4 \times 10^8$
45	134,454	2,298	$7.7 \times 10^7$
50	51,156	996	$2.5 \times 10^7$
55	20,293	444	$8.4 \times 10^6$
60	8,227	203	$2.9 \times 10^6$

**Table 4.16. Threshold of Fractional and Absolute Property Changes, and Associated Aging Times at 40°C where a Statistically Significant Aging Response is Expected to be Experimentally Observable in Banded U-6Nb. The lower and upper bounds of aging time are prediction intervals.**

Property	Threshold of change		Time at 40C to realize change					
			years, except where bolded			log(time in minutes)		
	f	ΔP	Lower Bound	Mean	Upper Bound	Lower Bound	Mean	Upper Bound
TE	0.1610	-6.31	163	3,880	1,810,000	7.934	9.309	11.977
UE	0.0420	-1.00	20	326	940,000	7.029	8.234	11.694
1YS	0.0078	8.1	<b>8 day</b>	<b>40 day</b>	50	4.035	4.765	7.416
1YS*	0.0410	42.7	<b>251 day</b>	3	196	5.5584	6.2460	8.0138
1YM	0.1286	8573	<b>1 day</b>	<b>27 day</b>	41	3.229	4.594	7.337
2YS	0.0171	9.3	5	41	49,600	6.381	7.331	10.416
UTS	0.0160	6.1	972	25,200	5,420,000,000	8.708	10.122	15.455
HV	0.0540	23.4	8	60	4,240	6.606	7.502	9.348

\* Threshold set to reach 200 MPa; see Section 4.1.3 for details.

**Table 4.17. Threshold of Fractional and Absolute Property Changes, and Associated Aging Times at 40°C where a Statistically Significant Aging Response is Expected to be Experimentally Observable in Nonbanded U-5.6Nb. The lower and upper bounds of aging time are prediction intervals.**

Property	Threshold of change		Time at 40C to realize change					
			years, except where bolded			log(time in minutes)		
	f	ΔP	Lower Bound	Mean	Upper Bound	Lower Bound	Mean	Upper Bound
TE	0.4182	-10.84	2,310	90,100	8,160,000	9.085	10.675	12.632
UE	0.2433	-5.63	1,260	24,600	2,840,000	8.820	10.112	12.174
1YS	0.0299	32.1	<b>129 day</b>	2	143	5.268	5.961	7.876
1YM	0.2231	15062	<b>9 day</b>	<b>199 day</b>	120	4.093	5.457	7.801
2YS	0.1310	85.8	1,910	17,000	1,180,000	9.003	9.950	11.792
UTS	0.2527	103.1	2,630,000	89,000,000	29,800,000,000	12.141	13.670	16.195
HV	0.0393	17.8	2	17	1,280	6.063	6.959	8.829

**Table 4.18. Threshold of Fractional and Absolute Property Changes, and Associated Aging Times at 40°C where a Statistically Significant Aging Response is Expected to be Experimentally Observable in Nonbanded U-7.7Nb. The lower and upper bounds of aging time are prediction intervals.**

Property	Threshold of change		Time at 40C to realize change					
			years, except where bolded			log(time in minutes)		
	f	ΔP	Lower Bound	Mean	Upper Bound	Lower Bound	Mean	Upper Bound
TE	0.2628	-10.25	1,890	99,200	114,000,000	8.997	10.717	13.779
UE	0.0687	-1.95	813,000	22,100,000	103,000,000,000	11.631	13.065	16.732
1YS	0.0256	33.3	<b>1 day</b>	<b>6 day</b>	3	2.971	3.928	6.246
1YM	0.1476	7972	<b>38 day</b>	<b>286 day</b>	26	4.737	5.614	7.142
2YS	0.0438	39.0	<b>91 day</b>	3	277	5.116	6.175	8.163
UTS	0.0418	29.3	371,000	3,100,000	1,060,000,000	11.290	12.212	14.744
HV	0.0149	7.2	<b>5 min</b>	<b>5 hr</b>	37	0.659	2.479	7.292

**Table 4.19. Notional Tensile Property Equivalency Table that Would Result from a Future Systematic Study of the Effects of Tensile Geometry and Machining Damage. Values for the zero artificial age condition are provided from the data made available in this report; such tables could also be generated for several representative artificial ages where the properties differ considerably from the zero age condition.**

Material Pedigree	Machining Damage Condition	Tensile Geometry	1YS slope		1YS stress		2YS stress	
			Value	StDev	Value	StDev	Value	StDev
Banded RFP U-6Nb	MA	Fig. 2.1						
Banded RFP U-6Nb	AM	Fig. 2.1						
Banded RFP U-6Nb	MA	Fig. 2.2						
Banded RFP U-6Nb	AM	Fig. 2.2	53333	5774	157.3	4.7	655.0	4.4
Banded RFP U-6Nb	MA	Alternate #1						
Banded RFP U-6Nb	AM	Alternate #1						
Nonbanded U-5.6Nb	MA	Fig. 2.1	63800	17254	125.4	16.4	545.2	46.8
Nonbanded U-5.6Nb	AM	Fig. 2.1						
Nonbanded U-5.6Nb	MA	Fig. 2.2						
Nonbanded U-5.6Nb	AM	Fig. 2.2						
Nonbanded U-5.6Nb	MA	Alternate #1						
Nonbanded U-5.6Nb	AM	Alternate #1						

Material Pedigree	Machining Damage Condition	Tensile Geometry	UTS stress		Plastic Elongation			
			Value	StDev	Uniform		Total	
					Value	StDev	Value	StDev
Banded RFP U-6Nb	MA	Fig. 2.1						
Banded RFP U-6Nb	AM	Fig. 2.1						
Banded RFP U-6Nb	MA	Fig. 2.2						
Banded RFP U-6Nb	AM	Fig. 2.2	818.7	2.5	0.2382	0.0062	0.3920	0.0424
Banded RFP U-6Nb	MA	Alternate #1						
Banded RFP U-6Nb	AM	Alternate #1						
Nonbanded U-5.6Nb	MA	Fig. 2.1	792.0	62.1	0.2006	0.0114	0.0111	0.0089
Nonbanded U-5.6Nb	AM	Fig. 2.1						
Nonbanded U-5.6Nb	MA	Fig. 2.2						
Nonbanded U-5.6Nb	AM	Fig. 2.2						
Nonbanded U-5.6Nb	MA	Alternate #1						
Nonbanded U-5.6Nb	AM	Alternate #1						

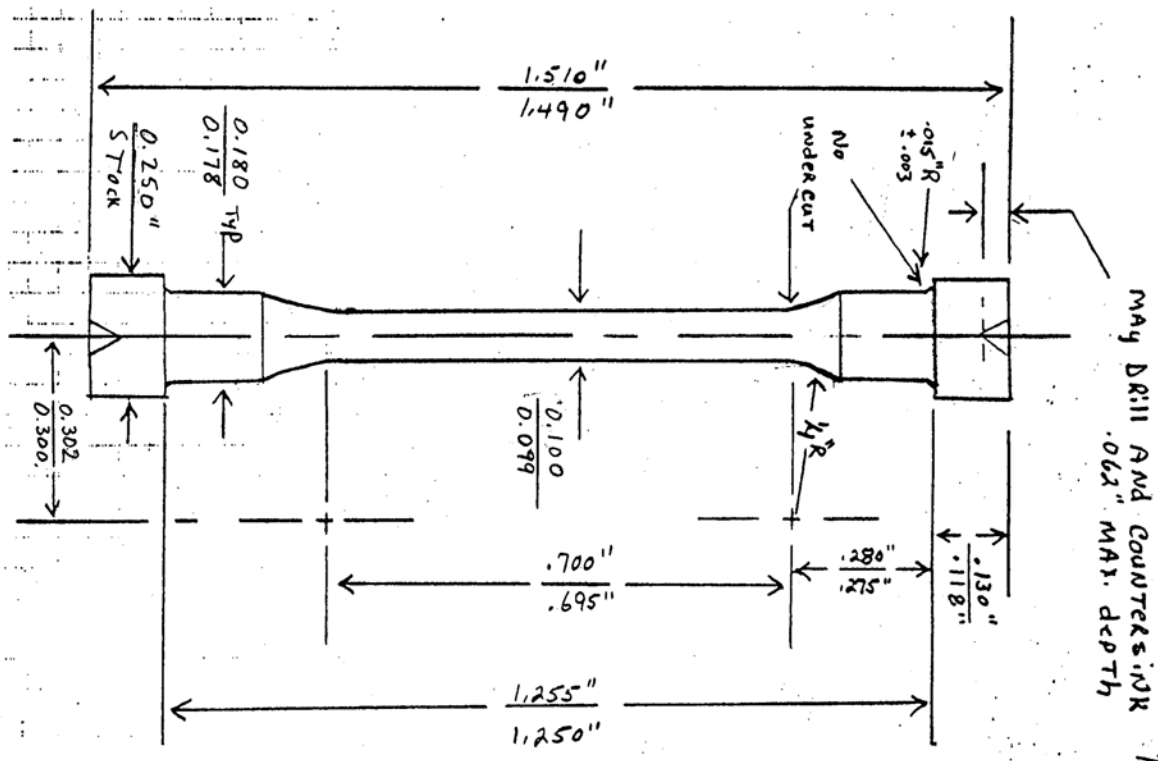


Figure 2.1. Cylindrical tensile specimen geometry used for the nonbanded U-5.6Nb and U-7.7Nb studies for both model fitting and for validation. Dimensions are in inches.

1 inch round button head tensile sample

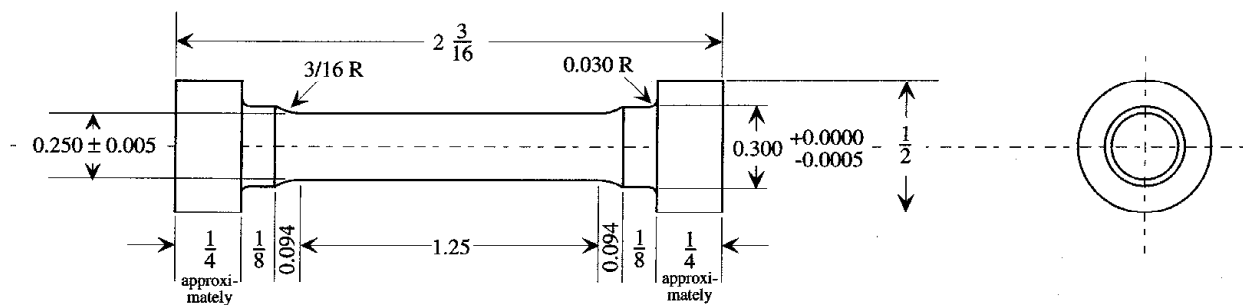


Figure 2.2. Cylindrical tensile specimen geometry used for the banded U-6Nb validation experiments. Dimensions are in inches.

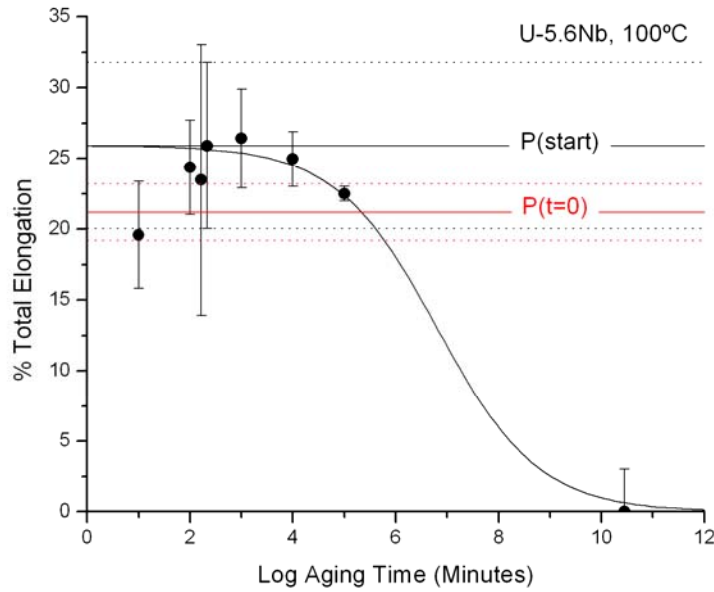


Figure 3.1. Total elongation at 100°C for U-5.6Nb. The black and red dotted lines indicate  $\pm 1$  standard deviation about the mean values (solid lines) of  $P(start)$  and  $P(t = 0)$ , respectively. A fictitious end-of-hardening (peak age) point has been added at  $x = 10.44$  to guide the Boltzmann fit in the previous study. All other solid points are data, with  $\pm 1$  standard deviation shown.

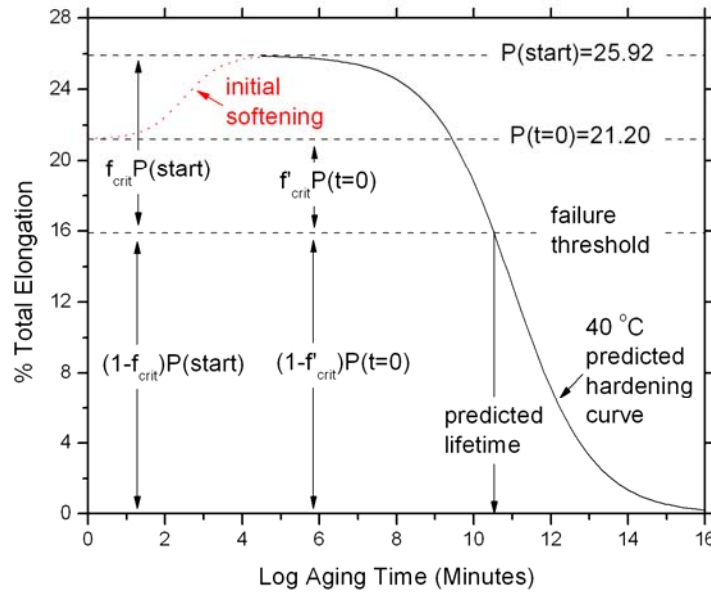


Figure 3.2. Predicted TE (solid curve) and lifetime at 40°C for U-5.6Nb (solid curve). The defining relationships between the failure threshold,  $P(start)$ ,  $P(t = 0)$ ,  $f_{crit}$  and  $f'_{crit}$  are graphically depicted. The differentiation between  $f_{crit}$  and  $f'_{crit}$  is due to the initial softening transient that is schematically depicted (red dotted curve). See the text for further details.

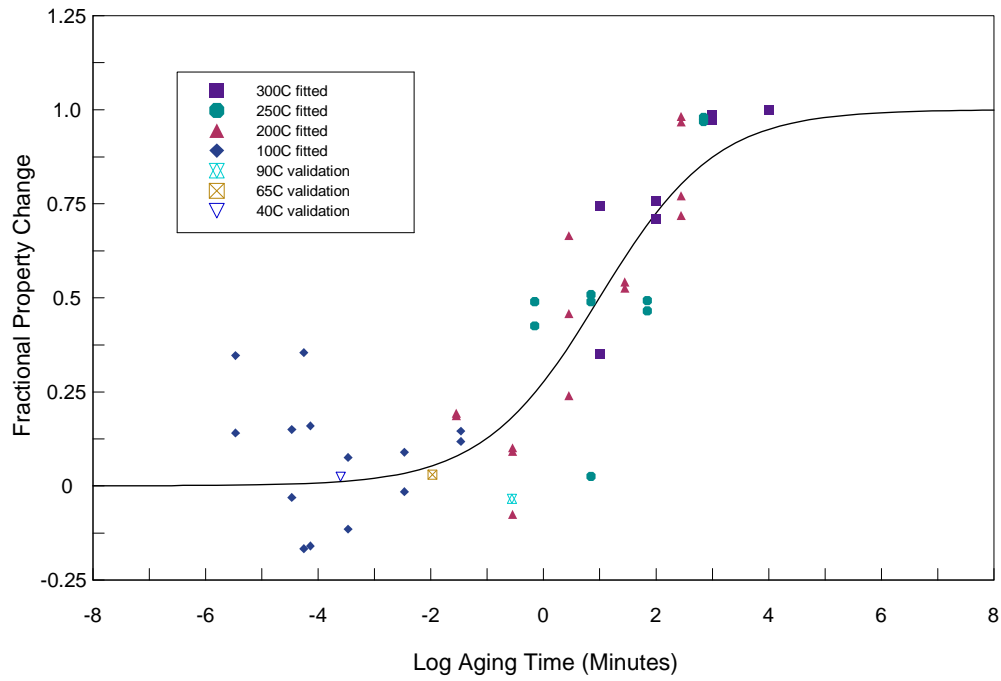


Figure 4.1. Universal plot of U-5.6Nb TE data (points) and model fit to data (solid line).

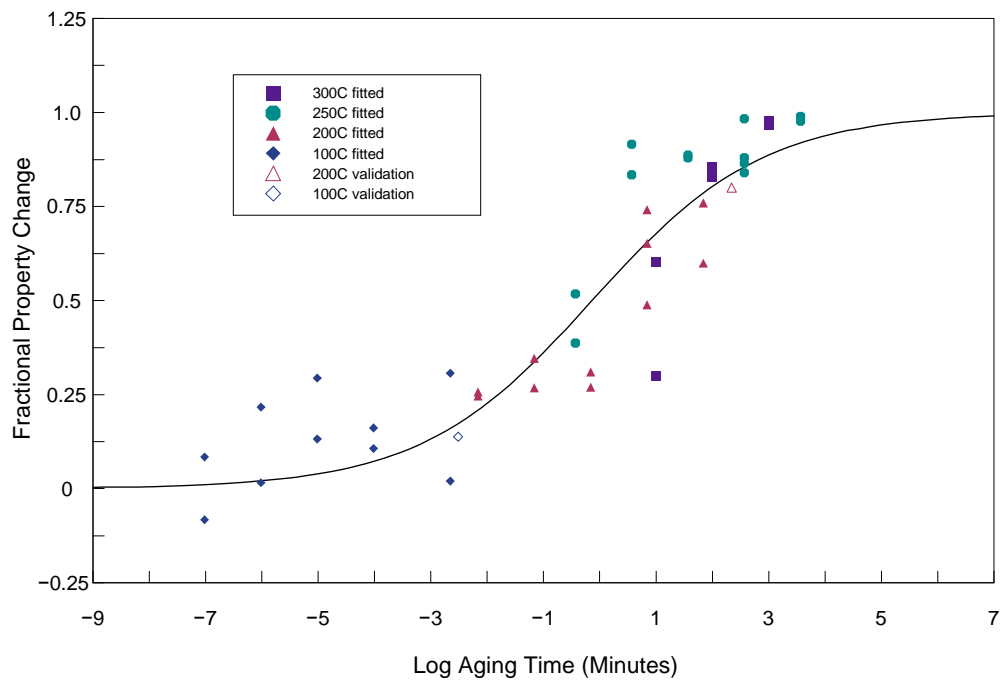


Figure 4.2. Universal plot of U-7.7Nb TE data (points) and model fit to data (solid line).

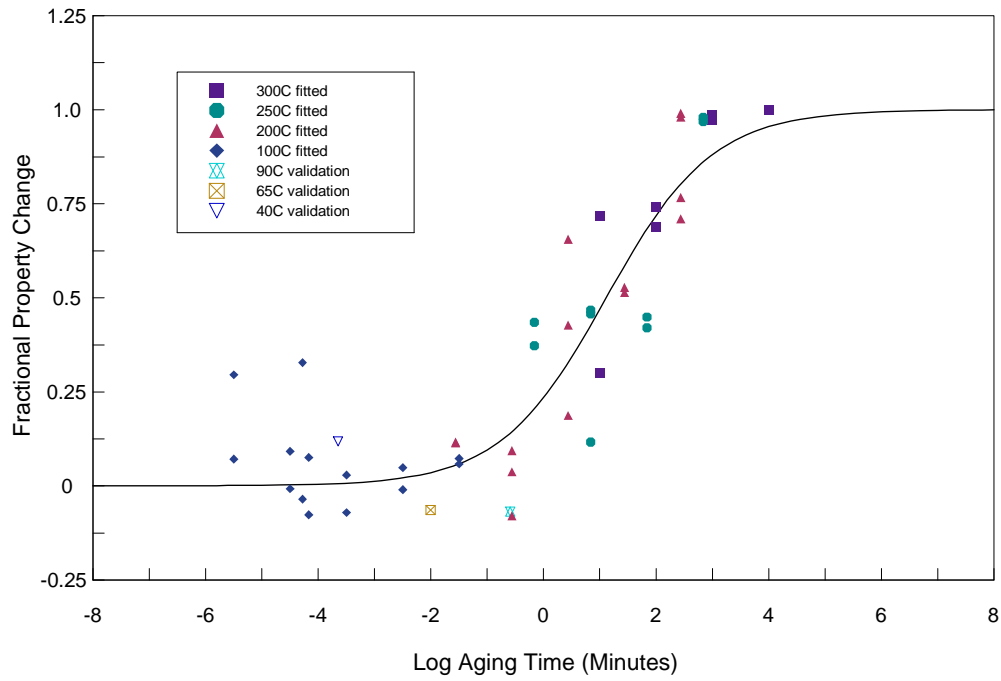


Figure 4.3. Universal plot of U-5.6Nb UE data (points) and model fit to data (solid line).

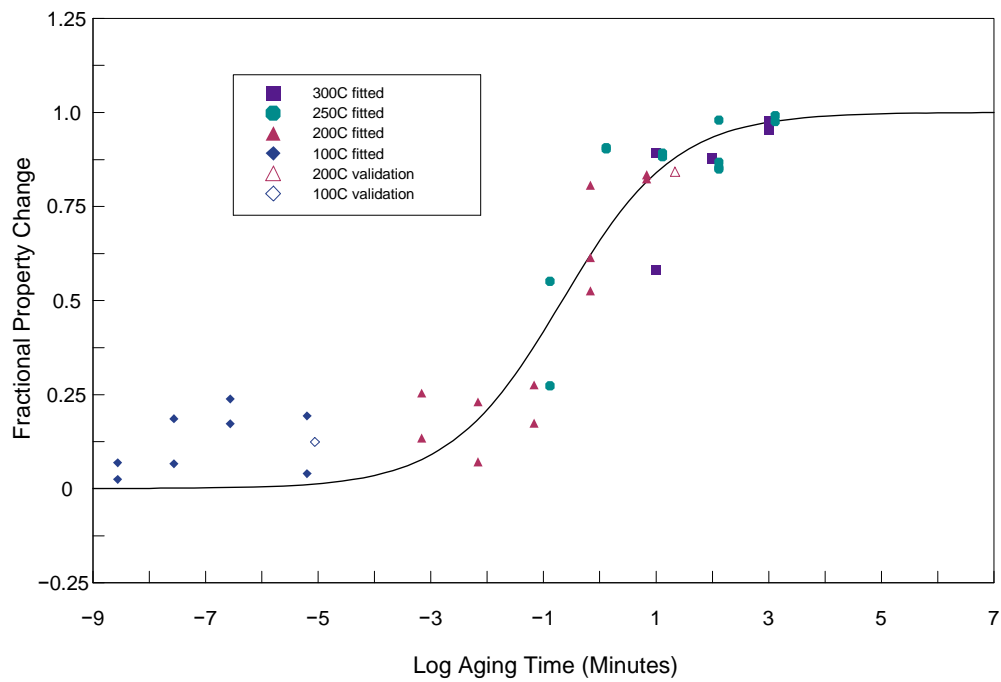


Figure 4.4. Universal plot of U-7.7Nb UE data (points) and model fit to data (solid line).

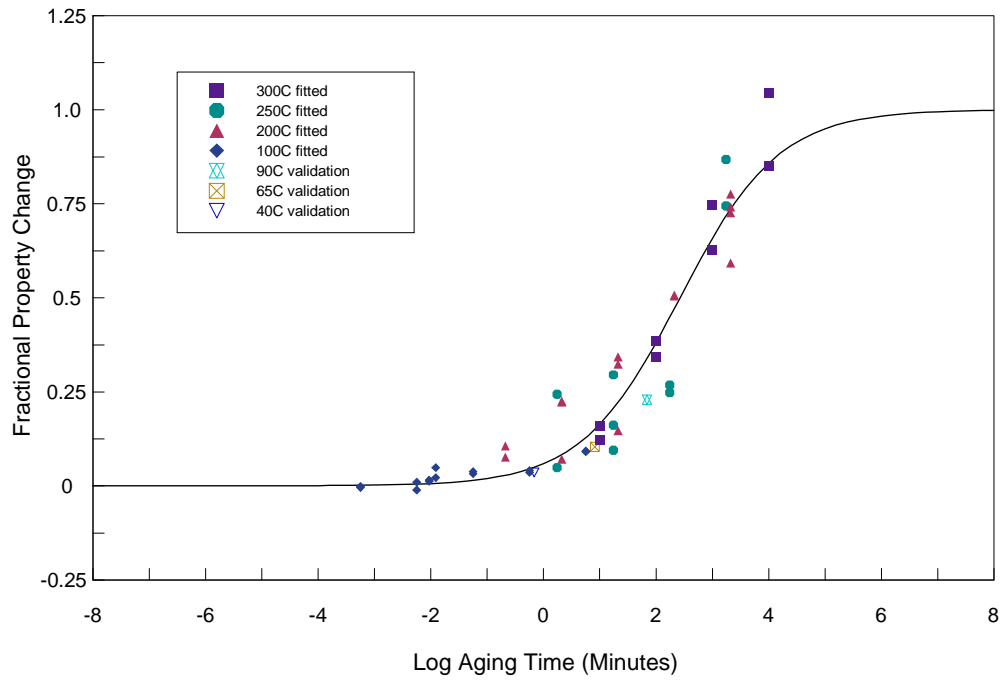


Figure 4.5. Universal plot of U-5.6Nb 1YS data (points) and model fit to data (solid line).

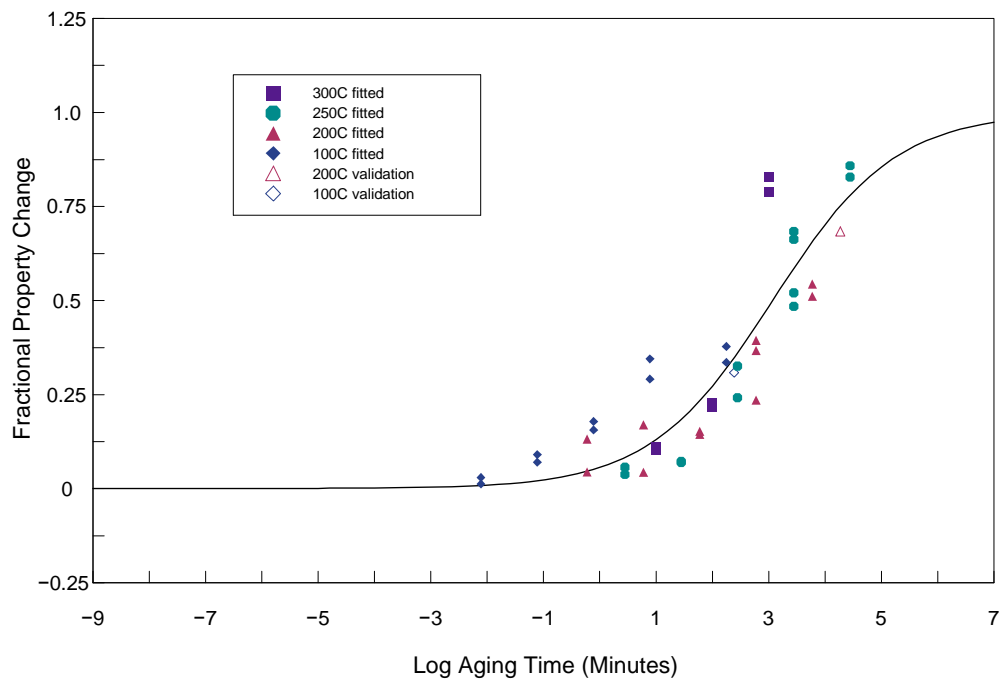


Figure 4.6. Universal plot of U-7.7Nb 1YS data (points) and model fit to data (solid line).

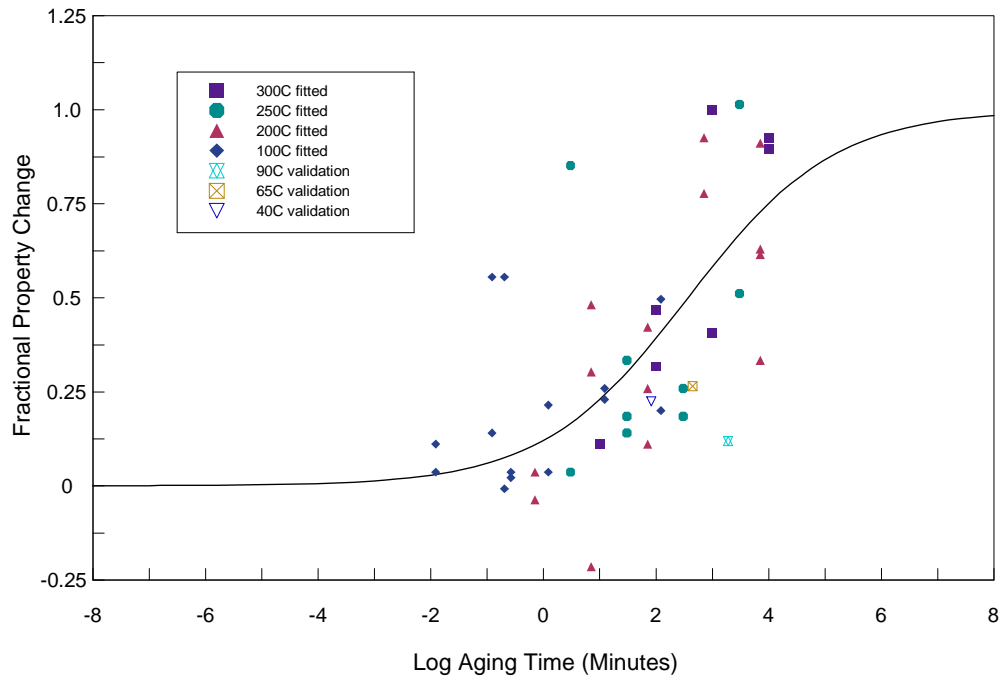


Figure 4.7. Universal plot of U-5.6Nb 1YM data (points) and model fit to data (solid line).

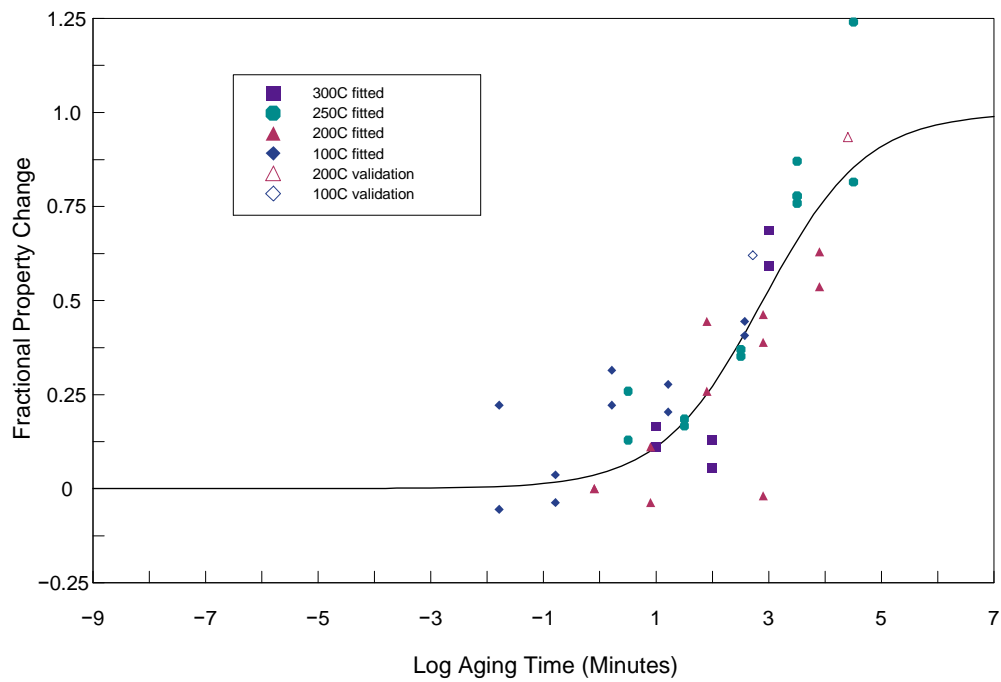


Figure 4.8. Universal plot of U-7.7Nb 1YM data (points) and model fit to data (solid line).

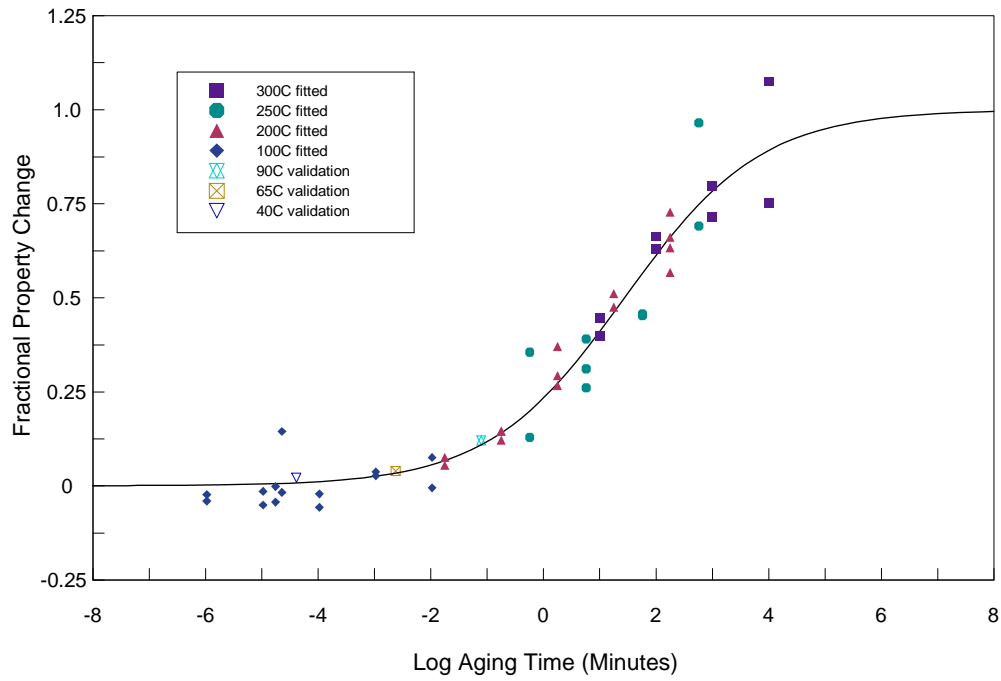


Figure 4.9. Universal plot of U-5.6Nb 2YS data (points) and model fit to data (solid line).

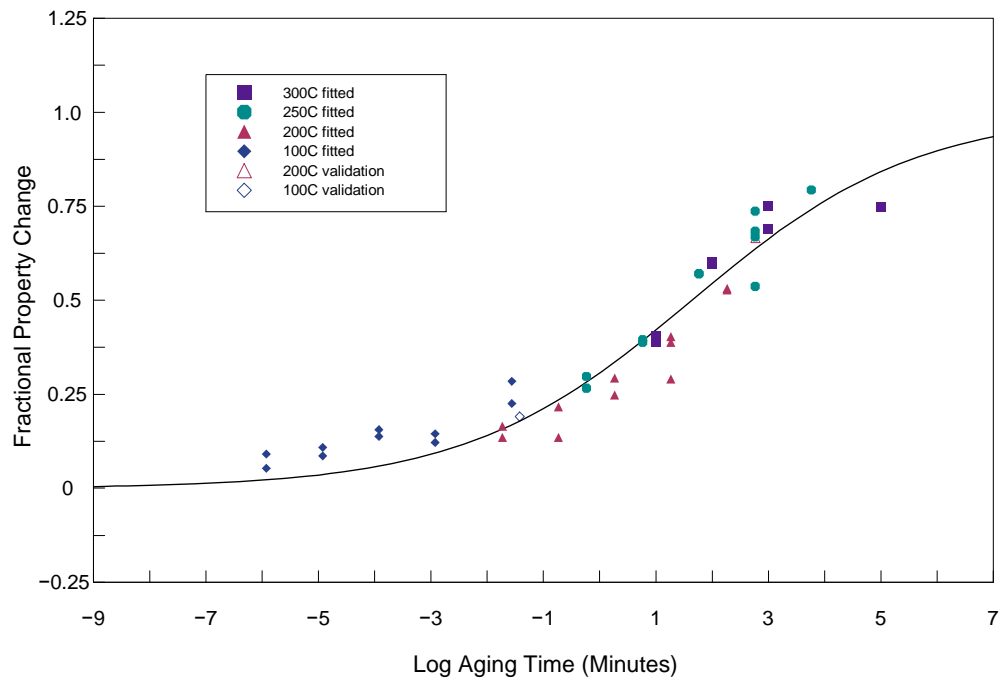


Figure 4.10. Universal plot of U-7.7Nb 2YS data (points) and model fit to data (solid line).

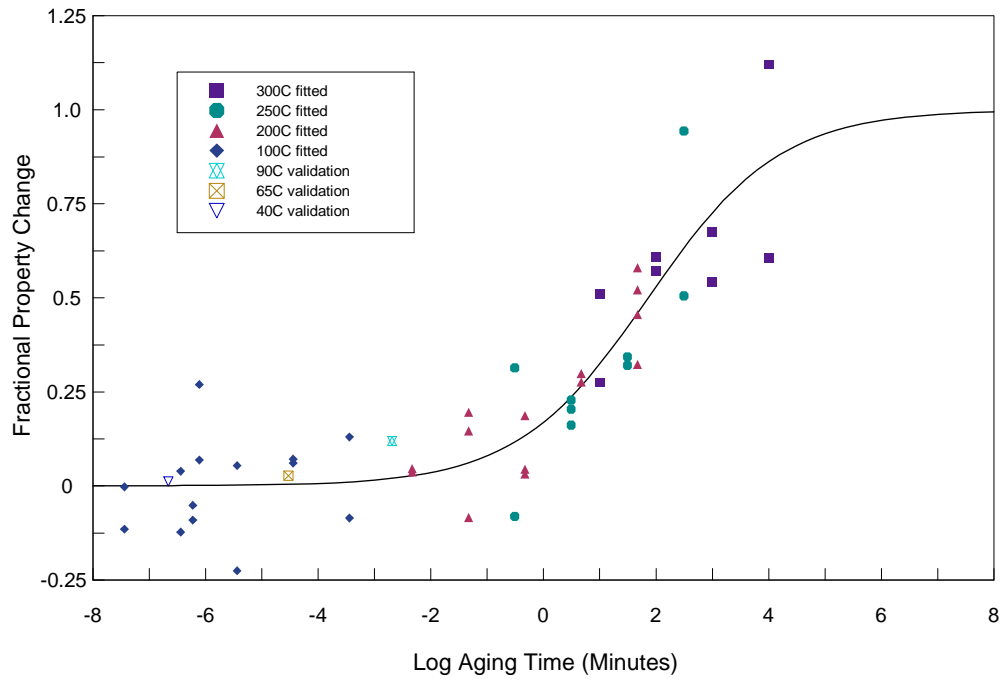


Figure 4.11. Universal plot of U-5.6Nb UTS data (points) and model fit to data (solid line).

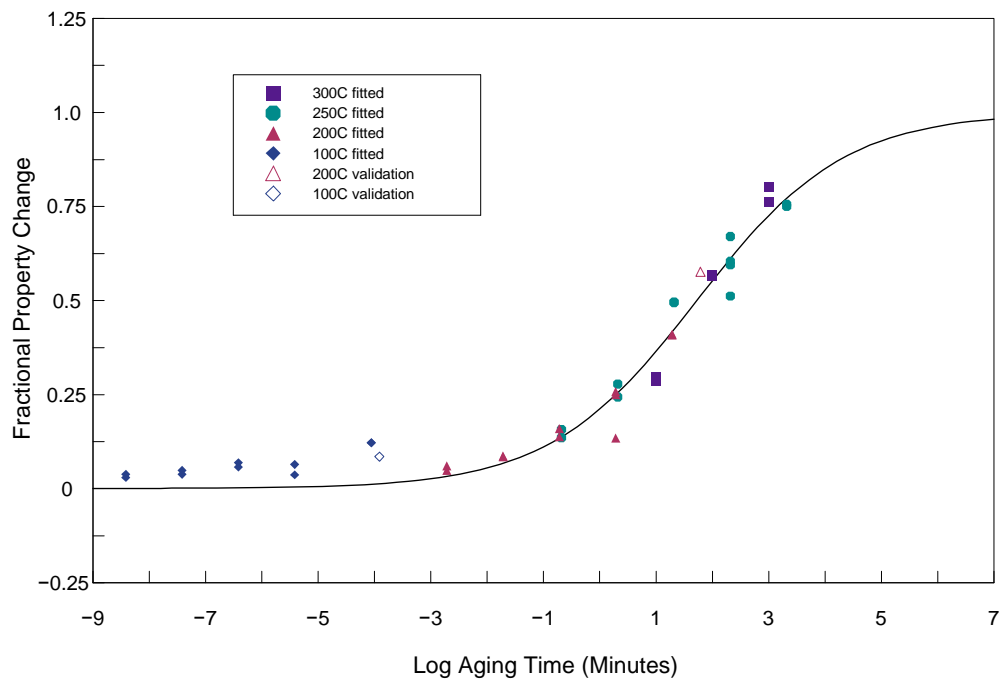


Figure 4.12. Universal plot of U-7.7Nb UTS data (points) and model fit to data (solid line).

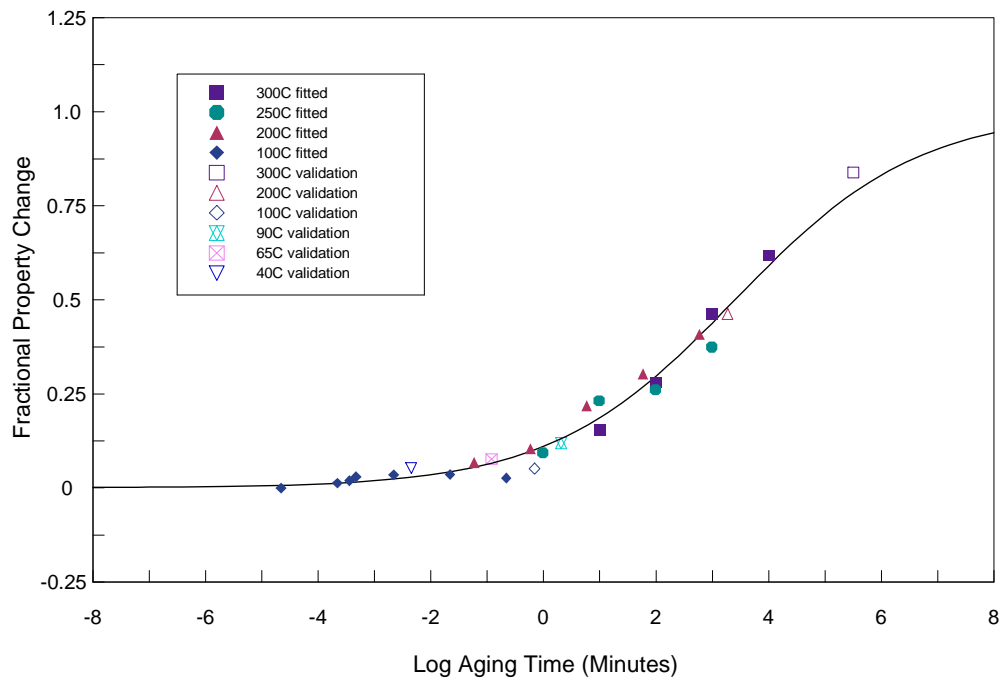


Figure 4.13. Universal plot of U-5.6Nb HV data (points) and model fit to data (solid line).

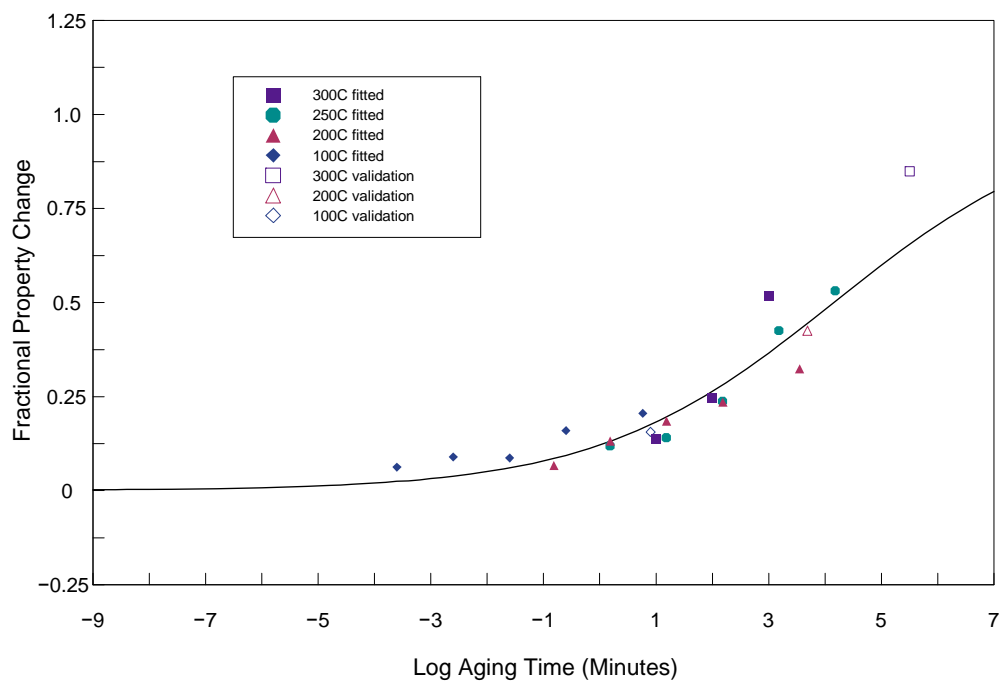


Figure 4.14. Universal plot of U-7.7Nb HV data (points) and model fit to data (solid line).

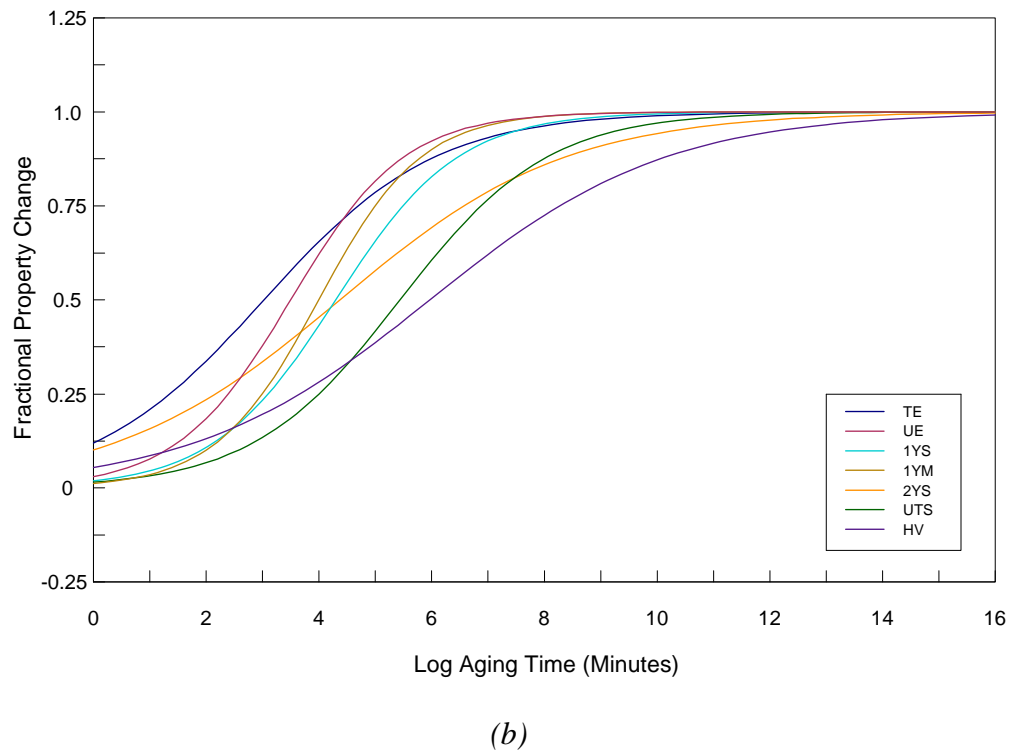
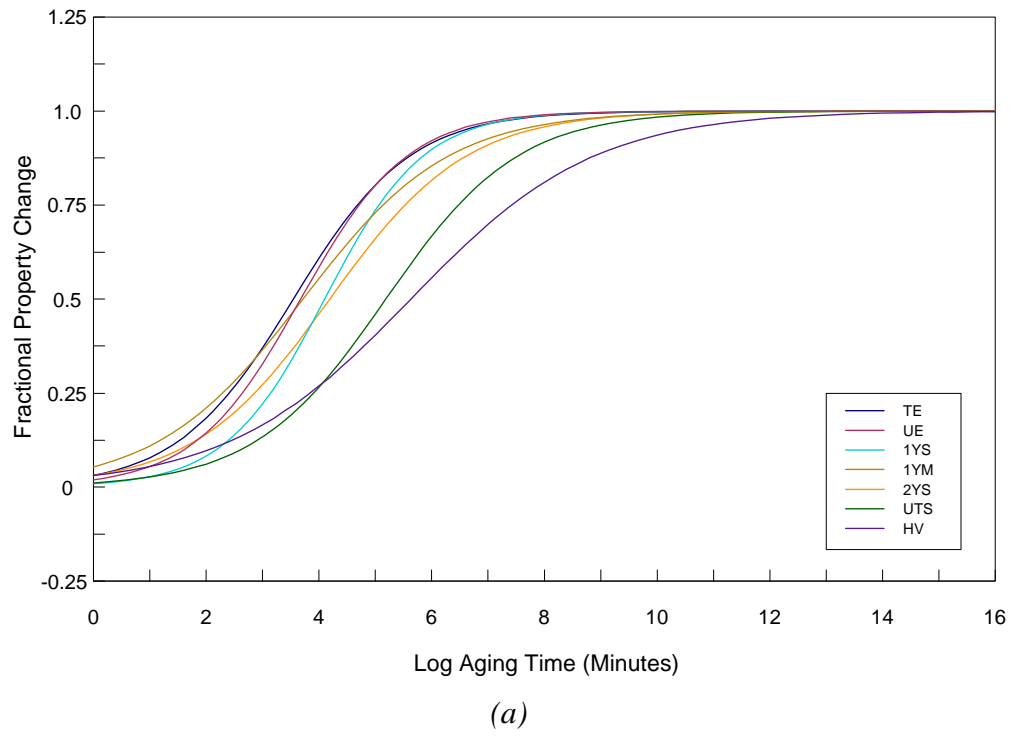


Figure 4.15. Consolidated aging response model fits at 200°C for (a) U-5.6Nb and (b) U-7.7Nb.

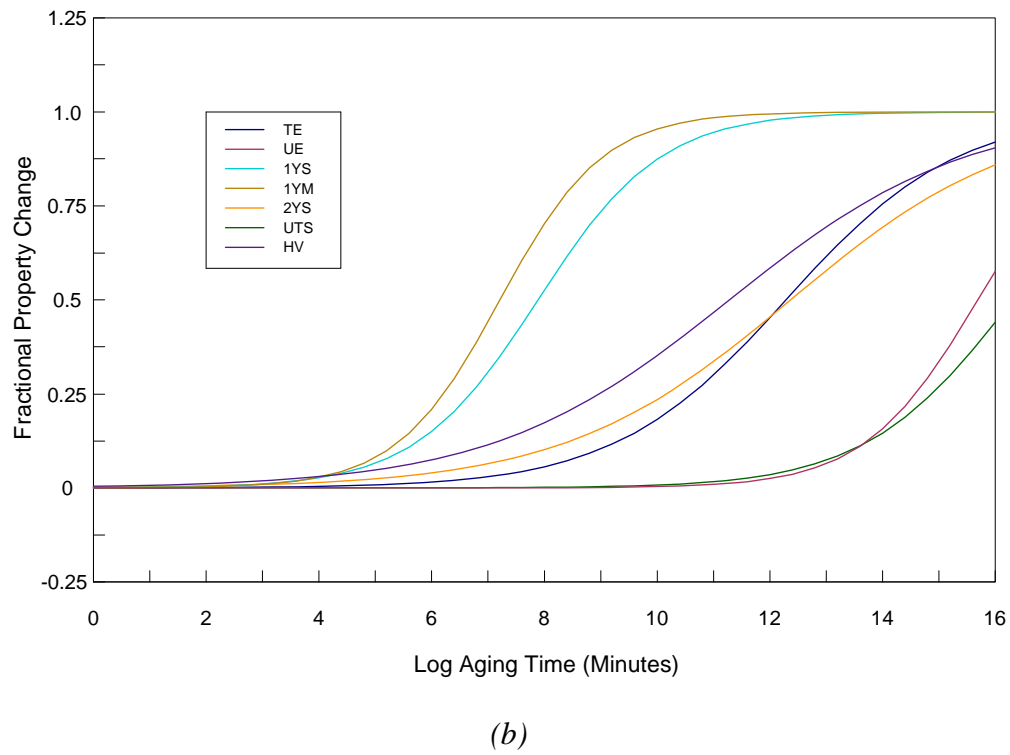
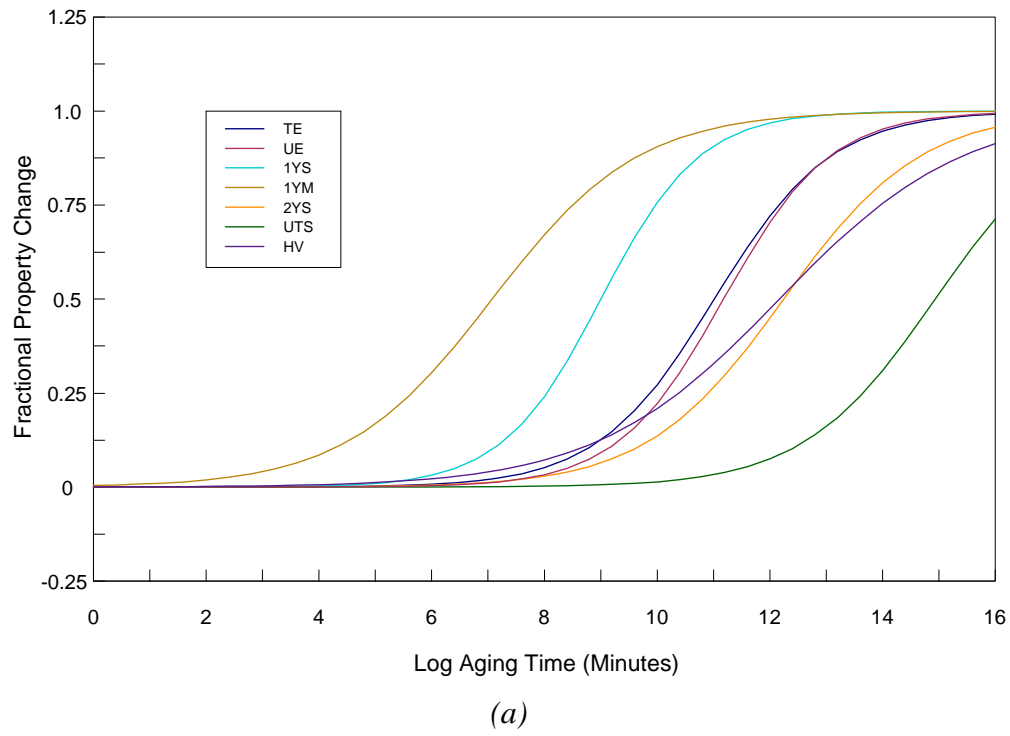


Figure 4.16. Consolidated aging response predictions at 40°C for (a) U-5.6Nb and (b) U-7.7Nb.

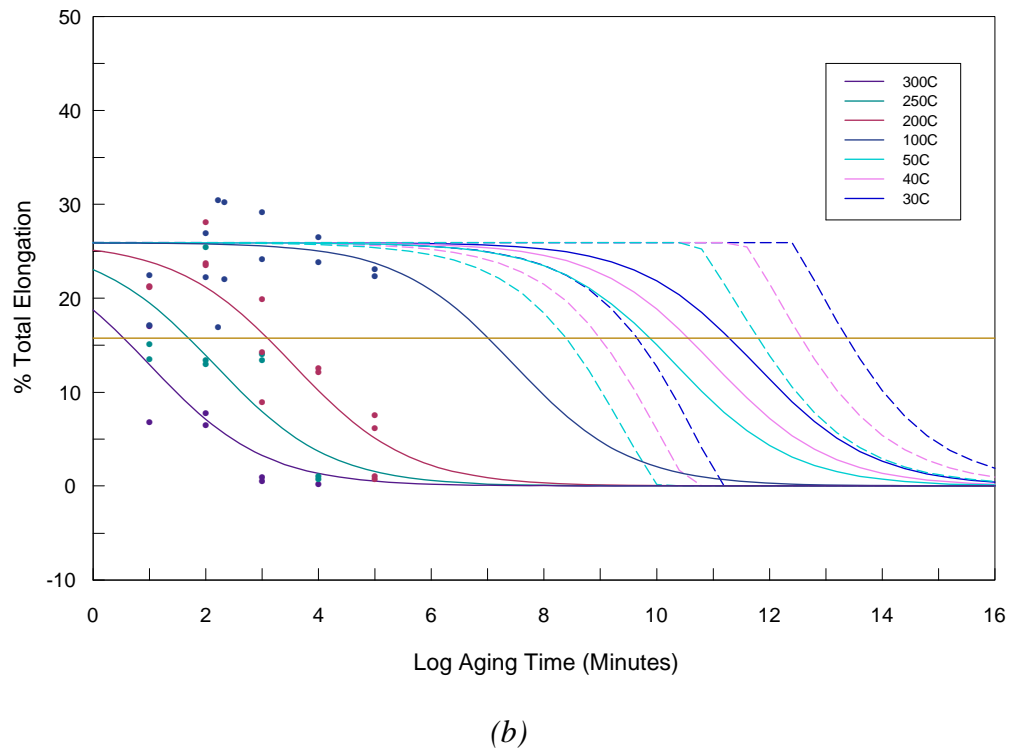
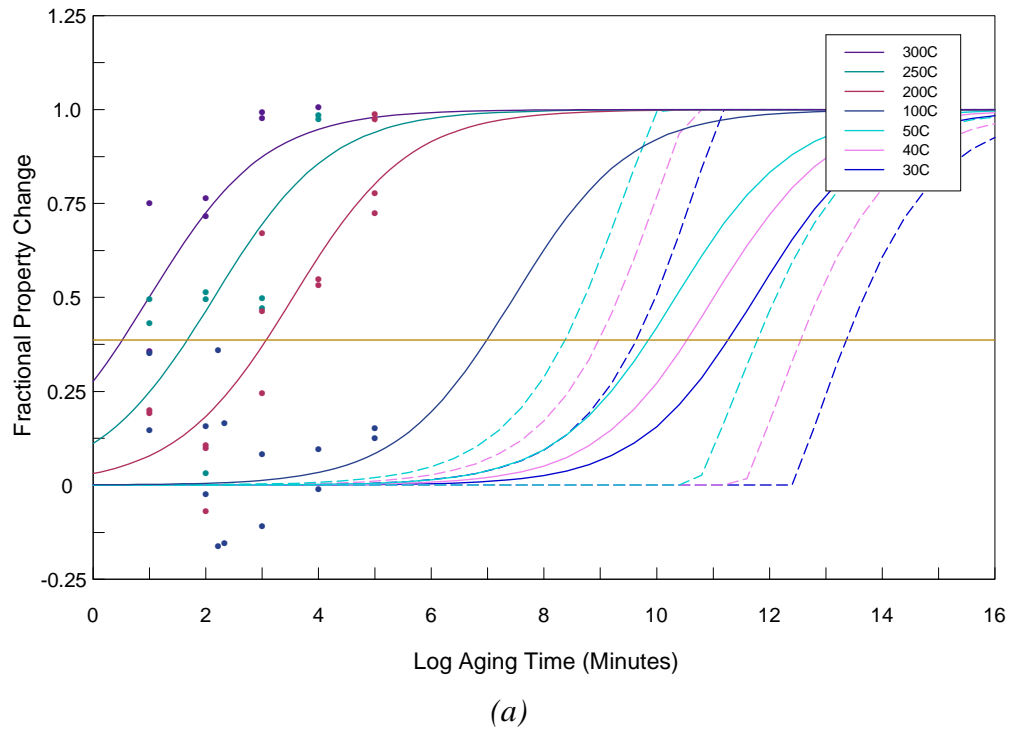
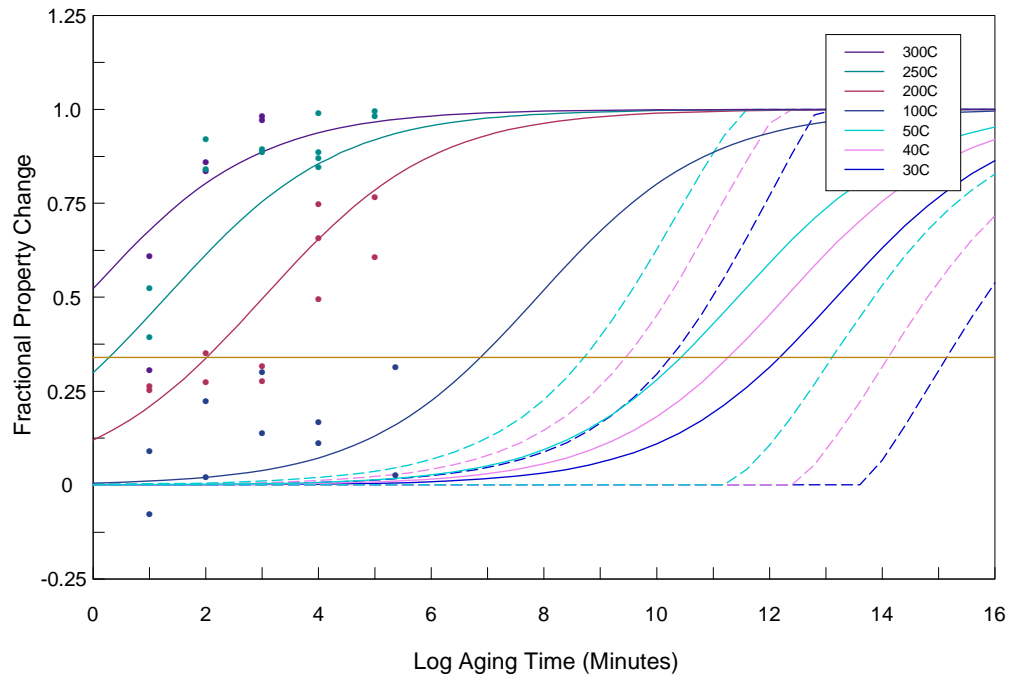
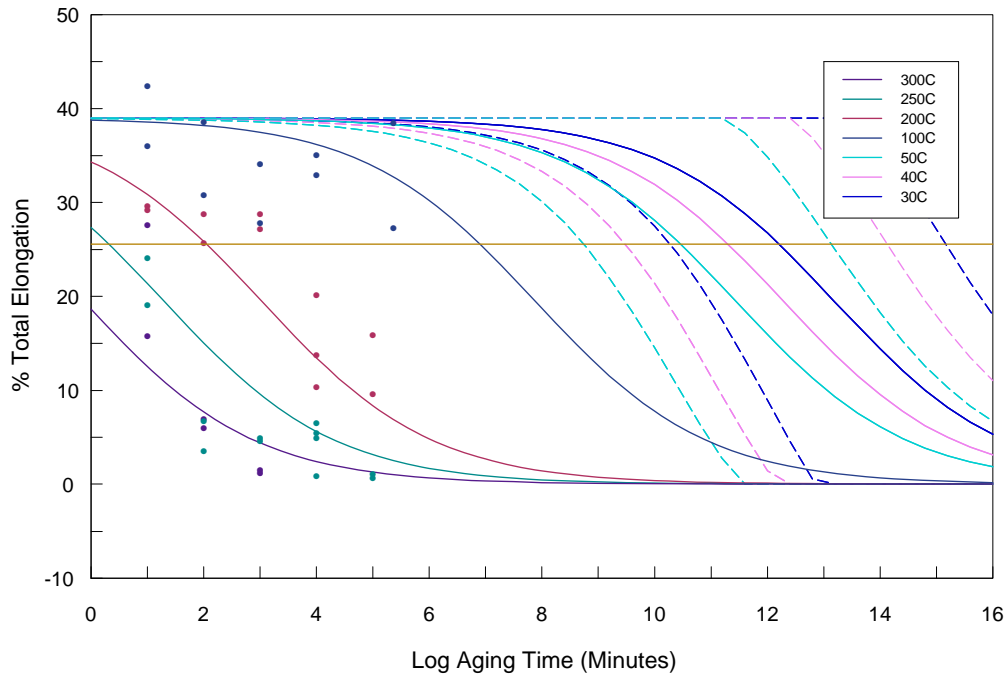


Figure 4.17. U-5.6Nb TE data (points), model fits to data (solid lines), and low-temperature model predictions (solid line—mean, dashed lines—95% confidence intervals). (a) in terms of  $f$ , (b) in terms of absolute property. The yellow line is the failure threshold.



(a)



(b)

Figure 4.18. U-7.7Nb TE data (points), model fits to data (solid lines), and low-temperature model predictions (solid line—mean, dashed lines—95% confidence intervals). (a) in terms of  $f$ , (b) in terms of absolute property. The yellow line is the failure threshold.

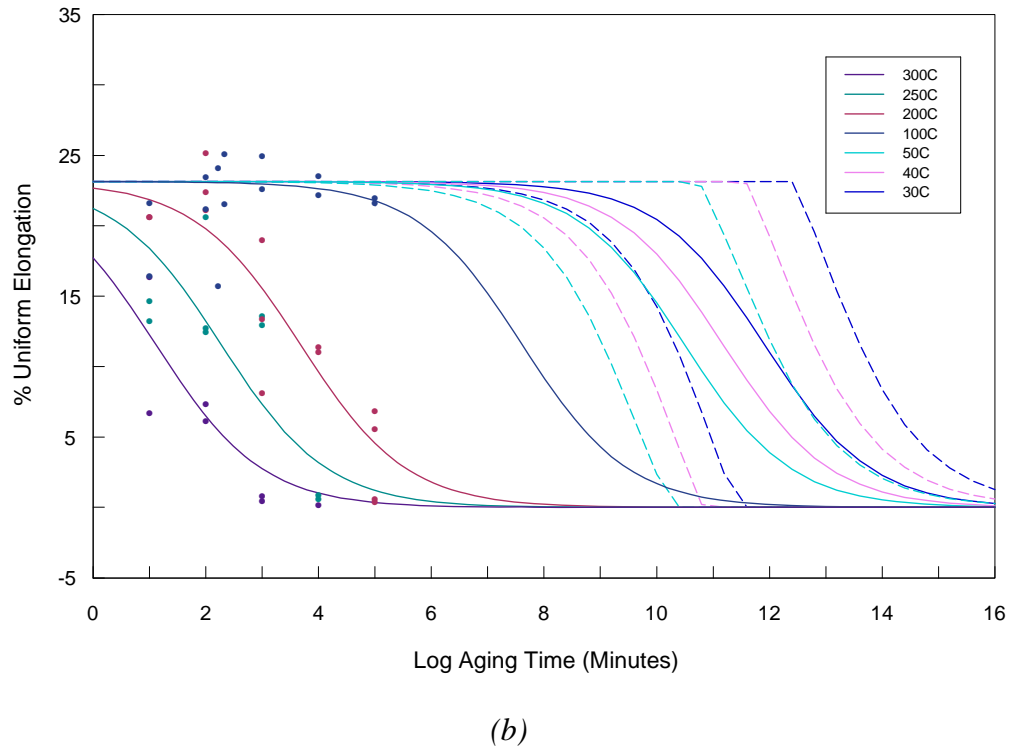
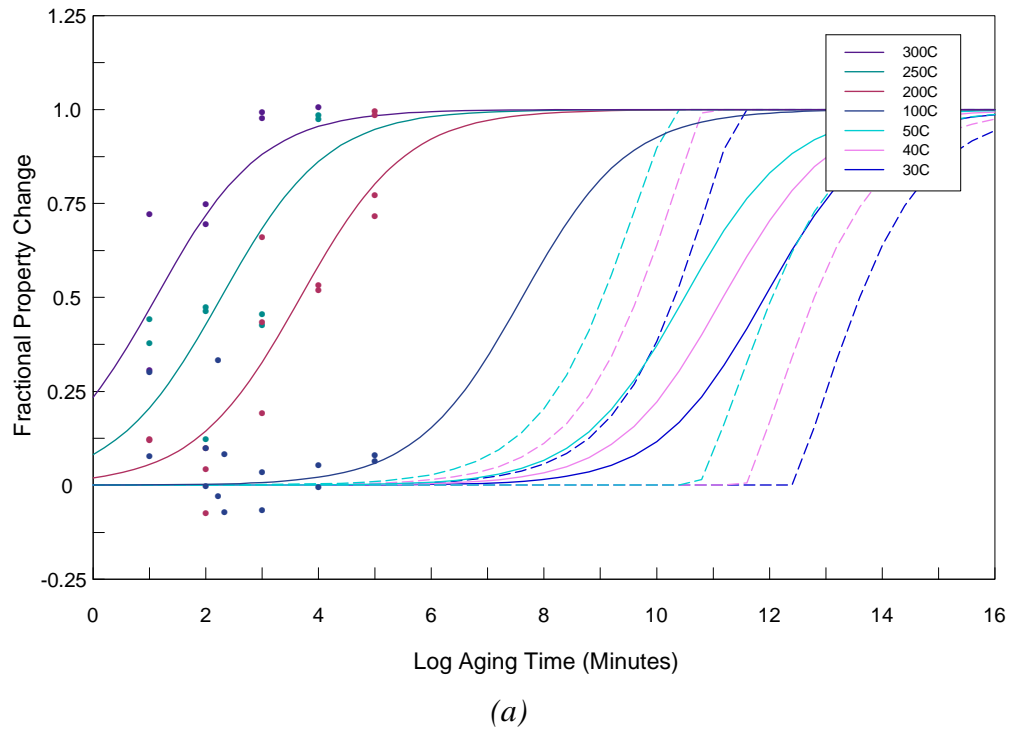


Figure 4.19. U-5.6Nb UE data (points), model fits to data (solid lines), and low-temperature model predictions (solid line—mean, dashed lines—95% confidence intervals). (a) in terms of  $f$ , (b) in terms of absolute property.

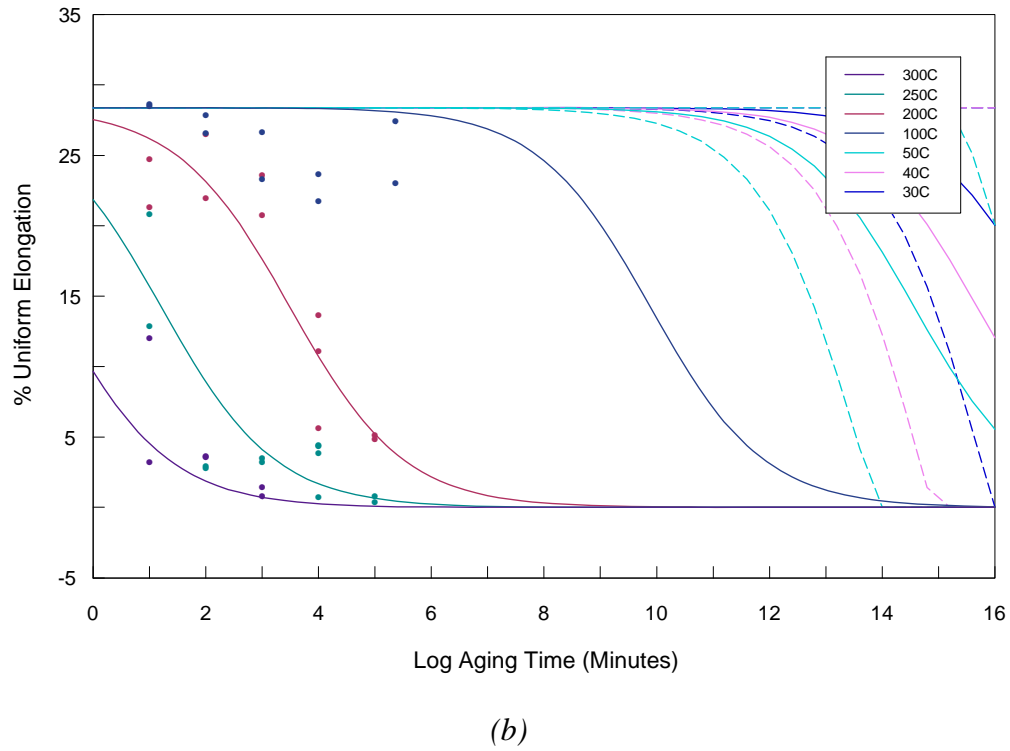
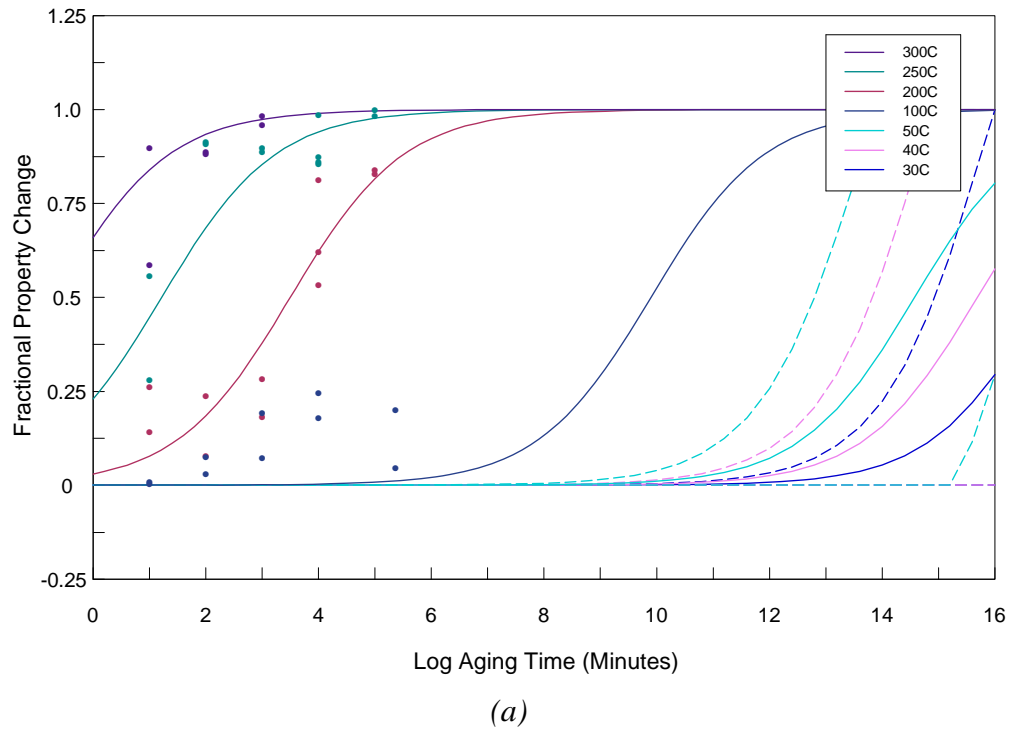


Figure 4.20. U-7.7Nb UE data (points), model fits to data (solid lines), and low-temperature model predictions (solid line—mean, dashed lines—95% confidence intervals). (a) in terms of  $f$ , (b) in terms of absolute property.

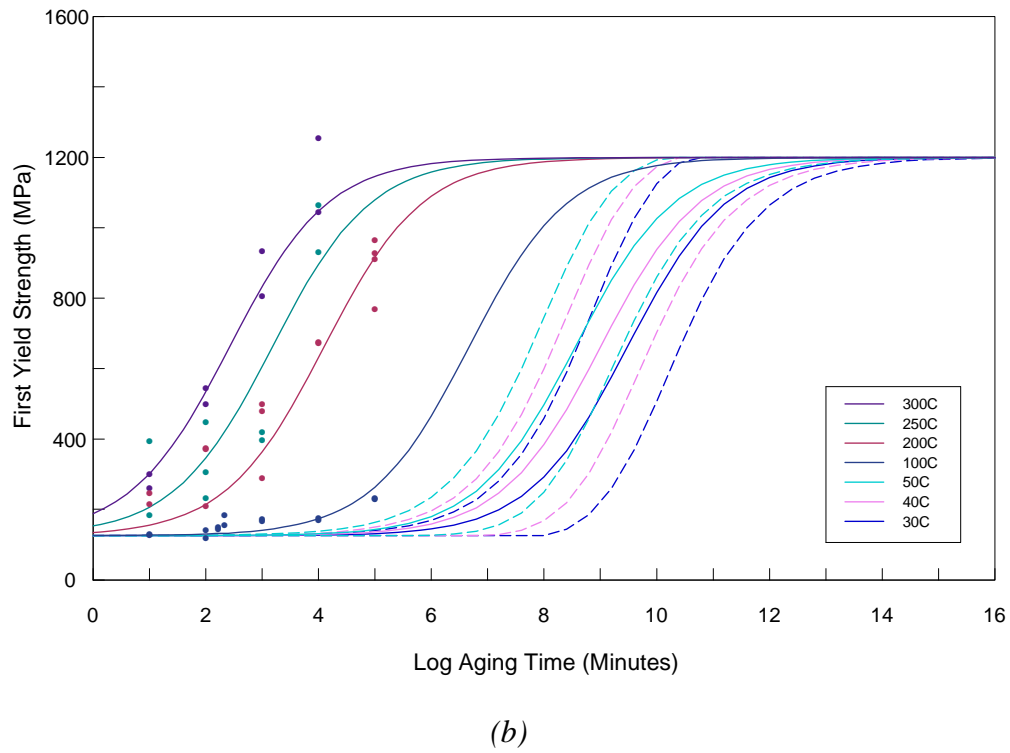
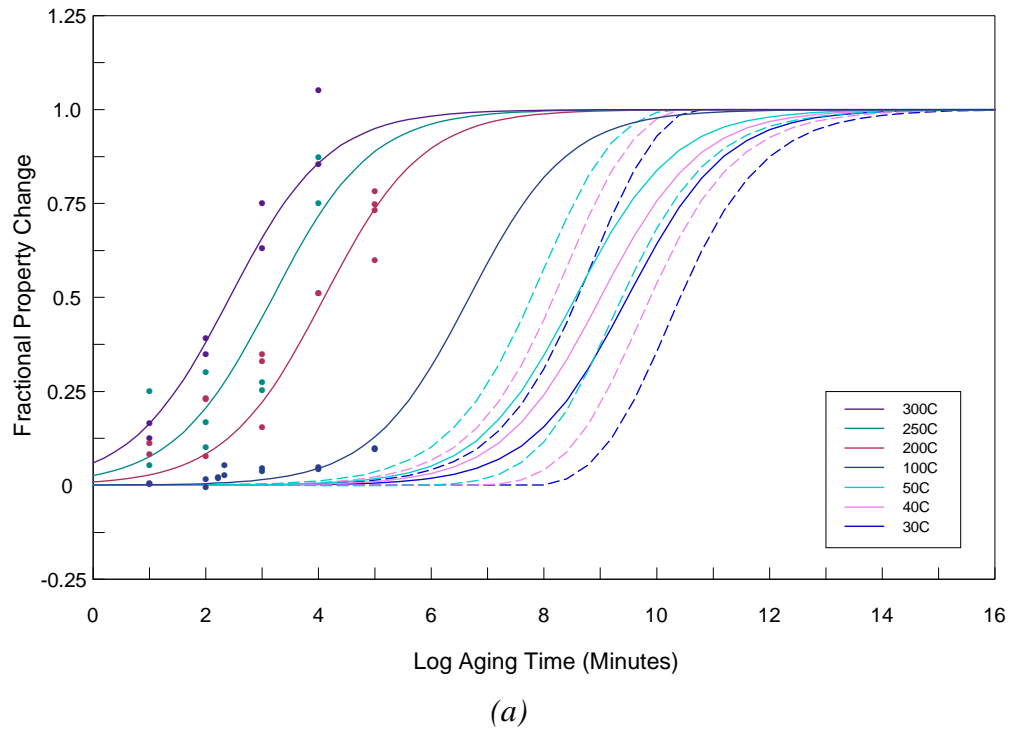


Figure 4.21. U-5.6Nb 1YS data (points), model fits to data (solid lines), and low-temperature model predictions (solid line—mean, dashed lines—95% confidence intervals). (a) in terms of  $f$ , (b) in terms of absolute property.

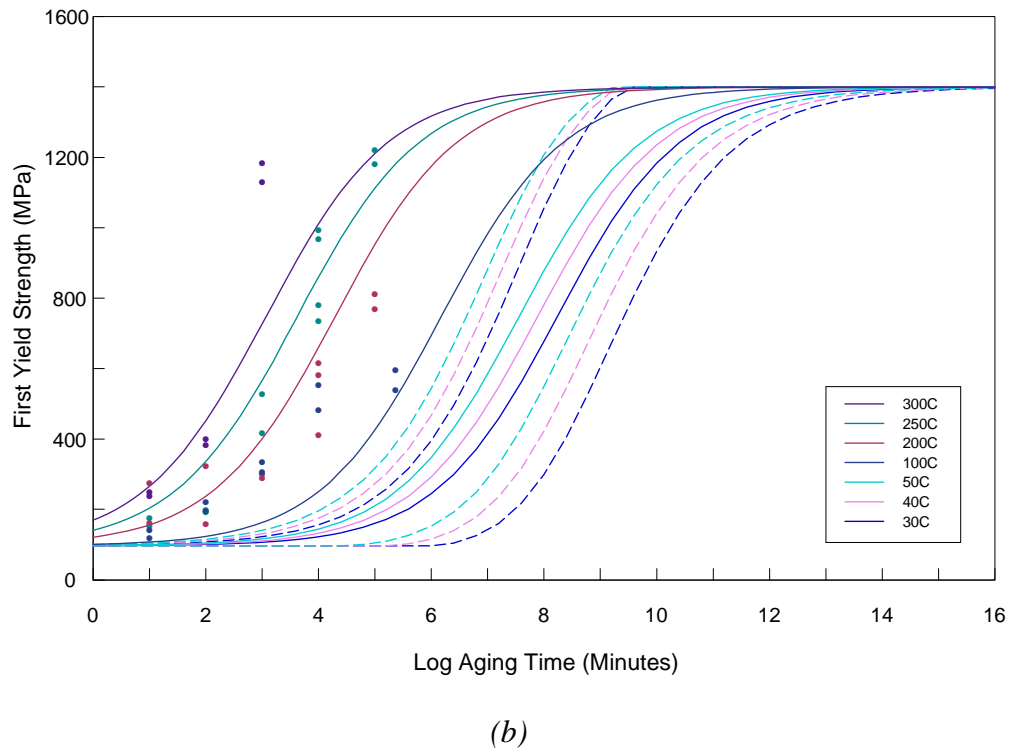
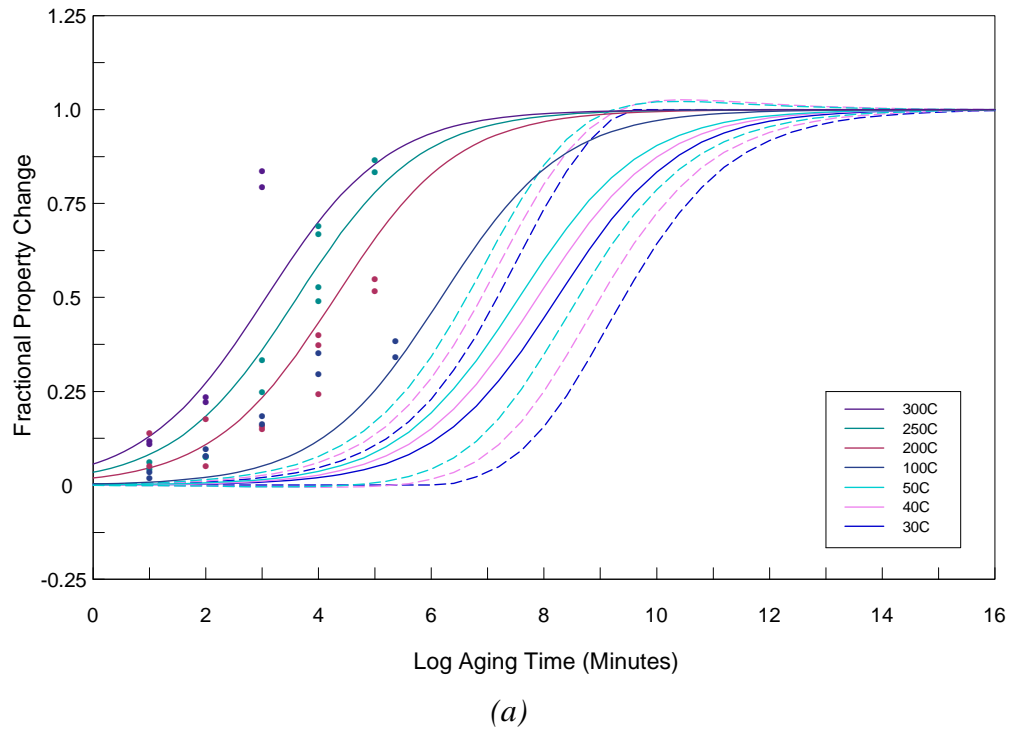


Figure 4.22. U-7.7Nb 1YS data (points), model fits to data (solid lines), and low-temperature model predictions (solid line—mean, dashed lines—95% confidence intervals). (a) in terms of  $f$ , (b) in terms of absolute property.

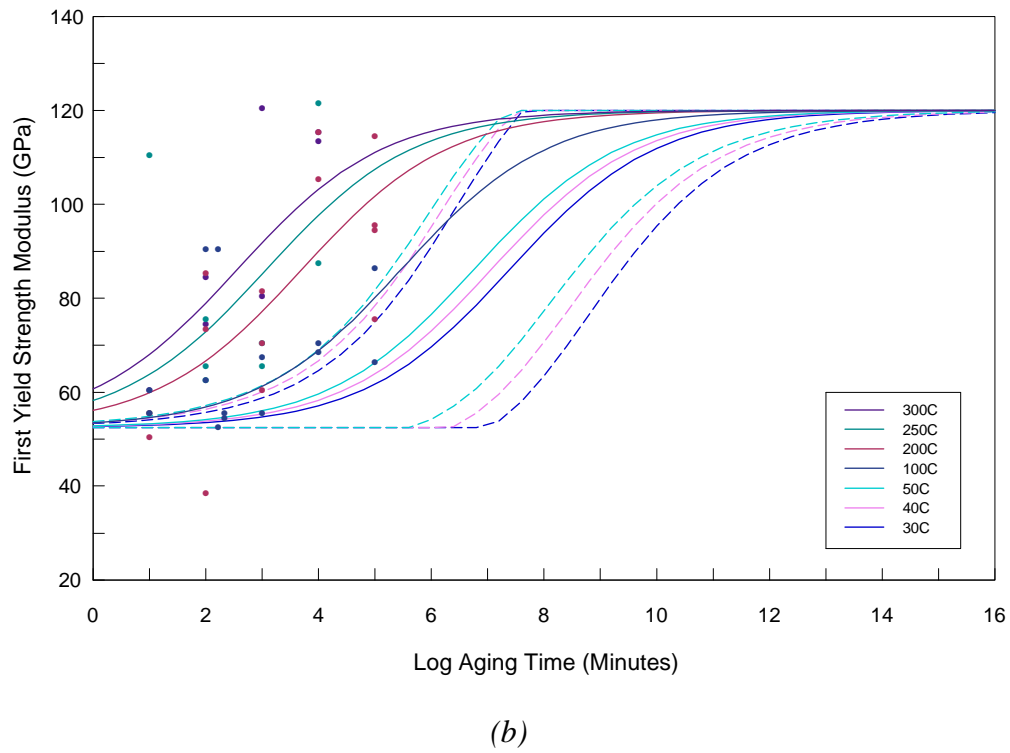
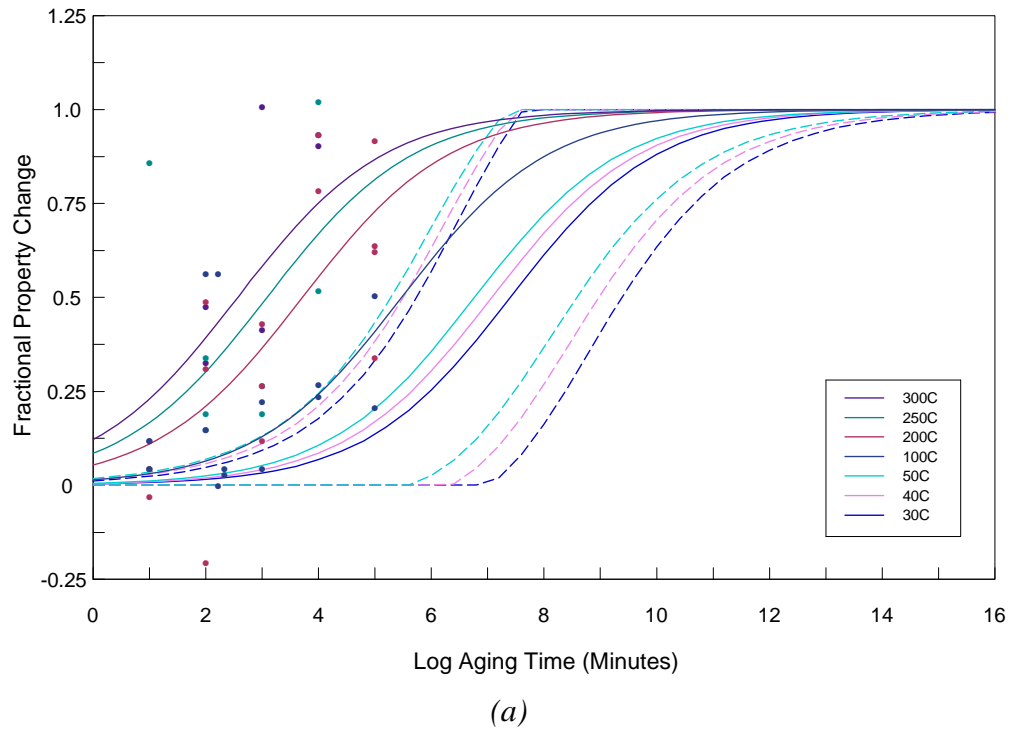


Figure 4.23. U-5.6Nb 1YM data (points), model fits to data (solid lines), and low-temperature model predictions (solid line—mean, dashed lines—95% confidence intervals). (a) in terms of  $f$ , (b) in terms of absolute property.

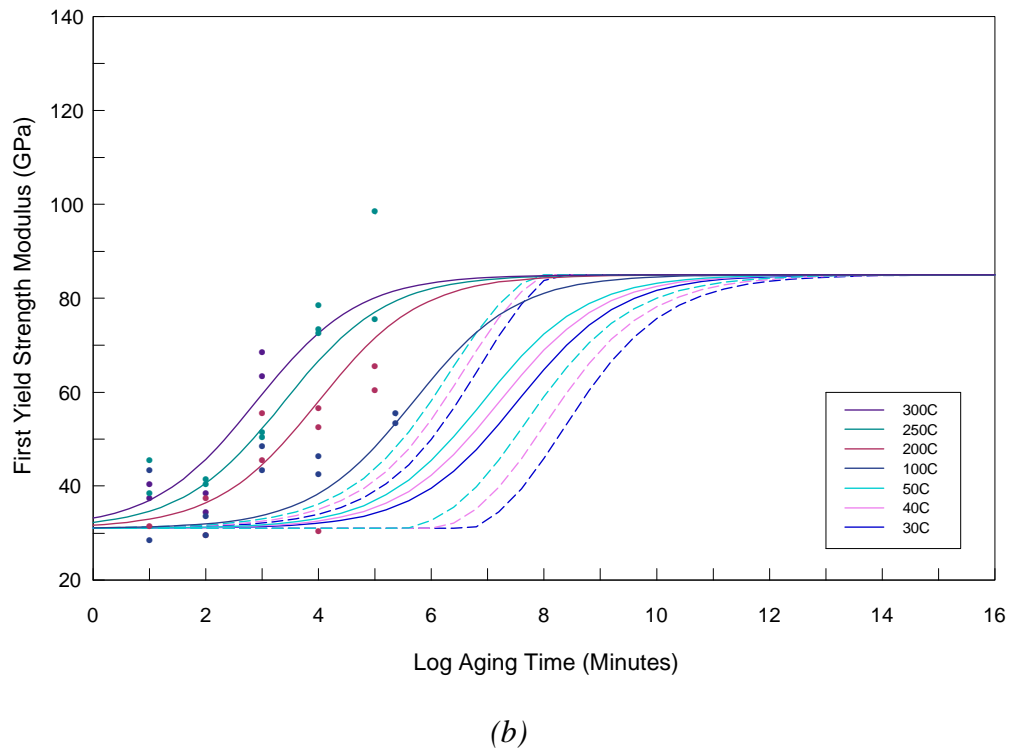
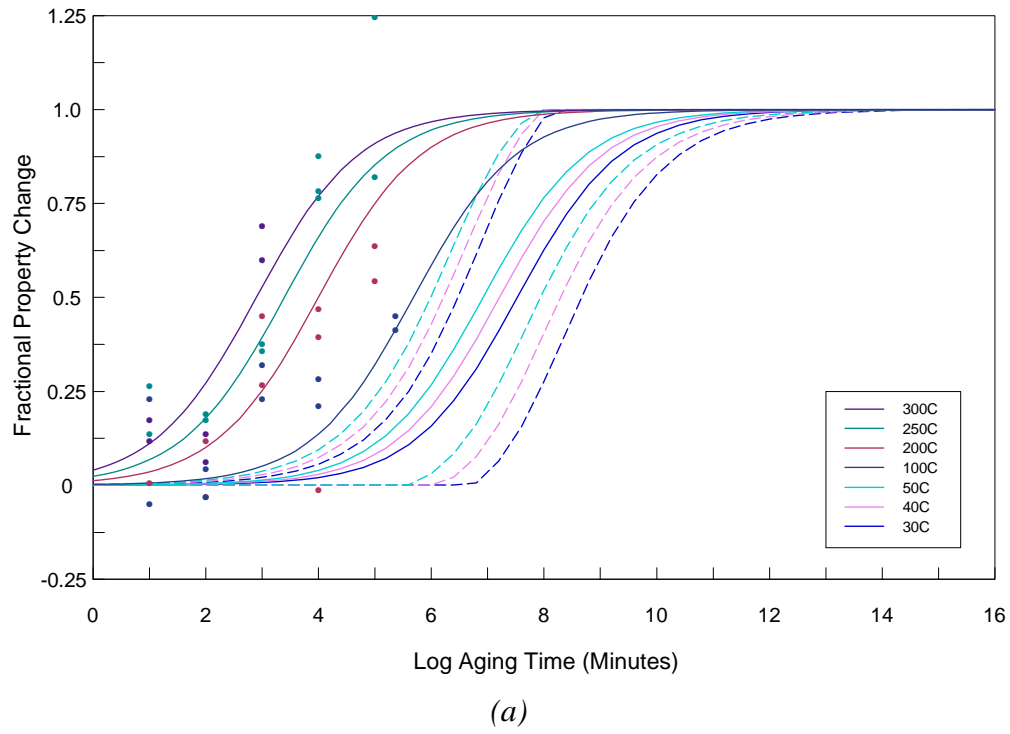


Figure 4.24. U-7.7Nb 1YM data (points), model fits to data (solid lines), and low-temperature model predictions (solid line—mean, dashed lines—95% confidence intervals). (a) in terms of  $f$ , (b) in terms of absolute property.

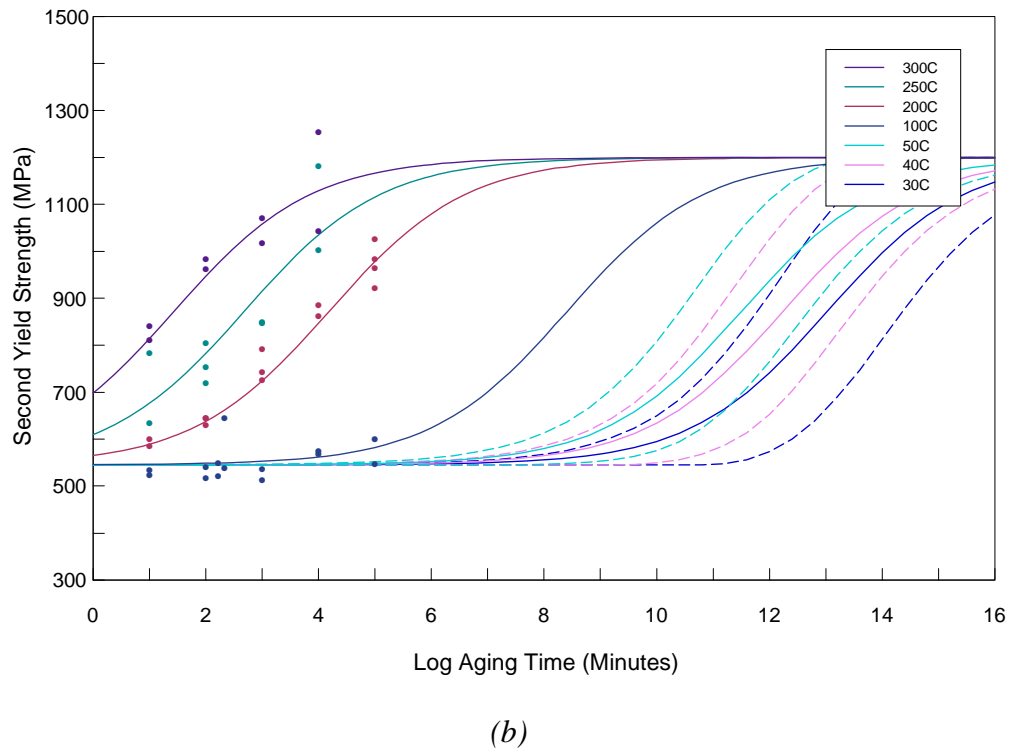
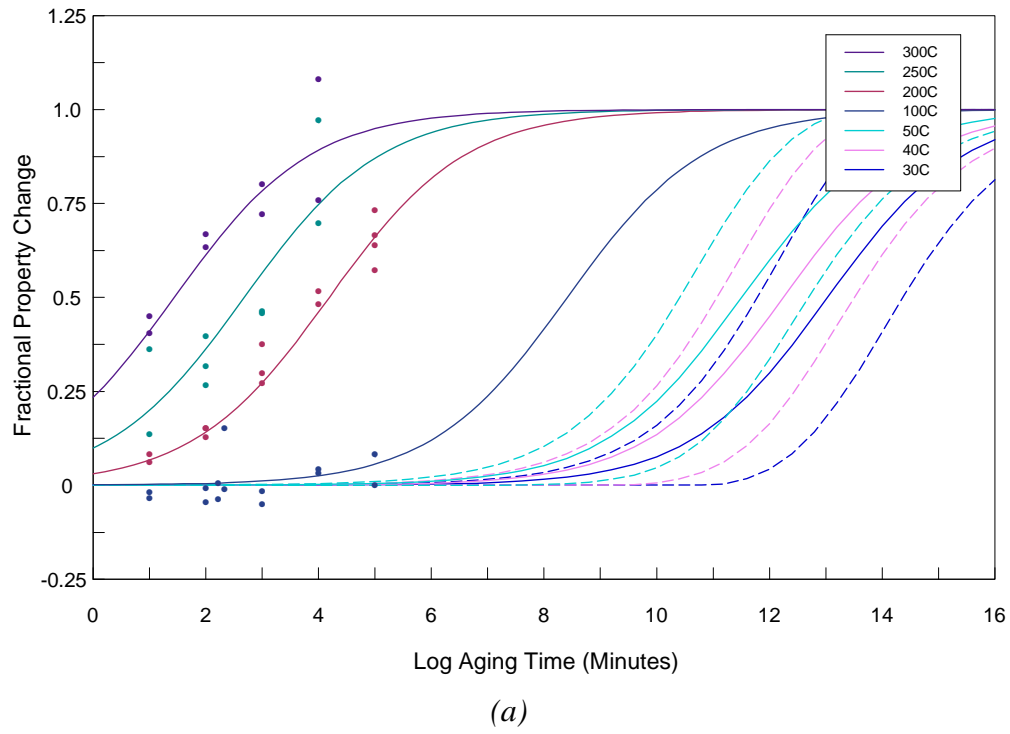


Figure 4.25. U-5.6Nb 2YS model data (points), model fits to data (solid lines), and low-temperature model predictions (solid line—mean, dashed lines—95% confidence intervals). (a) in terms of  $f$ , (b) in terms of absolute property.

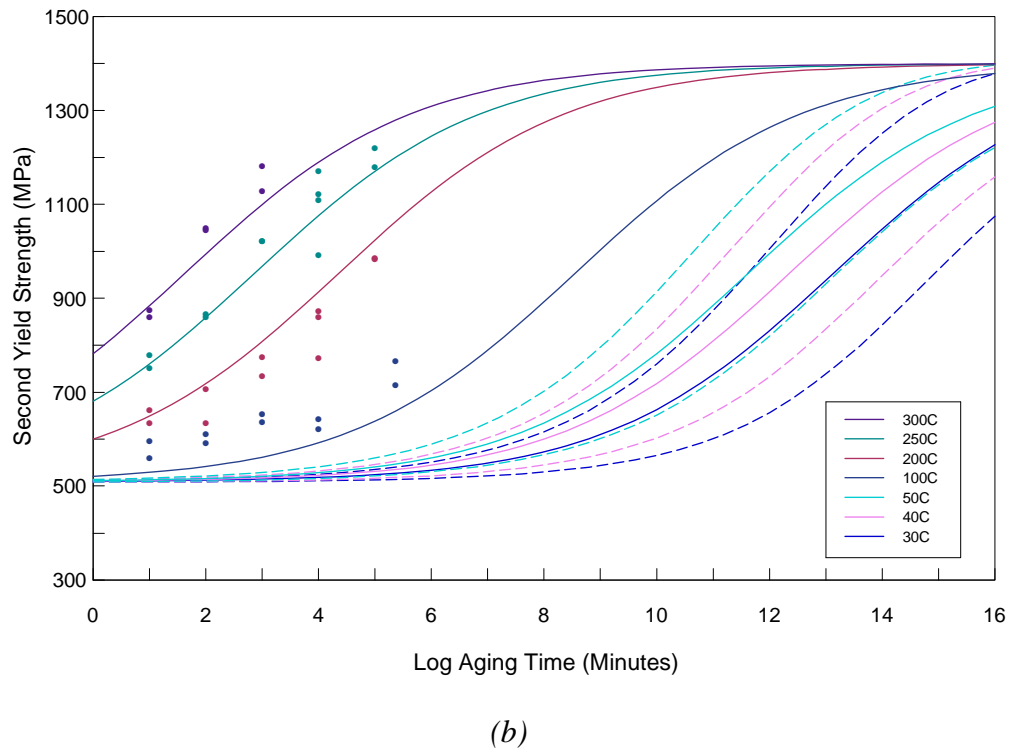
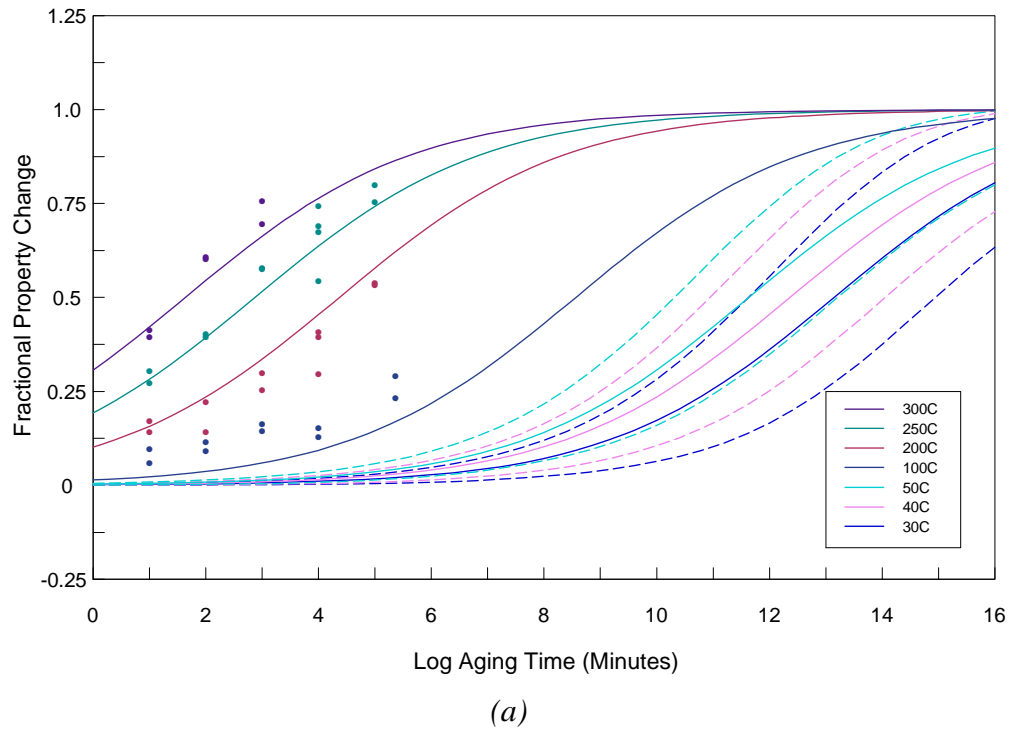


Figure 4.26. U-7.7Nb 2YS data (points), model fits to data (solid lines), and low-temperature model predictions (solid line—mean, dashed lines—95% confidence intervals). (a) in terms of  $f$ , (b) in terms of absolute property.

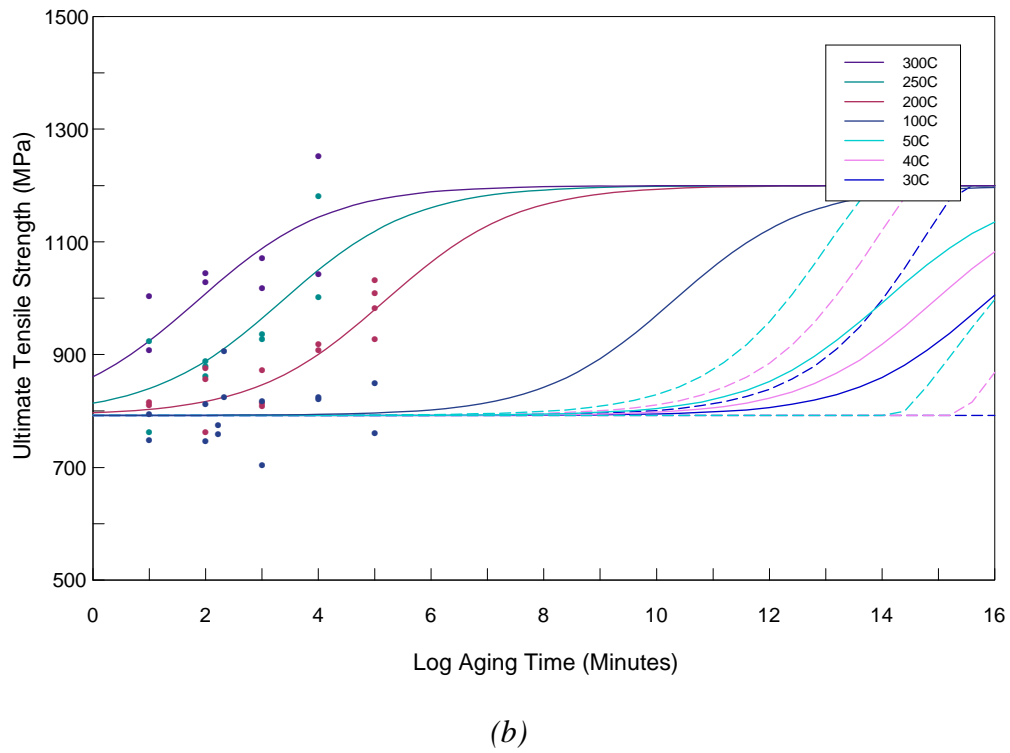
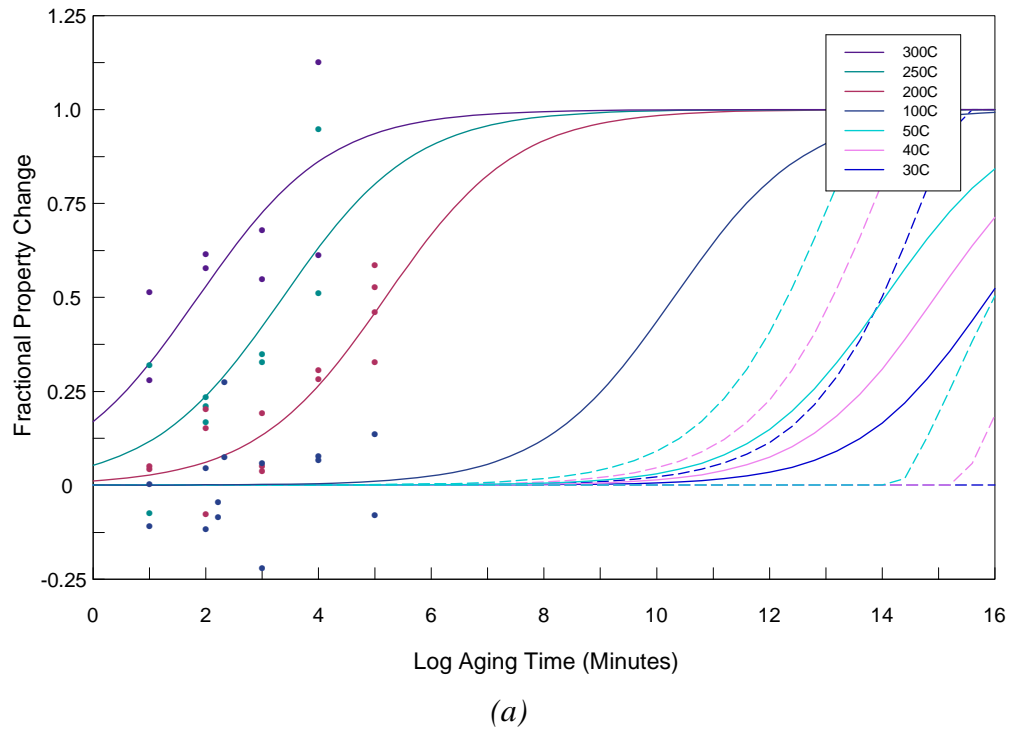


Figure 4.27. U-5.6Nb UTS data (points), model fits to data (solid lines), and low-temperature model predictions (solid line—mean, dashed lines—95% confidence intervals). (a) in terms of  $f$ , (b) in terms of absolute property.

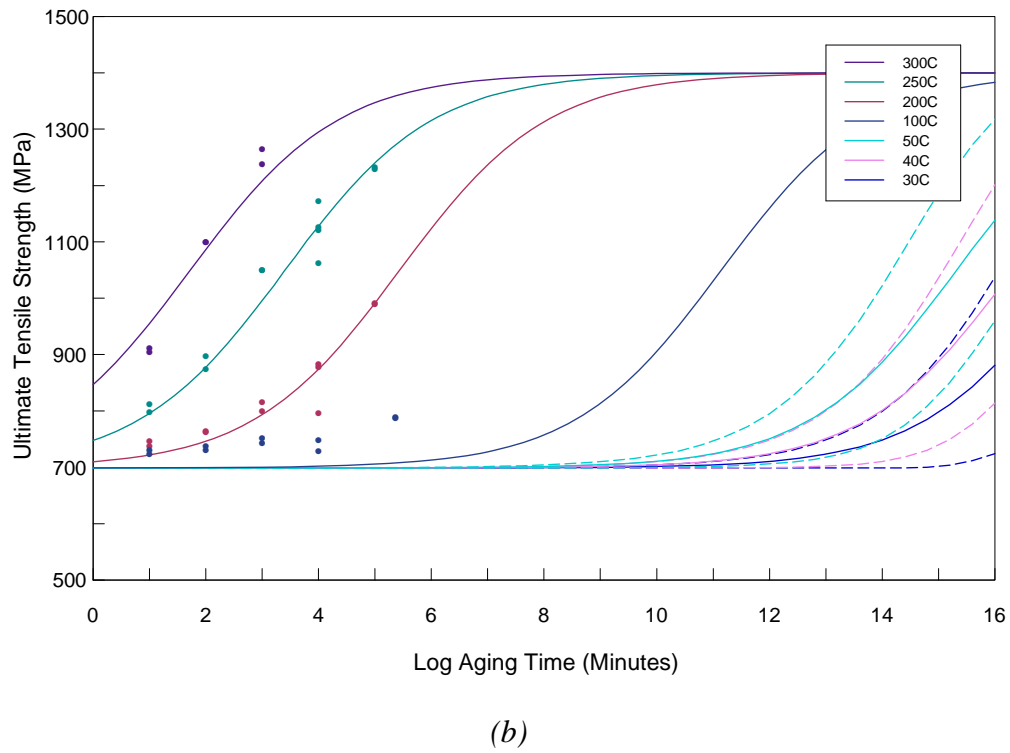
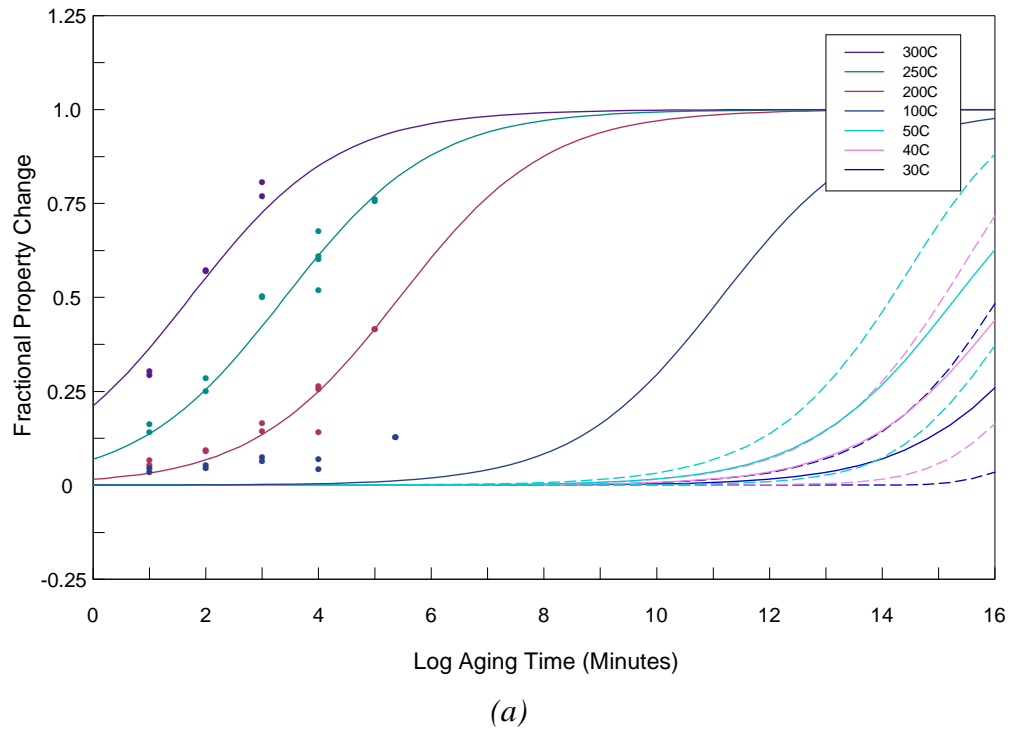


Figure 4.28. U-7.7Nb UTS data (points), model fits to data (solid lines), and low-temperature model predictions (solid line—mean, dashed lines—95% confidence intervals). (a) in terms of  $f$ , (b) in terms of absolute property.

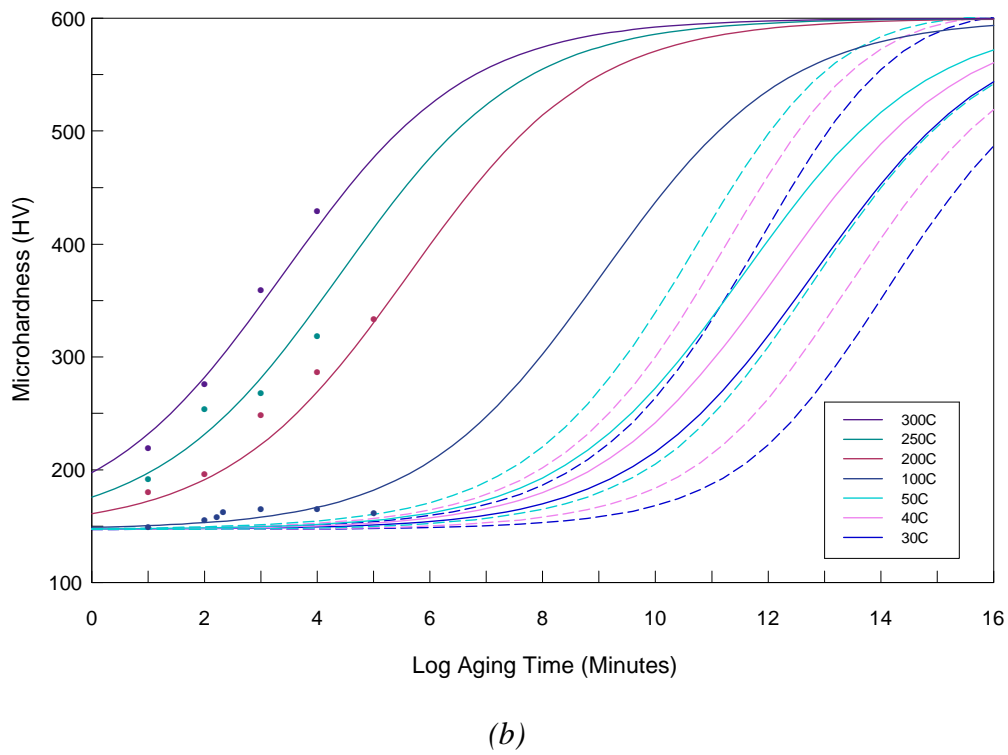
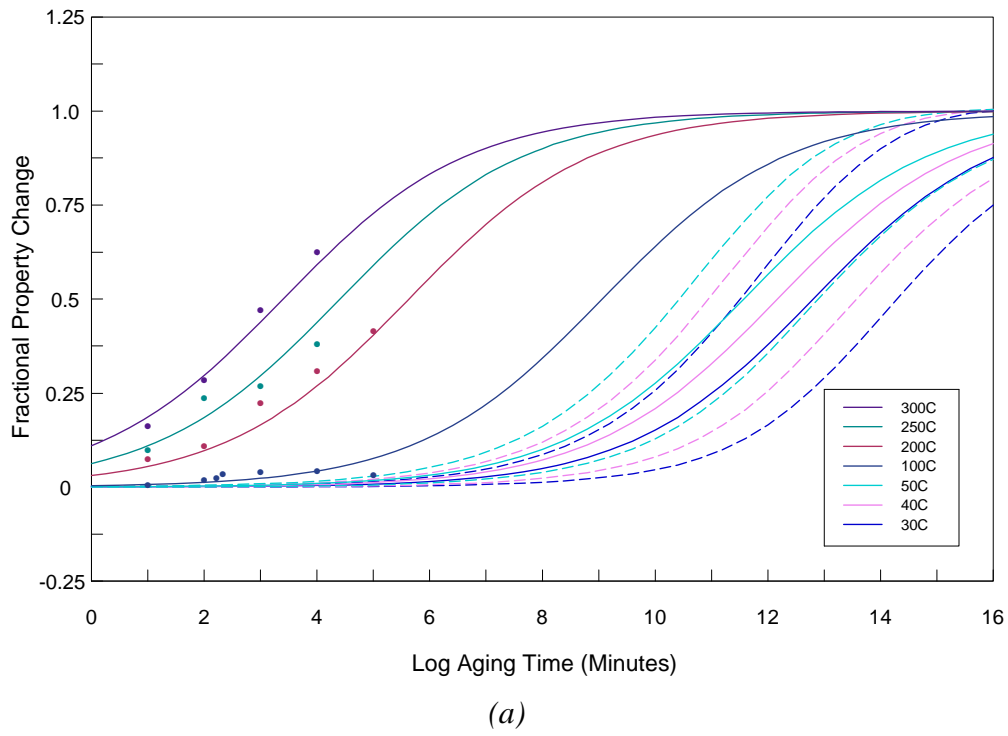


Figure 4.29. U-5.6Nb HV data (points), model fits to data (solid lines), and low-temperature model predictions (solid line—mean, dashed lines—95% confidence intervals). (a) in terms of  $f$ , (b) in terms of absolute property.

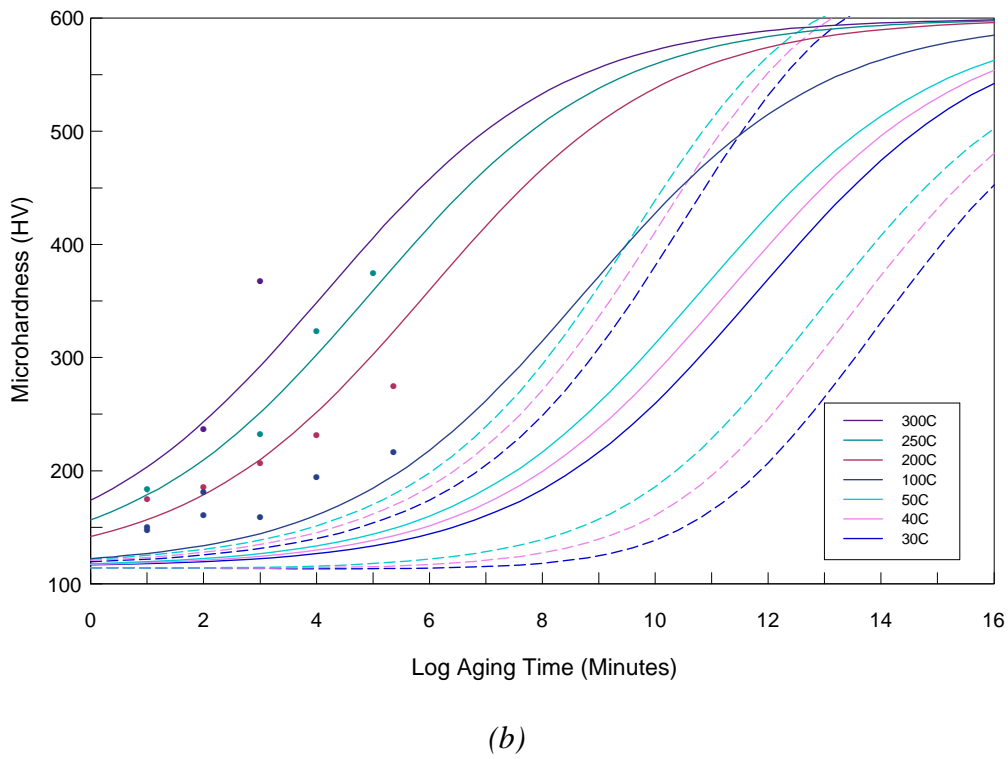
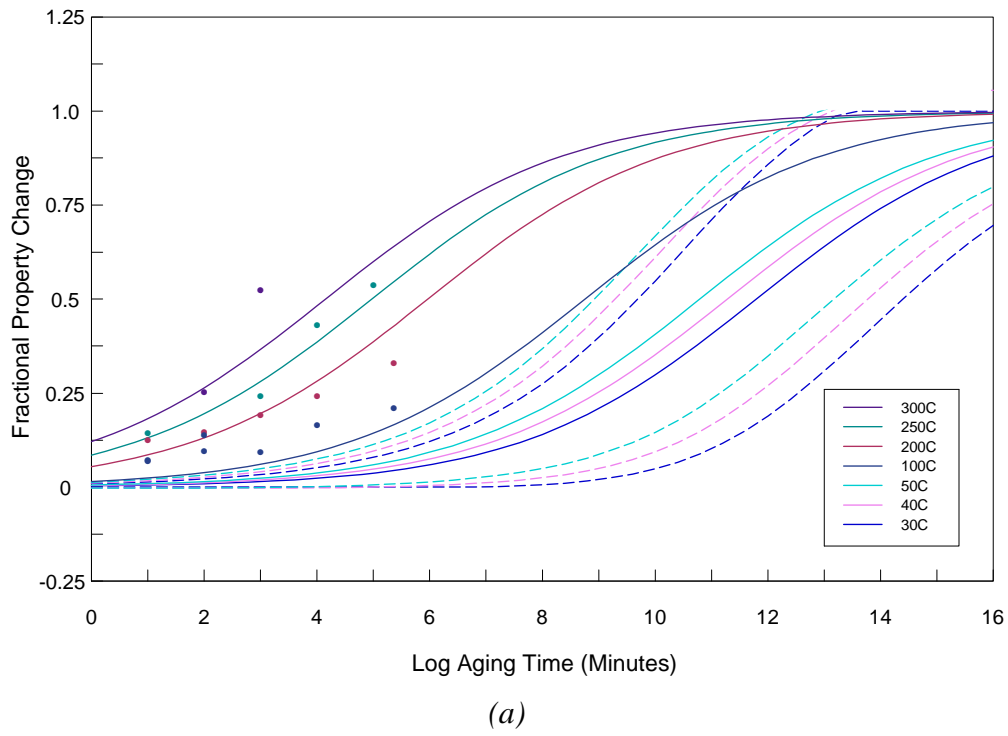


Figure 4.30. U-7.7Nb HV data (points), model fits to data (solid lines), and low-temperature model predictions (solid line—mean, dashed lines—95% confidence intervals). (a) in terms of  $f$ , (b) in terms of absolute property.

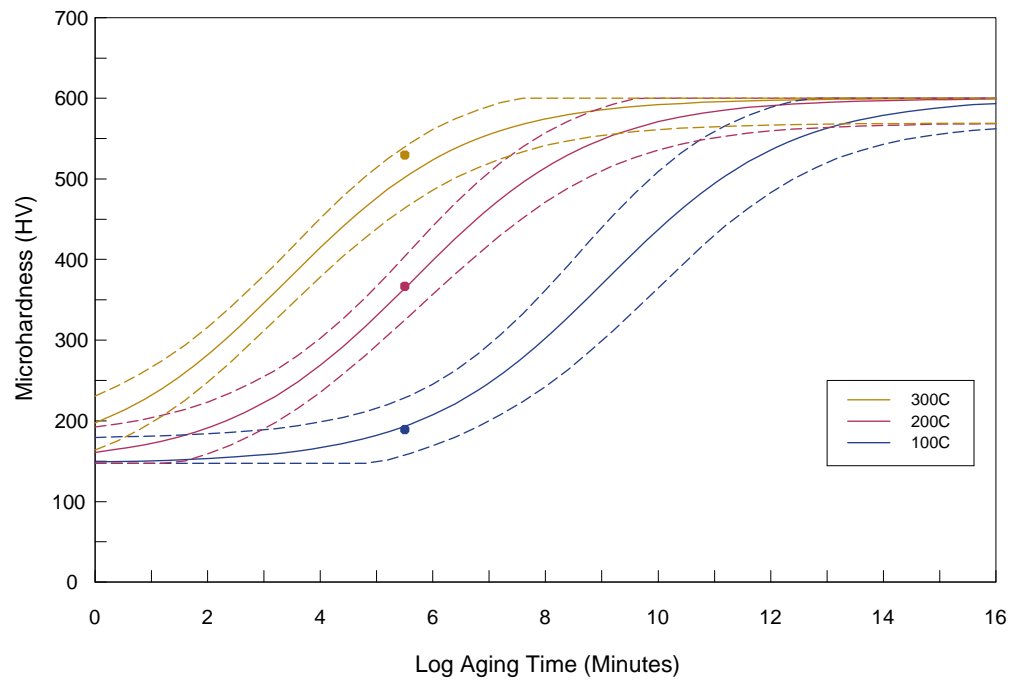


Figure 4.31. U-5.6Nb validation HV data (points) and model predictions (solid lines—mean, dashed lines—95% prediction intervals).

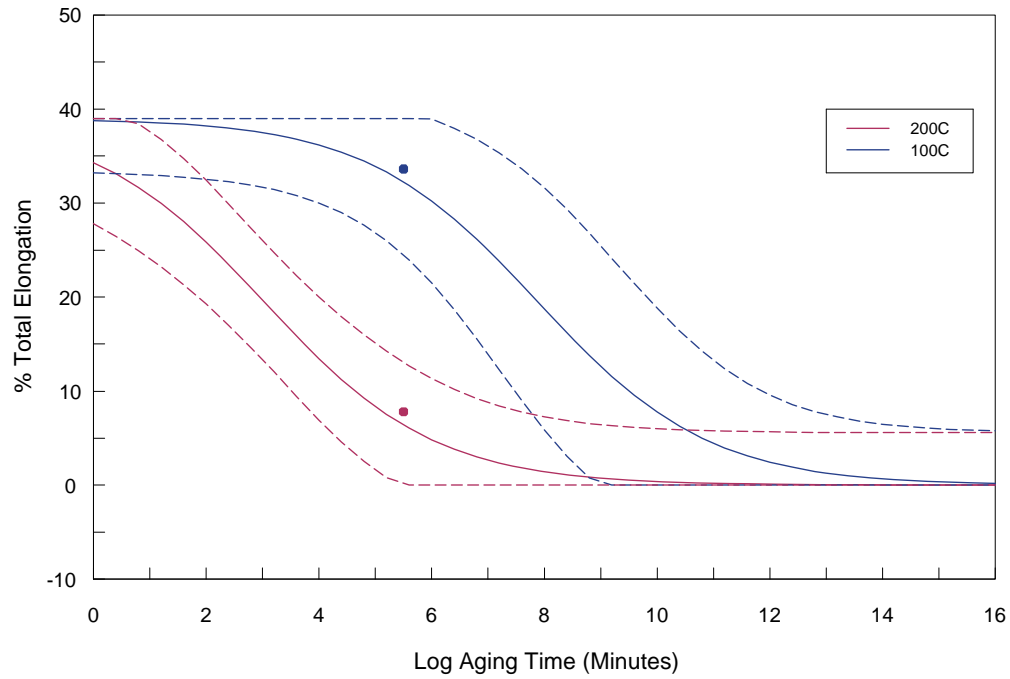


Figure 4.32. U-7.7Nb validation TE data (points) and model predictions (solid lines—mean, dashed lines—95% prediction intervals).

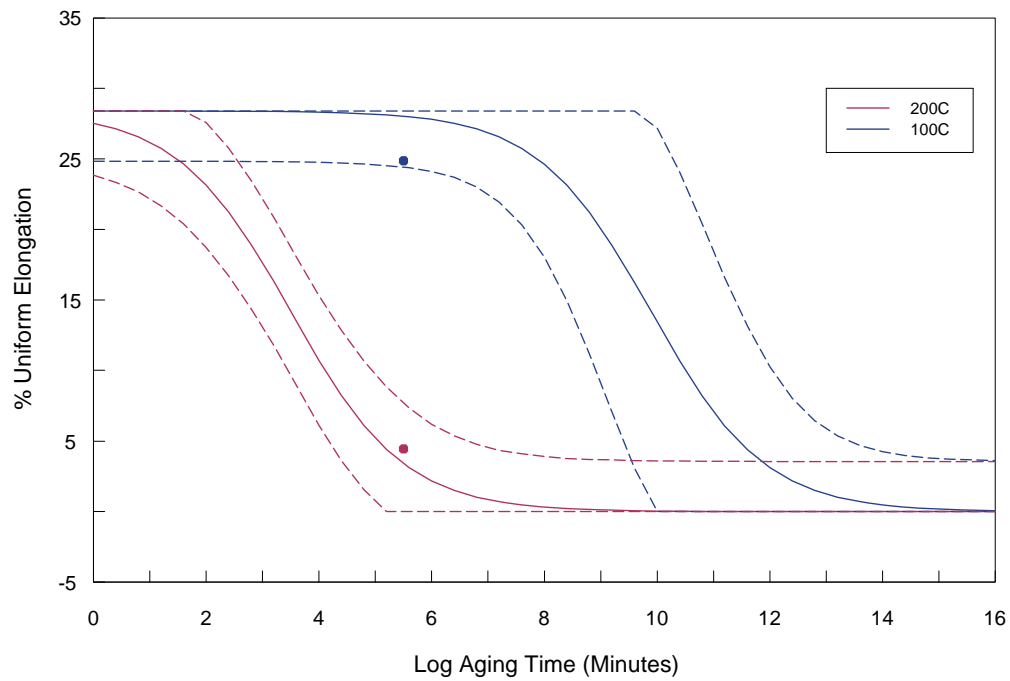


Figure 4.33. U-7.7Nb validation UE data (points) and model predictions (solid lines—mean, dashed lines—95% prediction intervals).

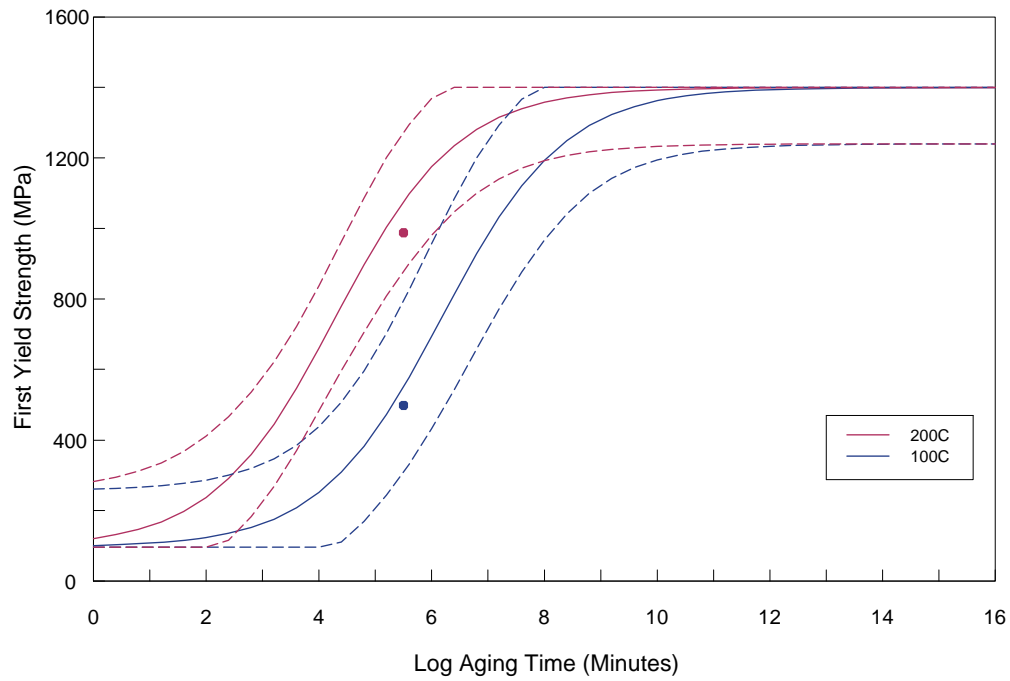


Figure 4.34. U-7.7Nb validation 1YS data (points) and model predictions (solid lines—mean, dashed lines—95% prediction intervals).

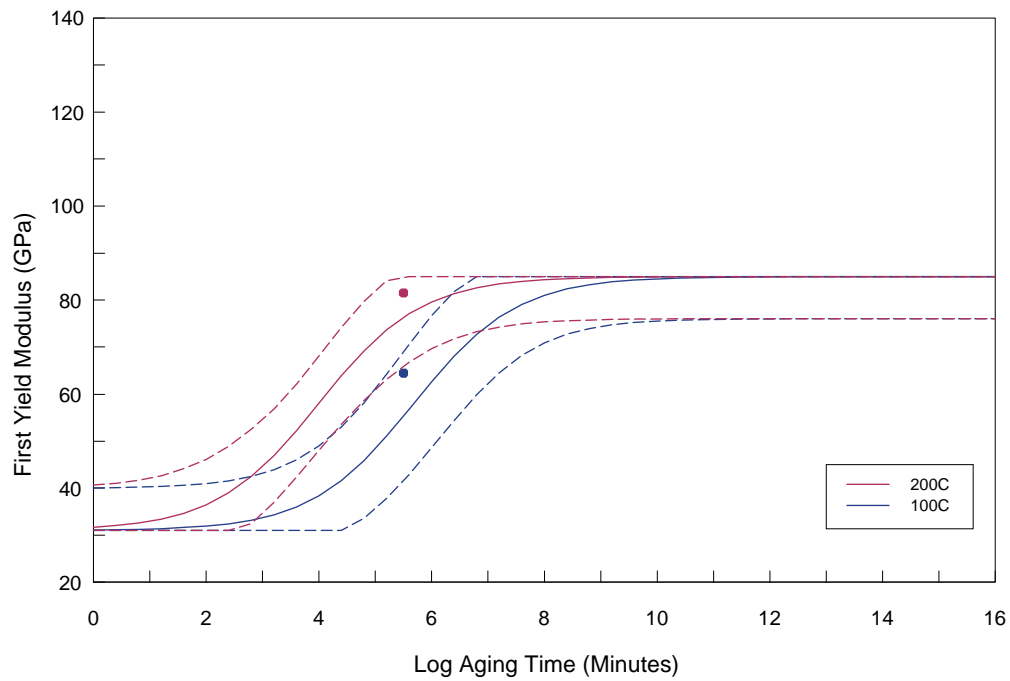


Figure 4.35. U-7.7Nb validation 1YM data (points) and model predictions (solid lines—mean, dashed lines—95% prediction intervals).

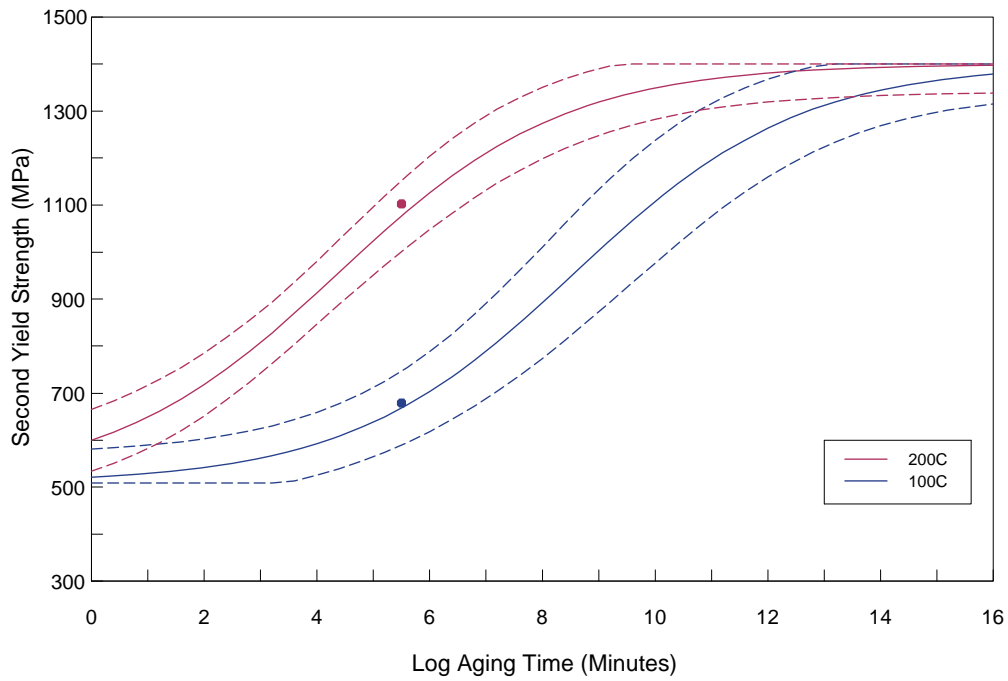


Figure 4.36. U-7.7Nb validation 2YS data (points) and model predictions (solid lines—mean, dashed lines—95% prediction intervals).

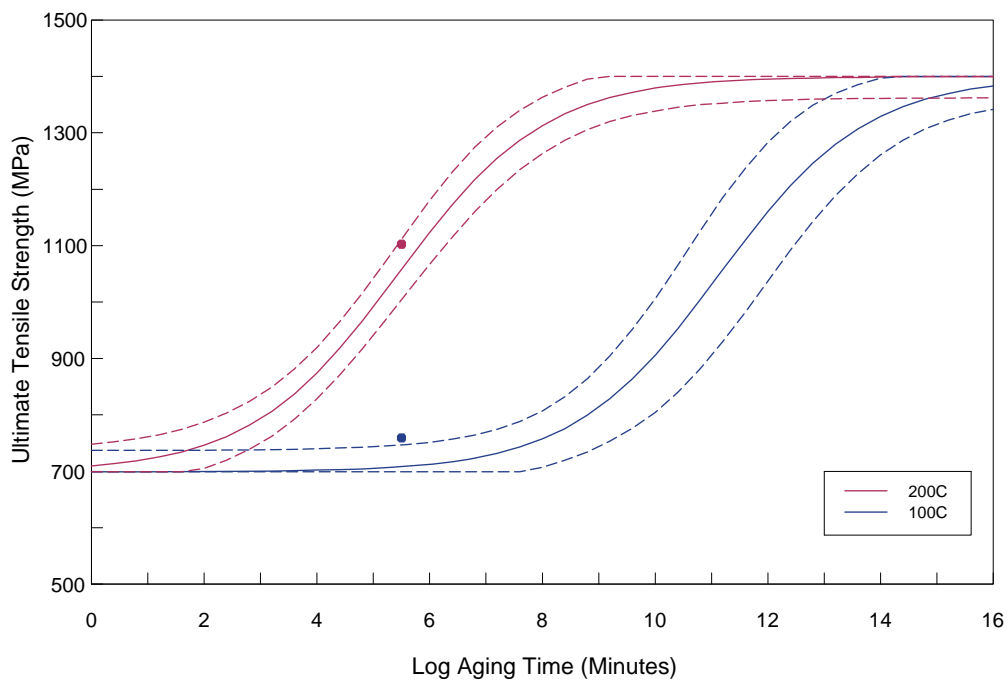


Figure 4.37. U-7.7Nb validation UTS data (points) and model predictions (solid lines—mean, dashed lines—95% prediction intervals).

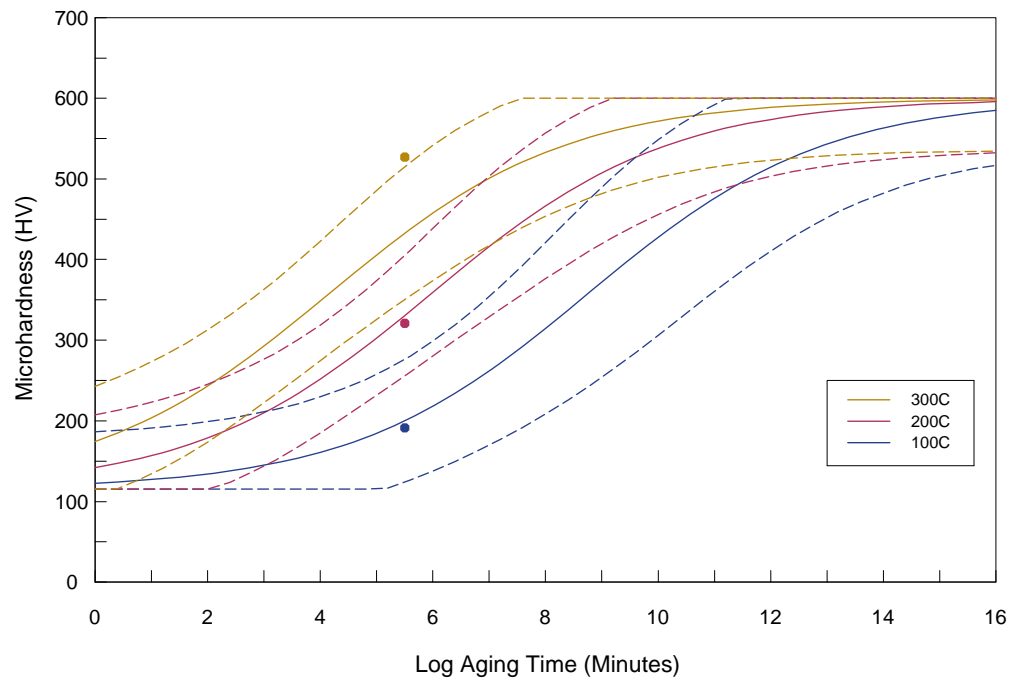


Figure 4.38. U-7.7Nb validation HV data (points) and model predictions (solid lines—mean, dashed lines—95% prediction intervals).

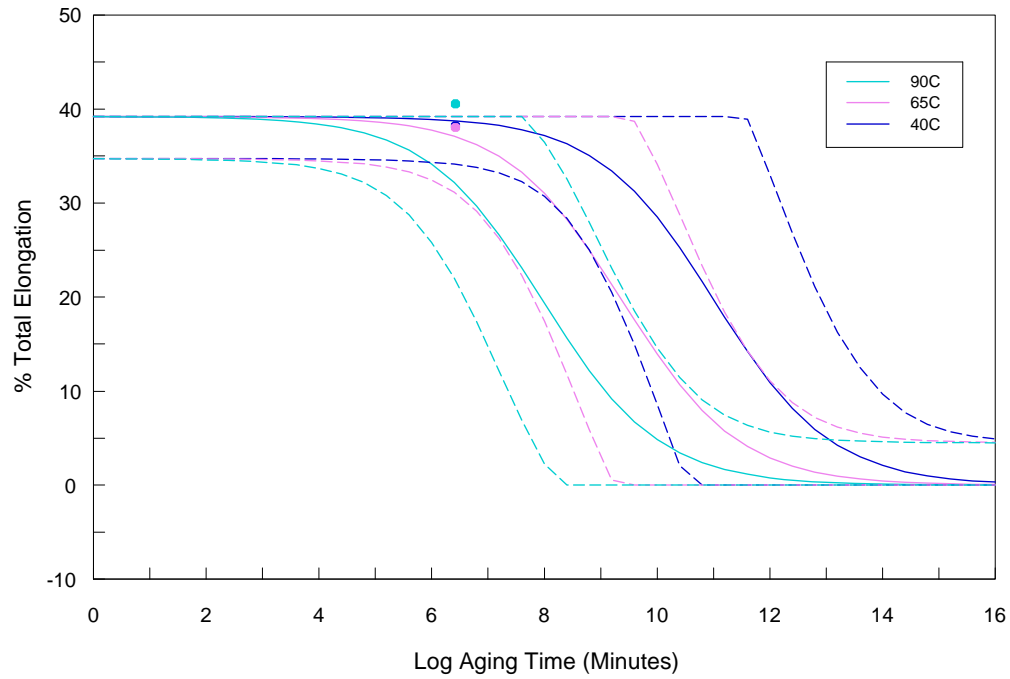


Figure 4.39. U-6Nb validation TE data (points) and model predictions (solid lines—mean, dashed lines—95% prediction intervals).

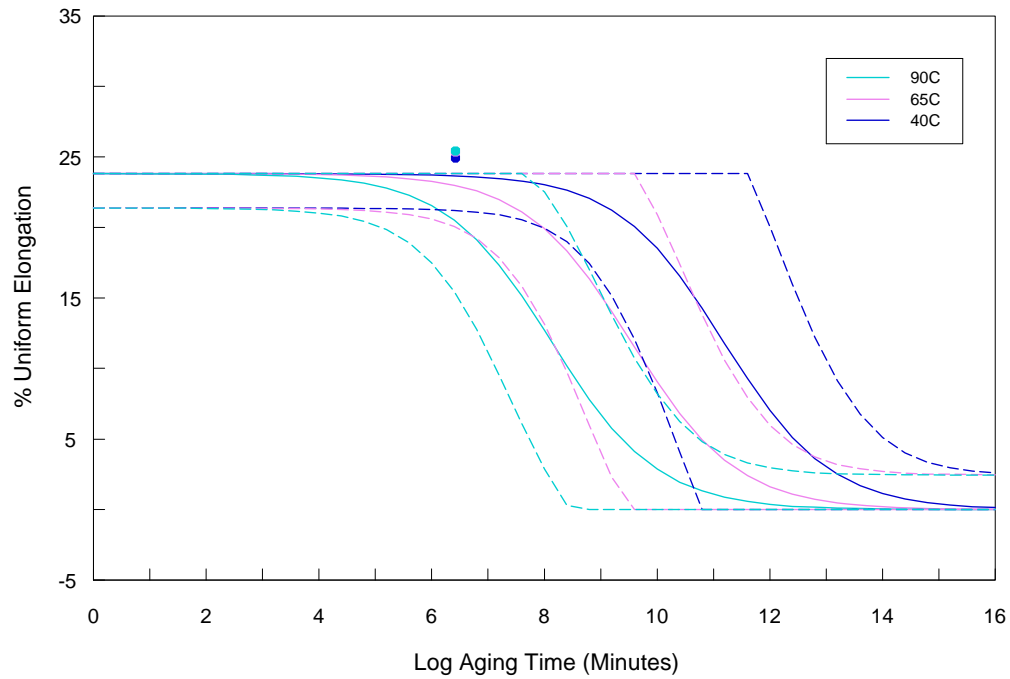


Figure 4.40. U-6Nb validation UE data (points) and model predictions (solid lines—mean, dashed lines—95% prediction intervals).

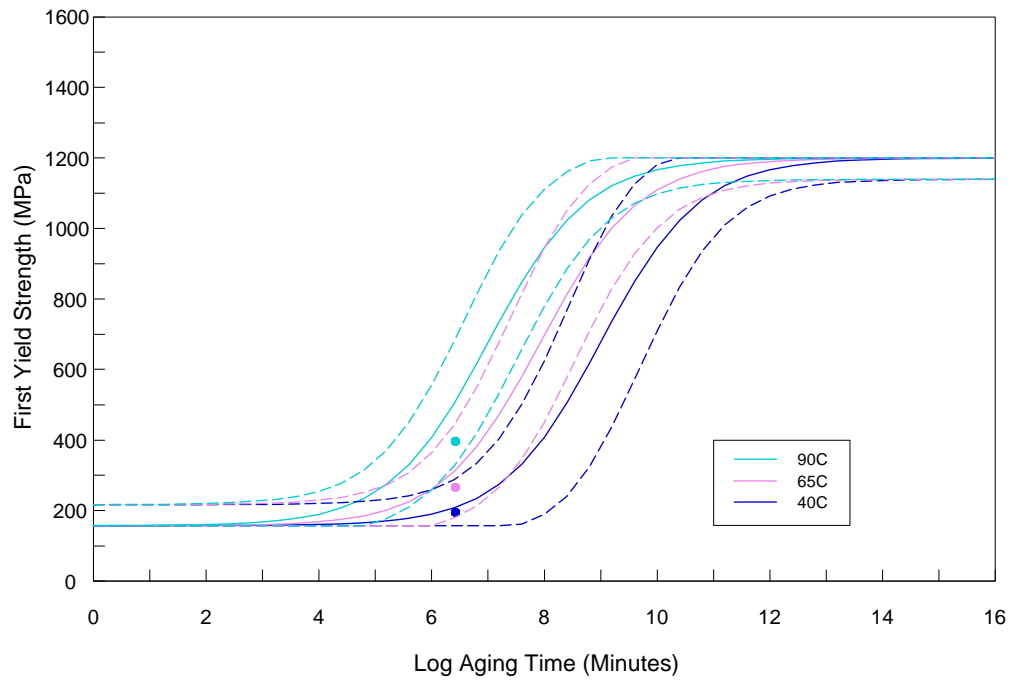


Figure 4.41. U-6Nb validation 1YS data (points) and model predictions (solid lines—mean, dashed lines—95% prediction intervals).

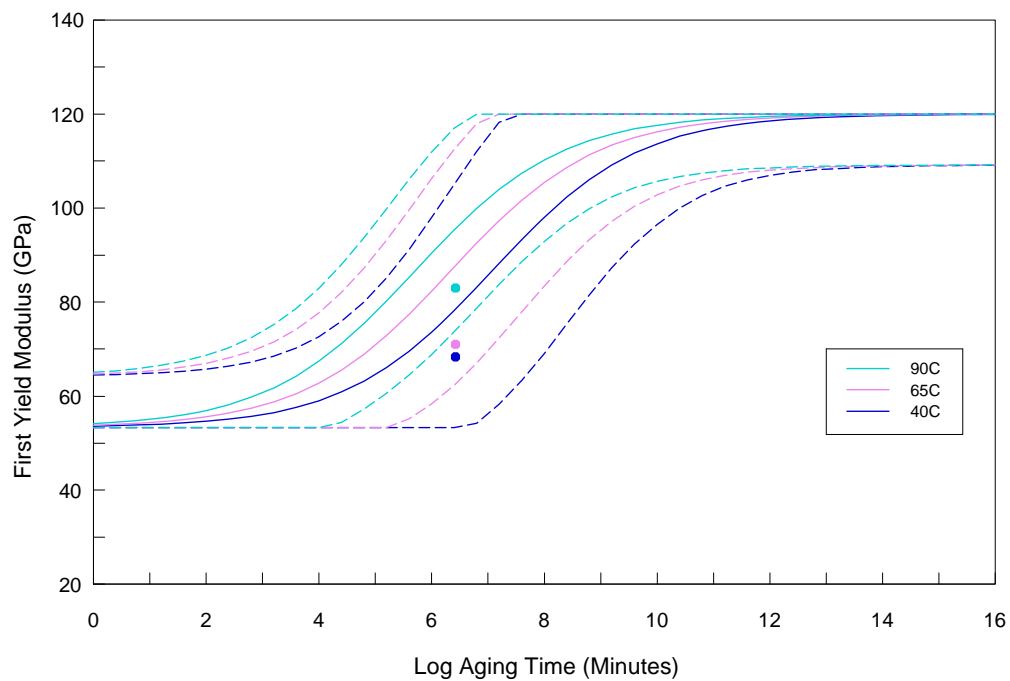


Figure 4.42. U-6Nb validation 1YM data (points) and model predictions (solid lines—mean, dashed lines—95% prediction intervals).

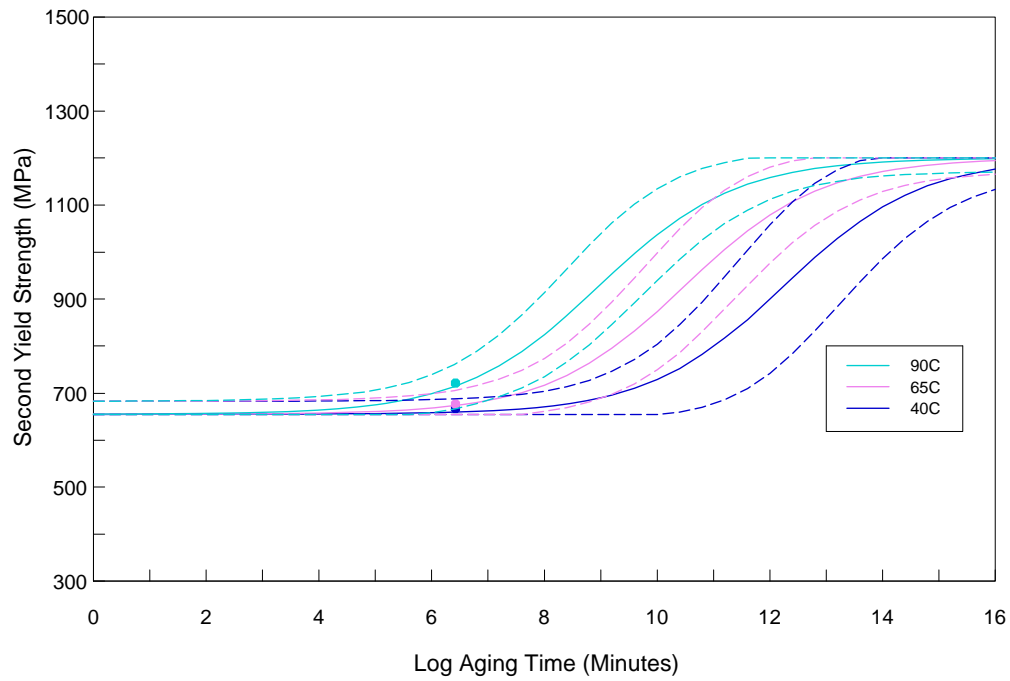


Figure 4.43. U-6Nb validation 2YS data (points) and model predictions (solid lines—mean, dashed lines—95% prediction intervals).

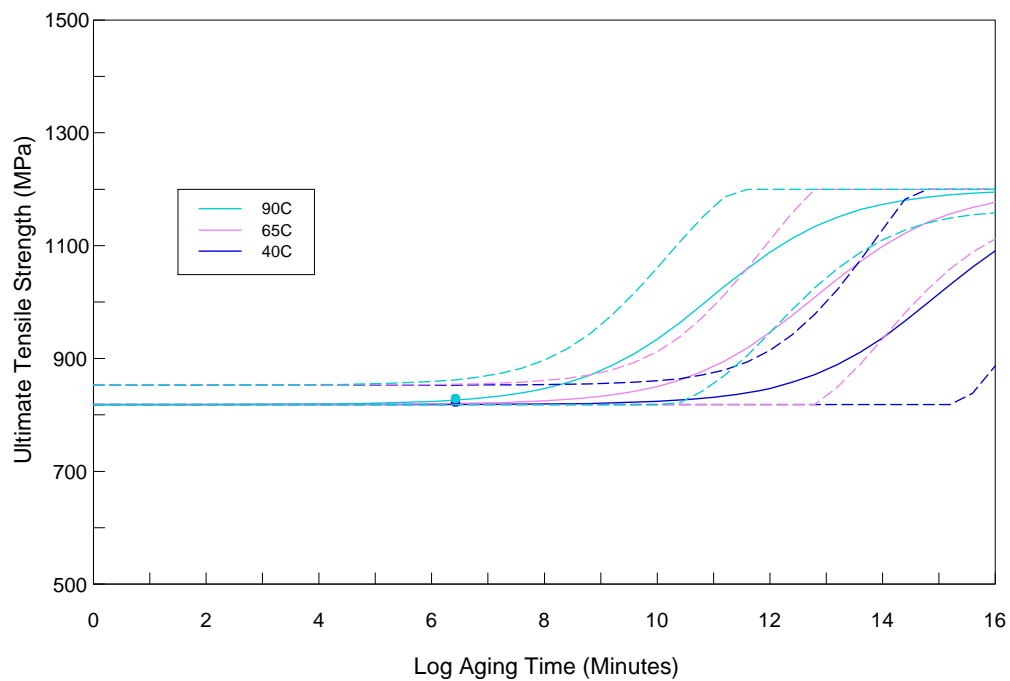


Figure 4.44. U-6Nb validation UTS data (points) and model predictions (solid lines—mean, dashed lines—95% prediction intervals).

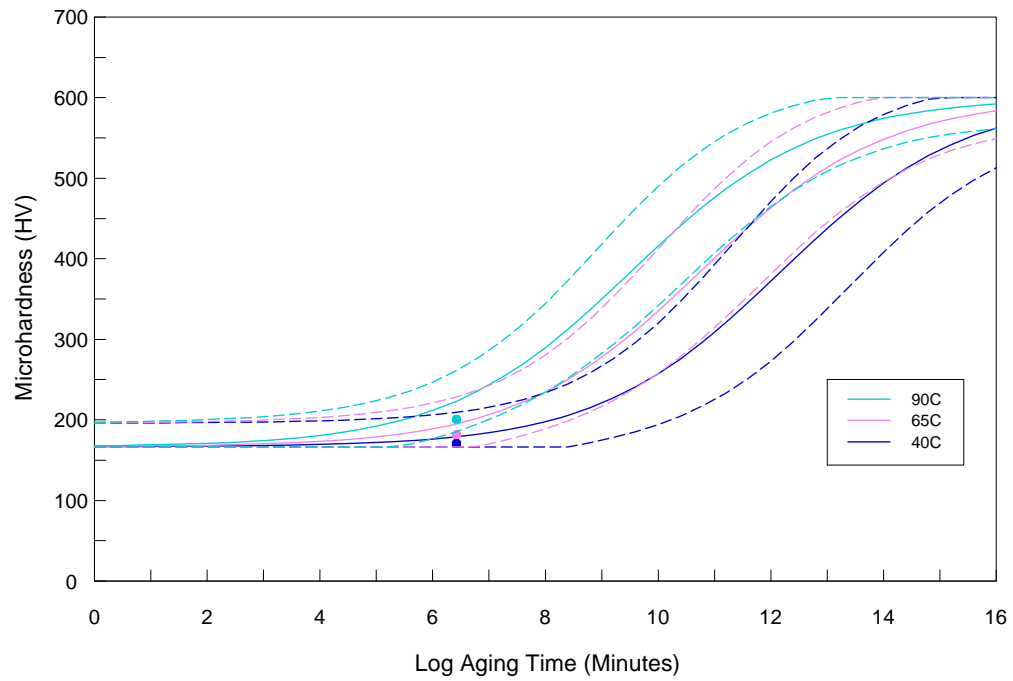


Figure 4.45. U-6Nb validation HV data (points) and model predictions (solid lines—mean, dashed lines—95% prediction intervals).

## APPENDIX 1: SOURCES AND MAGNITUDES OF SCATTER

For completeness, the origin and impact of all the known or expected sources of scatter is detailed here. It is grouped by whether the scatter originates from a material-specific issue or from a testing or data-reduction issue.

### 1. **Intrinsic Material Variability.** The plate synthesis report provides further details [2007hac1].

- a. *Chemistry.* Differences in Nb content among replicates is expected to be the most significant material-specific contributor to the variability in all age-sensitive properties. Bulk chemical analysis (ICP-MS) on ~10 replicates from the nonbanded plates provided the following average  $\pm 1$  *SD* wt% Nb:  $5.60 \pm 0.56$  and  $7.69 \pm 0.33$ . The average of ~50 points taken from more localized electron microprobe (EPMA) scans were  $5.30 \pm 0.21$  and  $7.75 \pm 0.13$ . The smaller *SD* from the localized EPMA scans indicate that the Nb content is fairly homogeneous within any given replicate, while the larger scatter from the ICP-MS data indicate that Nb differences among different replicates are more significant. The fact that the coring wavelength and the bulk Nb content measured at eight different positions in the as-cast material showed no systematic variation (top-to-bottom or side-to-side in the mold) indicate that the point-to-point Nb variations were stochastic and not originating in slow heat flow during solidification, which is normally the main driver of chemical inhomogeneities in alloys, including banded U-6Nb [1978sny1, 1978sny2].
- b. *Microstructure.* Property scatter arising from inclusions and crystal distributions are expected to be minor for this material. With few exceptions, the carbo-oxy-nitride inclusions that affect ductility are uniformly distributed throughout the microstructure. Any crystal anisotropy impacting tensile deformation is expected to be minor because the small average prior gamma grain diameter (~200 microns) and martensite twin width (20–50 nm) are considerably smaller than the tensile gage diameter (2,540 microns), allowing any anisotropy to be averaged out.
- c. *Specimen correlations.* The ~30 coupon and ~60 tensile specimens used in this study were machined from predetermined zones within the plate. However, the replicates for any given age were randomly selected from a bag where they were mixed, so no systematic scatter is expected because of correlation between any replicate and its location in the plate before machining with respect to other replicates or ages.

### 2. **Experimental and Data Reduction.** Further details are from [2007hac2, 2008ale].

- a. *Heat treatment Temperatures.* Temperatures of the furnace used for 800°C or 850°C solutionizing and furnaces and sand pot employed for aging were calibrated with an independent thermocouple, ensuring a mean set-point temperature value accurate to within 1°C. Deviations from this mean value during furnace or sand pot operation are expected to be  $\pm 2^\circ\text{C}$ .
- b. *Heat treatment times.* The impact of the expected scatter in the 800°C or 850°C solutionizing heat treatment times ( $\pm 30$  seconds) is considered to be negligible for a 30-minute nominal time. There is an error in the aging process because of the time it took for the vacuum-encapsulated specimens to reach the aging temperature upon heating to the aging temperature, and to reach ambient temperature (23°C) upon subsequent cooling. All aging heat treatments carried out for times <1,000 minutes

had 10 minutes added to the nominal aging time to account for the time it took to heat up to the aging temperature. (The times quoted here and elsewhere [2007hac2] are the nominal times) This was done on the basis of a preliminary experiment that showed it took ~10 minutes for the center of a vacuum-encapsulated DU specimen to attain a temperature within 5°C of the set point irrespective of whether the set point was 100°C, 200°C, 250°C, or 300°C [2007hac2]. Table A1.1 lists the absolute errors in aging time attributable to the combined effects of (assumed) exponential heating and cooling to/from the aging temperature for both the <1,000-minute ages (for which the extra 10 minutes was added) and the ≥1,000-minute ages (for which no extra time was added). The aging equivalency was numerically evaluated in a spreadsheet using the Arrhenius relationship with the indicated activation energy  $Q$ . The specimens aged <1,000 minutes experienced an 1–2 minute surplus of aging, whereas those aged 1,000 minutes or longer experienced a 7–8 minute deficit of aging. These absolute errors are about ten times larger than the actual operator error in pulling the specimen out of the furnace or sand pot at exactly the prescribed time. Table A1.2 shows that the relative aging time error is largest for the 10 minutes (10–20%) and 100 minutes (1–2%), but for all other ages it is 1% or less. The aging time errors were not accounted for in this study since they are 0.01–1% in the intermediate- to long-time regimes where the sensitivity to such errors in the time-series fitting process would be the highest because of their higher leveraging

- c. *Solutionizing and quenching replicate specimens in different encapsulations.* All the AQ specimens were solution treated and quenched in the same capsule. Because of their quantity, the specimens meant to be subsequently aged were solutionized and quenched in several different capsules, with no attempt to keep track of which specimens came from which capsule. Given the relative quench-insensitivity of U-Nb alloys (≥20 K/s cooling rates are sufficient for this purpose [1984eck]) and the fact that the operator reported no problems or anomalies with this step in the experiment, the impact of using multiple capsules is considered to be minor.
- d. *Aging replicate specimens in different encapsulations.* Two tensile specimen replicates and a single coupon for hardness were aged in the same encapsulated tube at the outset, ensuring that they experience the same aging treatment. In instances where the first two tensile replicates (labeled #1 and #2) for a given age gave significantly different stress-strain responses, one or two additional tensile specimen replicates (labeled #3 and #4) were heat treated and tested to provide better statistics. It was often the case that the replicates 3 and 4 showed the same scatter amongst themselves as replicates 1 and 2 showed amongst themselves. Such an outcome indicates that the scatter in replicate results is due to the intrinsic point-to-point variability in the chemistry and/or microstructure of the nonbanded plate material and not due to a defective heat treatment. One might consider that a bias is introduced because only the apparently anomalous ages (not all ages) were subjected to further tensile replicate testing. However, this potential source of bias was not considered further.
- e. *Hardness testing (HV).* The observed ±~8 HV *SD* scatter (Tables 2.2 and 2.4) is a combination of indenter errors (force and size measurement), and the intrinsic chemistry and microstructural variability, and the unavoidable situation where a hard carbo-oxy-nitride inclusion is present just below the surface of indentation, which

skews a small portion of the data points higher than normal. Deconvolution of these error sources is neither practical nor necessary.

- f. *Elastic moduli (1YS, 2YS slopes)*. The 1YS slope was determined by trial-and-error (with the aid of graphing software) on the engineering stress-engineering strain curves. The analyst eyeballed the best linear fit to the curve near the origin. The analyst's error in determining any given 1YS slope is estimated to be  $\pm 2500$  MPa *SD*. The 2YS slope<sup>11</sup> was determined by doing a linear fit to the curve in the region of its inflection, and therefore is subject to less absolute error (estimated at  $\pm 250$  MPa *SD*) than that of the 1YS slope. Both of these are dwarfed by the material variability observed in the actual scatter among replicates (Tables 2.1 and 2.3)
- g. *Tensile stresses (1YS, 2YS, UTS)*. The MTS screw-driven tensile testing machines have load cells that were calibrated to an accuracy better than 0.1% relative, which translates to a measurement error of 1 MPa at a typical 1,000 MPa flow stress observed in U-Nb. The initial cross-sectional area measurement (done with calipers and an optical microscope) has a relative error of 0.04%, which translates to an additional stress measurement error of 0.4 MPa at the 1,000 MPa level. These stress errors are smaller than those because of the analyst's error in determining any given 1YS slope that propagates through the analysis to give a 1YS *SD* of  $\pm 5$ –10 MPa. More significantly, all of the foregoing errors pale in view of the intrinsic material variability, which reflected in the wide differences in *SD* (spanning 1.4–180.3 MPa) as implied from the data in Tables 2.1 and 2.3, and explicitly reported in Tables 6.1 and 6.3 in [2007hac2]. (It is noted that the analyst's errors in measuring 2YS and UTS values for any given stress-strain curve are much smaller than those for measuring 1YS.)
- h. *Tensile elongations (uniform and total)*. The strain gages used were calibrated to be within 0.1% relative, which translates to an engineering strain measurement error of 0.00025 at a typical 0.25 total strain (elongation) to failure. Considering the propagation of the error in determining any given 1YS slope translates to an error in the uniform and total plastic elongation of 0.00025. The material variability again dominates the observed scatter in uniform and TEs, typically  $>0.01$  (Tables 2.1 and 2.3). In line with past metallurgical experience, the UE has a smaller scatter than the TE, because the latter is affected by stochastic phenomenon arising from internal defects and surface damage, but the former is not. The uniform (and nonuniform) elongation did, however, suffer from problems with determining the instability point from Considere's criterion on the true-stress ( $\sigma$ )-true strain ( $\epsilon$ ) curves, as the slope  $d\sigma/d\epsilon$  crossed the  $\sigma$ - $\epsilon$  curve multiple times (and had considerable noise as well); it was decided that the highest-strain intersection of these two curves was the true point of instability. This decision was validated by the fact that the engineering stress evaluated at this assumed instability point was always within 1 MPa of the UTS, which is consistent with typical metallic tensile behavior. In any event, this instability issue does not factor into the TE evaluation.

---

<sup>11</sup> Although the 2YS slope is age-sensitive, it was not analyzed in this study but is included in Tables 2.1, 2.3, 2.5, and 2.9 for the sake of completeness.

**Table A1.1. Calculated Absolute Error in Aging Time (Evaluated at the Indicated Aging Temperature) due to Aging Attributable to Heating and Cooling that was Unaccounted for in the Nominal Aging Time and Heat Treat Practice.**

		Time error, minutes relative to the nominal aging time							
Q (kcal/mole)		25				30			
Aging temperature (C)		100	200	250	300	100	200	250	300
Nominal aging time (min)	<1000	1.693	1.887	2.047	2.199	1.087	1.438	1.625	1.794
	>=1000	-7.821	-7.325	-7.048	-6.795	-8.427	-7.773	-7.471	-7.200

**Table A1.2. Calculated Relative Percentage Error in Aging Time (Evaluated at the Indicated Aging Temperature) due to Aging Attributable to Heating and Cooling that was Unaccounted for in the Nominal Aging Time and Heat Treat Practice.**

		Time error, percent relative to the nominal aging time							
Q (kcal/mole)		25				30			
Aging temperature (C)		100	200	250	300	100	200	250	300
Nominal aging time (min)	10	16.9300	18.8700	20.4700	21.9900	10.8700	14.3800	16.2500	17.9400
	100	1.6930	1.8870	2.0470	2.1990	1.0870	1.4380	1.6250	1.7940
	165	1.0261	1.1436	1.2406	1.3327	0.6588	0.8715	0.9848	1.0873
	215	0.7874	0.8777	0.9521	1.0228	0.5056	0.6688	0.7558	0.8344
	1000	-0.7821	-0.7325	-0.7048	-0.6795	-0.8427	-0.7773	-0.7471	-0.7200
	10000	-0.0782	-0.0733	-0.0705	-0.0680	-0.0843	-0.0777	-0.0747	-0.0720
	100000	-0.0078	-0.0073	-0.0070	-0.0068	-0.0084	-0.0078	-0.0075	-0.0072
	230385	-0.0034	-0.0032	-0.0031	-0.0029	-0.0037	-0.0034	-0.0032	-0.0031
	318000	-0.0025	-0.0023	-0.0022	-0.0021	-0.0027	-0.0024	-0.0023	-0.0023
	1052400	-0.0007	-0.0007	-0.0007	-0.0006	-0.0008	-0.0007	-0.0007	-0.0007
	3153600	-0.0002	-0.0002	-0.0002	-0.0002	-0.0003	-0.0002	-0.0002	-0.0002

## APPENDIX 2: MODEL FITS AND PREDICTIONS ON AN ALTERNATE DEFINITION OF HARDNESS REPLICATES

For completeness, the current analysis method was repeated on the hardness data, using a different assumption on the definition of what constitutes a hardness replicate. The approach documented in the main text assumed that the hardness replicate was the average of all measurements from a single coupon. For all the model-fitting and validation data in this work, the number of hardness replicates,  $n$  or  $nv$  for any given age, is always equal to one. This Appendix presents the parallel results assuming that the hardness replicate is the individual hardness measurement. These replicate hardness measurements are provided in Tables 2.2 and 2.4 for the U-5.6Nb and U-7.7Nb model-fitting data ( $n$  varying over 7–15), and also for the validation HV measurements (Tables 2.6, 2.7, and 2.10, where  $n$  is even larger).

The parameters fitted on this alternate assumption are provided in Tables A2.1 and A2.2, which can be compared with the results of the baseline approach in Tables 3.18 and 3.19. The graphical depictions in Figures A2.1 and A2.2 can also be compared against Figures 4.15 and 4.16. The difference between the parameters is minimal, showing that the model fitting is not very sensitive to the replicate definition.

What is sensitive to the definition are the prediction intervals for the validation data, provided in Table A2.3. Compare this with the results from the baseline approach in Table 4.13. Note that the  $PI$  values in Table A2.3 are practically indistinguishable from the corresponding  $CI$  values. This is because as  $n$  increases, the quantity  $RSE/n$  approaches zero, and the expression for  $PI$  (Eq. A4.13) approaches that for the  $CI$  (Eq. A4.12); See Appendix 4. The sample size for future ages was set at a comparable number to the validation hardness data sets already available:  $nv = 160$  for U-6Nb and  $nv = 60$  for both U-5.6Nb and U-7.7Nb.

In general, the baseline approach (Table 4.13) gives better agreement between the existing validation data and the model predictions than does this alternate approach (Table A2.3), which gives some modest confidence in the baseline approach.

**Table A2.1. Vickers Hardness Kinetic Parameters for U-5.6Nb. The  $t$  value used to compute the confidence interval is 1.969. The units of  $Q$  are kcal/mol;  $A$  and  $B$  were assessed on the basis of the time in minutes.**

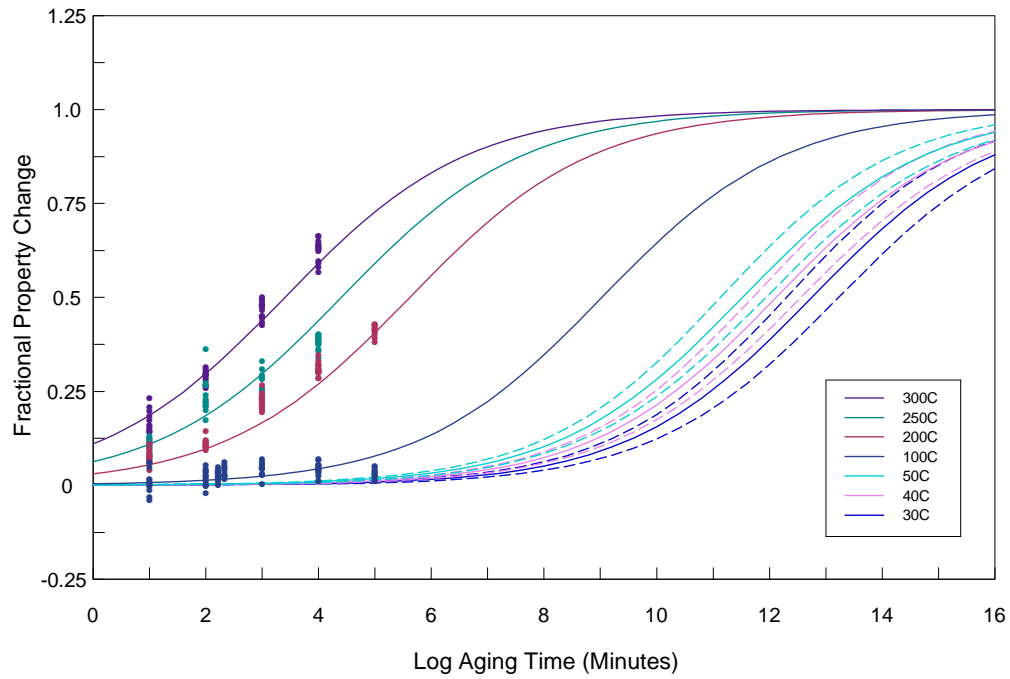
<b>U-5.6Nb Microhardness</b>				
Parameter	Estimate	Standard Error	95% Confidence Interval	
			Lower Bound	Upper Bound
$Q$	27.575	0.729	26.140	29.010
$A$	0.6148	0.0153	0.5847	0.6449
$B$	3.4009	0.0361	3.3298	3.4720

**Table A2.2. Vickers Hardness Kinetic Parameters for U-7.7Nb. The  $t$  value used to compute the confidence interval is 1.976. The units of  $Q$  are kcal/mol;  $A$  and  $B$  were assessed on the basis of the time in minutes.**

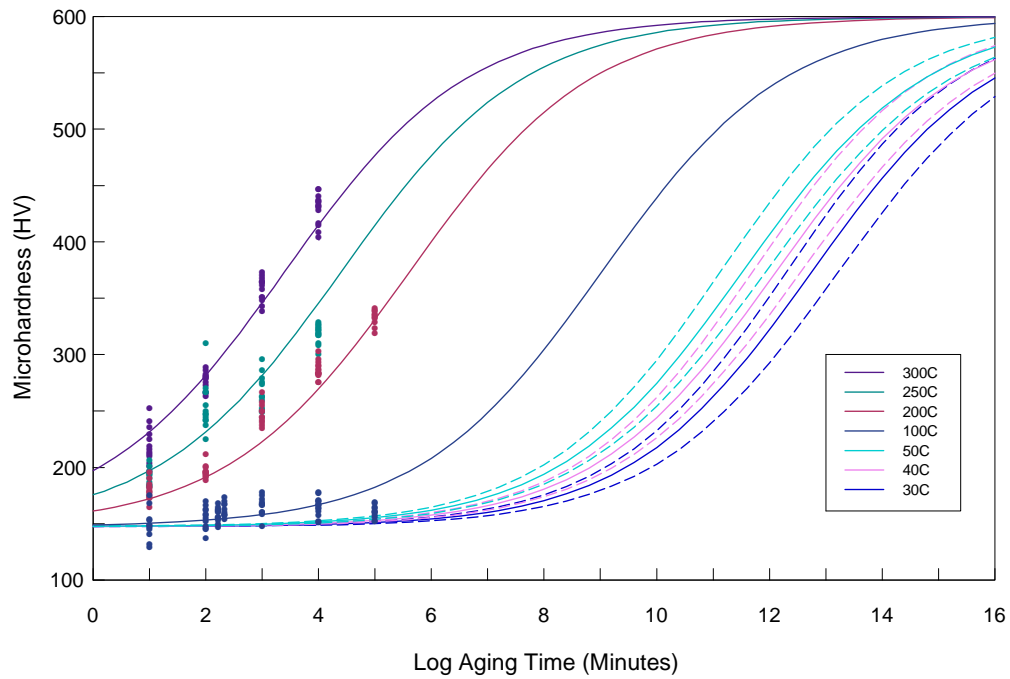
<b>U-7.7Nb Microhardness</b>				
Parameter	Estimate	Standard Error	95% Confidence Interval	
			Lower Bound	Upper Bound
$Q$	21.814	1.263	19.318	24.310
$A$	0.4555	0.0228	0.4104	0.5006
$B$	4.2665	0.1117	4.0458	4.4872

**Table A2.3. Experimentally Measured and Predicted and Mean HV Values for Various U-Nb Alloys for Current and Future Model Validation, from an Alternate Replicate Definition. The 95% prediction and confidence intervals are also given. The alloy identified as 6 wt% Nb is the RFP banded U-6Nb; the alloys identified as 5.6 wt% and 7.7 wt% are nonbanded. “NP” indicates that no data point is expected, because of material limitations.**

Alloy Wt.% Nb	Aging Temp. (C)	Aging Time		Vickers Microhardness					
		(min.)	(years)	Experimental Mean	Prediction Int.		Prediction Mean	Confidence Int.	
					lower	upper		lower	upper
6	40	328320	0.625		172.5	175.7	174.1	172.5	175.6
6	40	656640	1.25		173.6	177.4	175.5	173.6	177.4
6	40	1311840	2.5		175.0	179.5	177.3	175.0	179.5
6	40	2629440	5.0	171	176.7	182.0	179.4	176.7	182.0
6	40	5260320	10.0		178.7	185.0	181.8	178.7	185.0
6	40	10519200	20.0		181.0	188.5	184.8	181.1	188.5
6	40	21038400	40.0		183.8	192.7	188.3	183.9	192.7
6	65	328320	0.625		181.0	186.9	183.9	181.0	186.9
6	65	656640	1.25		183.8	190.7	187.2	183.8	190.7
6	65	1311840	2.5		187.0	195.3	191.2	187.1	195.3
6	65	2629440	5.0	182	191.0	200.6	195.8	191.0	200.6
6	65	5260320	10.0		195.6	206.9	201.3	195.6	206.9
6	65	10519200	20.0		201.2	214.3	207.7	201.0	214.3
6	65	21038400	40.0		207.3	222.8	215.0	207.3	222.8
6	90	328320	0.625		197.1	206.3	201.7	197.1	206.3
6	90	656640	1.25		202.7	213.5	208.1	202.7	213.5
6	90	1311840	2.5		209.3	221.8	215.6	209.3	221.8
6	90	2629440	5.0	201	217.0	231.5	224.2	217.0	231.5
6	90	5260320	10.0		225.7	242.5	234.1	225.7	242.5
6	90	10519200	20.0		235.7	254.9	245.3	235.7	254.9
6	90	21038400	40.0		247.0	268.9	257.9	247.0	268.9
5.6	100	318000	0.6	189	188.2	199.2	193.7	188.2	199.2
5.6	100	1052400	2.0		201.7	215.9	208.8	201.7	215.9
5.6	100	3153600	6.0		217.3	235.0	226.1	217.3	235.0
5.6	200	318000	0.6	367	357.8	373.0	365.4	357.9	373.0
5.6	200	1052400	2.0		392.6	410.3	401.5	392.7	410.3
5.6	200	3153600	6.0		423.7	442.9	433.3	423.7	442.9
5.6	300	318000	0.6	530	495.5	509.3	502.4	495.6	509.3
5.6	300	1052400	2.0		518.1	531.2	524.7	518.2	531.2
5.6	300	3153600	6.0		535.3	547.3	541.3	535.4	547.3
7.7	100	318000	0.6	191	194.3	218.1	206.2	194.3	218.1
7.7	100	1052400	2.0		211.0	239.1	225.0	211.0	239.0
7.7	100	3153600	6.0		228.2	260.8	244.5	228.3	260.8
7.7	200	318000	0.6	321	317.3	340.8	329.0	317.3	340.8
7.7	200	1052400	2.0		343.4	371.8	357.6	343.4	371.8
7.7	200	3153600	6.0		367.5	400.1	383.8	367.5	400.1
7.7	300	318000	0.6	527	408.3	439.9	424.1	408.3	439.8
7.7	300	1052400	2.0		433.0	466.3	449.7	433.0	466.3
7.7	300	3153600	6.0		454.2	488.2	471.2	454.3	488.1

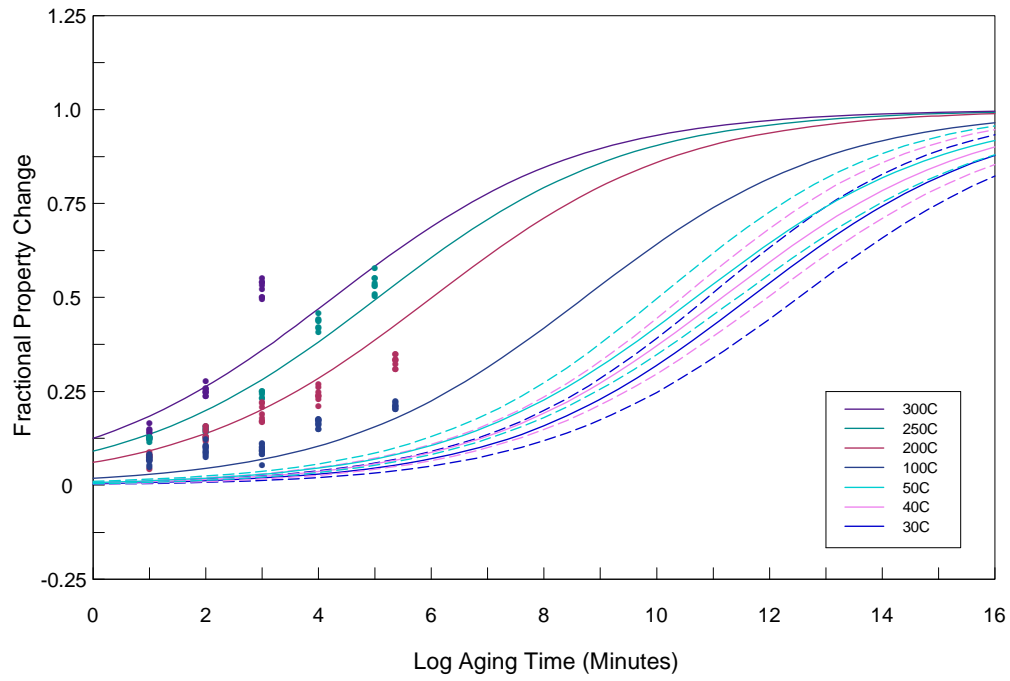


(a)

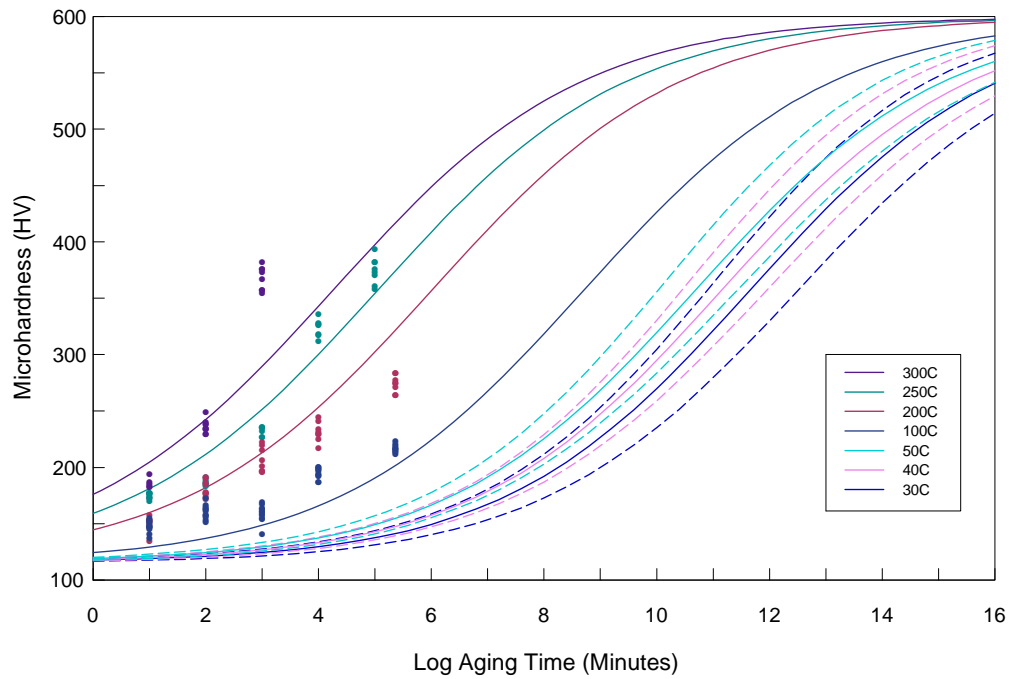


(b)

Figure A2.1. U-5.6Nb HV data (points), model fits to data (solid lines), and low-temperature model predictions (solid line—mean, dashed lines—95% confidence intervals). (a) in terms of  $f$ , (b) in terms of absolute property.



(a)



(b)

Figure A2.2. U-7.7Nb HV data (points), model fits to data (solid lines), and low-temperature model predictions (solid line—mean, dashed lines—95% confidence intervals). (a) in terms of  $f$ , (b) in terms of absolute property.

This page left blank intentionally.

### APPENDIX 3: MODEL EVALUATION

Residuals from a model fit are defined as the differences:

$$e_i = y_i - pred_i \quad \text{Eq. A3.1}$$

where  $y_i$  is an observed value for the  $i$ th replicate data point, and  $pred_i$  is the corresponding mean fitted value from the model. In other words, the errors are the differences between what is observed and what is predicted based on the model. Thus, we can think of the  $e_i$  as the observed errors if the model is correct. In regression analysis, it is assumed that the errors are independent, have a mean of 0 and a variance of  $\sigma^2$ , and follow a normal distribution. The assumption of the errors following a normal distribution is necessary for testing hypotheses about the model parameters and for computing confidence and prediction intervals. As part of the model evaluation process, residuals are examined to see if the assumptions hold. Plots of residuals from the models showed that the variance was constant over time, that successive error terms were independent, and that the errors appeared to follow a normal distribution. Normal probability plots of residuals plotted against the quartiles of a standard normal distribution are provided below in Figures A3.1 and A3.2. If the models provide an adequate fit to the data, then the points on these plots should fall along a straight line.

Another means of assessing the goodness of fit of a model is to look at the residual standard error (*RSE*) of the fit. In equation form, this is defined as

$$RSE = \sqrt{\sum_{i=1}^n \frac{(y_i - pred_i)^2}{(n-p)}} = \sqrt{\sum_{i=1}^n \frac{e_i^2}{(n-p)}} \quad \text{Eq. A3.2}$$

where the  $e_i$  are the residuals from the model fit, and the quantity  $(n-p)$  is the number of observations minus the number of parameters in the model, equal to the degrees of freedom (*df*). This value provides an overall summary of how well the model fits the observed data.

In the summary of the nonlinear model fit to the data, tests of hypotheses are examined to see whether or not the parameter estimates ( $Q$ ,  $A$ , and  $B$ ) are significantly different from 0. For the models chosen, all parameter estimates were significantly different from 0, indicating that all three parameters were significant and relevant for consideration as part of the model fitting.

Various methods have been developed for investigating the goodness of fit of a nonlinear model. For a more complete discussion, see Ratkowsky [1983rat] or Bates and Watts [1988bat]. In particular, for nonlinear models, there are methods for measuring the degree to which the model and its individual parameter estimates exhibit linearity. The method used for assessing the degree of departure from linearity for the nonlinear model parameters in this report involved two-dimensional profiles of the residual sum-of-squares function  $\tau$ . These plots are provided in Figures A3.3 and A3.4. For coordinate (as defined by each parameter) directions along which the approximate linear methods are accurate, a plot of the nonlinear t-statistic  $\tau$  against the parameter estimate over several standard deviations on either side of the maximum likelihood estimate should produce a straight line. The degree to which such plots exhibit nonlinearity represent the degree of potential bias and inaccuracy in the parameter estimates. See Venables and Ripley [1994ven] for more details.

For most of the models, the two-dimensional profile for each of the parameters appears to be fairly linear. Where there is some degree of nonlinearity in one or more of the parameter

estimates for a given property, the linear approximation for that parameter may be misleading. As a result, less confidence should be placed on these estimates.

Most notable among the exceptions to linearity in U-5.6Nb are the parameter estimates for  $Q$ ,  $A$ , and  $B$  for 1YM.

Most notable among the exceptions to linearity in U-7.7Nb are the following parameter estimates:

1.  $Q$  and  $B$  for TE,
2.  $A$  for 1YM,
3.  $A$  for UE, and
4.  $Q$  and  $B$  for HV.

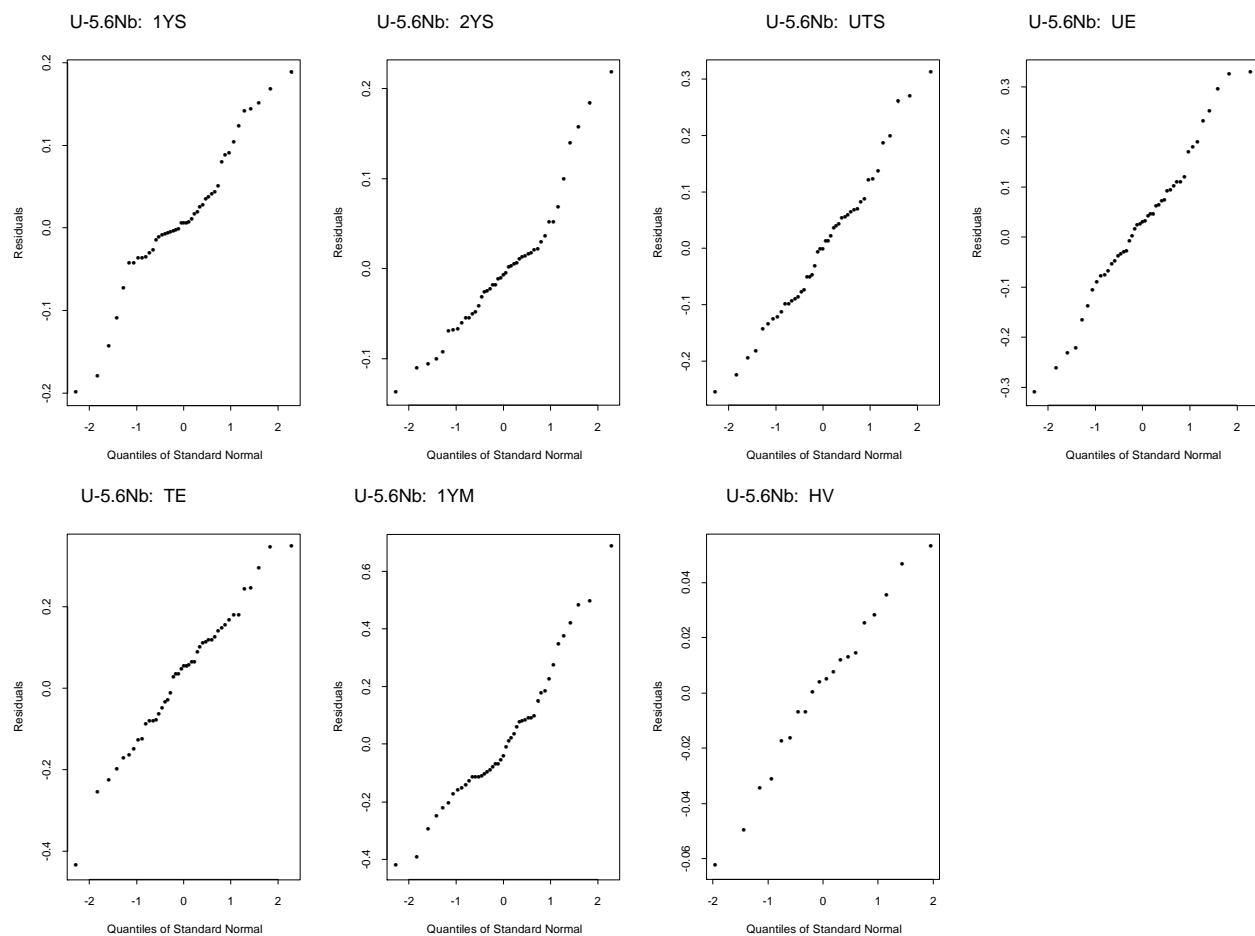


Figure A3.1. Normal probability plots of the residuals for U-5.6Nb model fits.

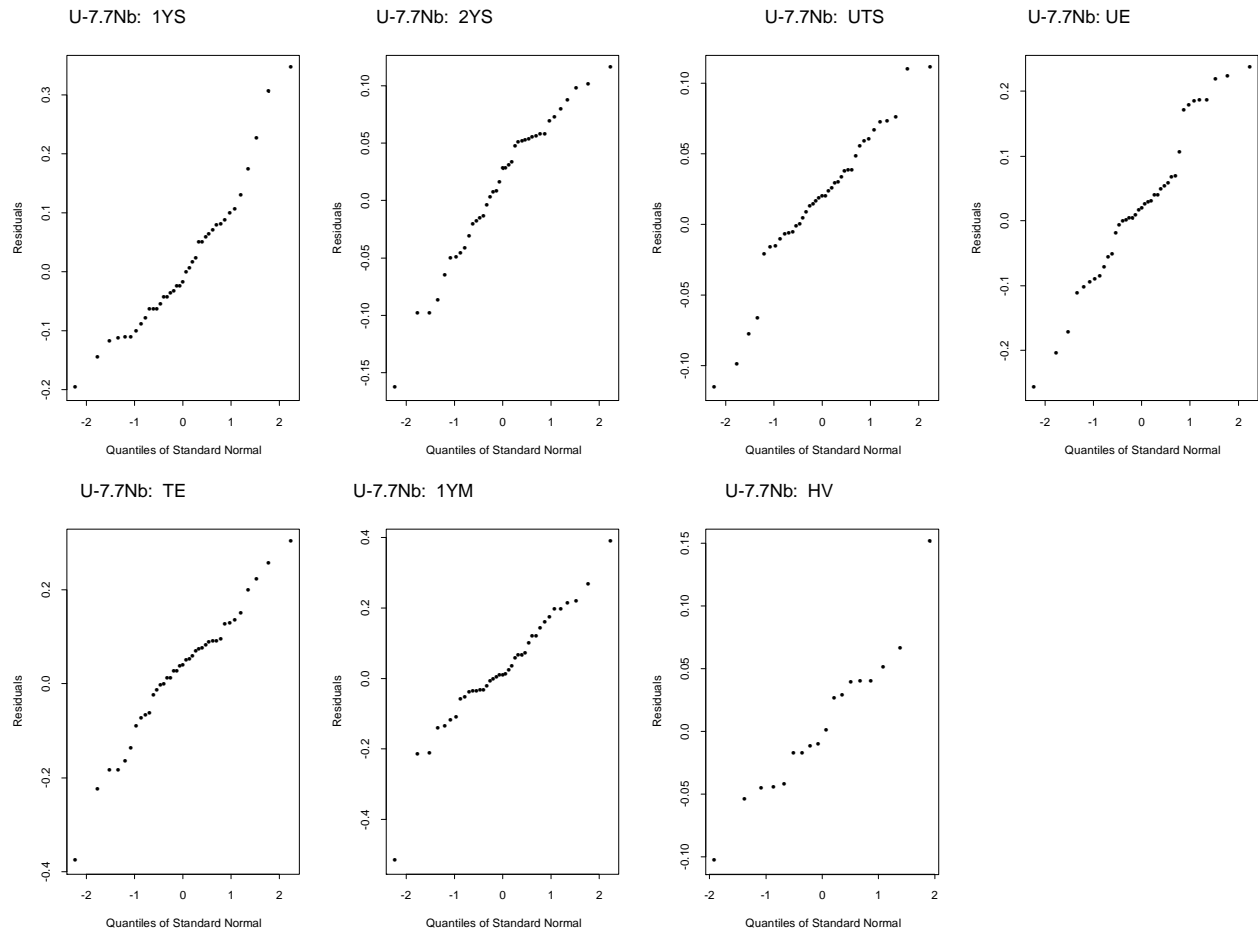


Figure A3.2. Normal probability plots of the residuals for U-7.7Nb model fits.

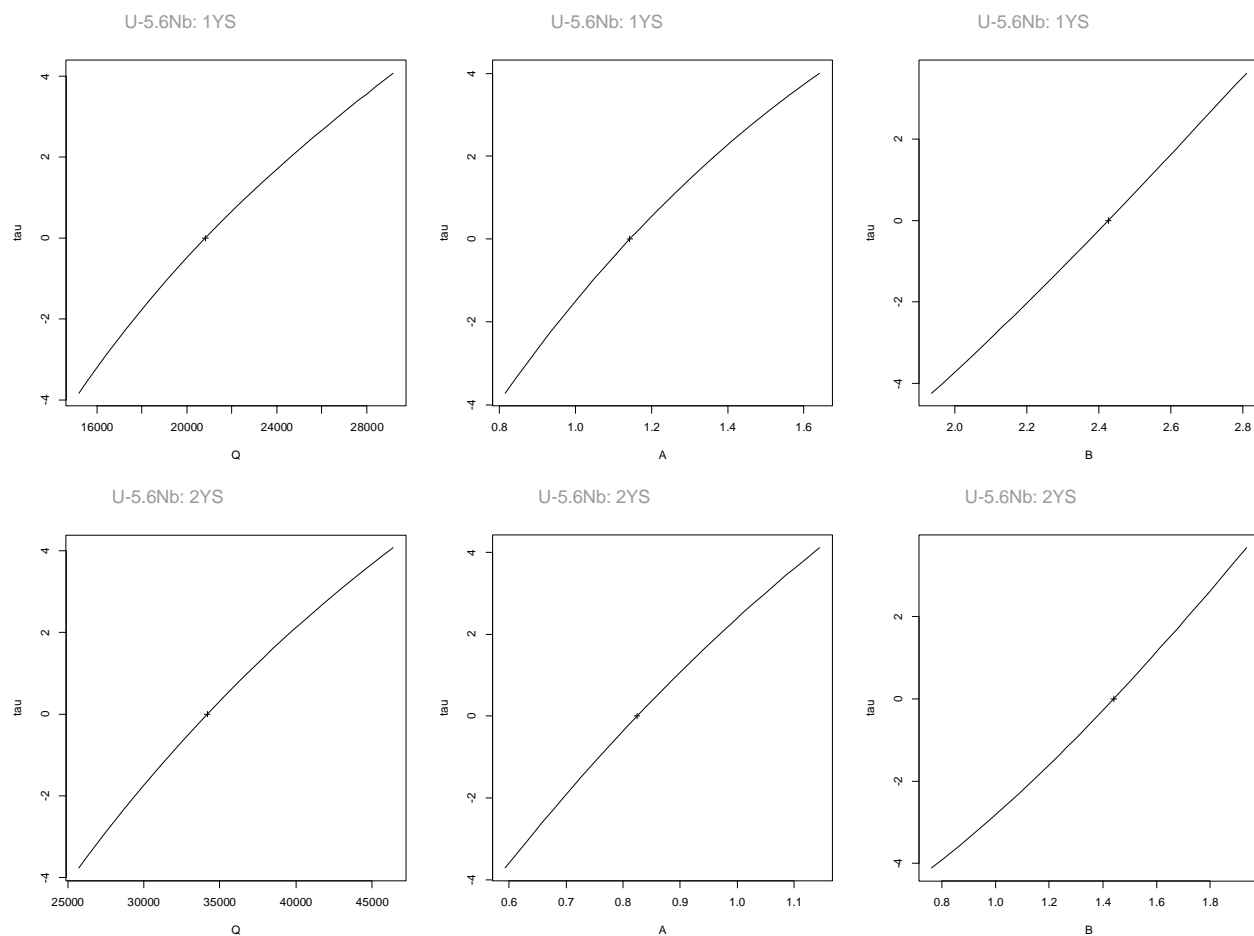


Figure A3.3. Two-dimensional profiles of the residual sum-of-squares function for U-5.6Nb model fits.

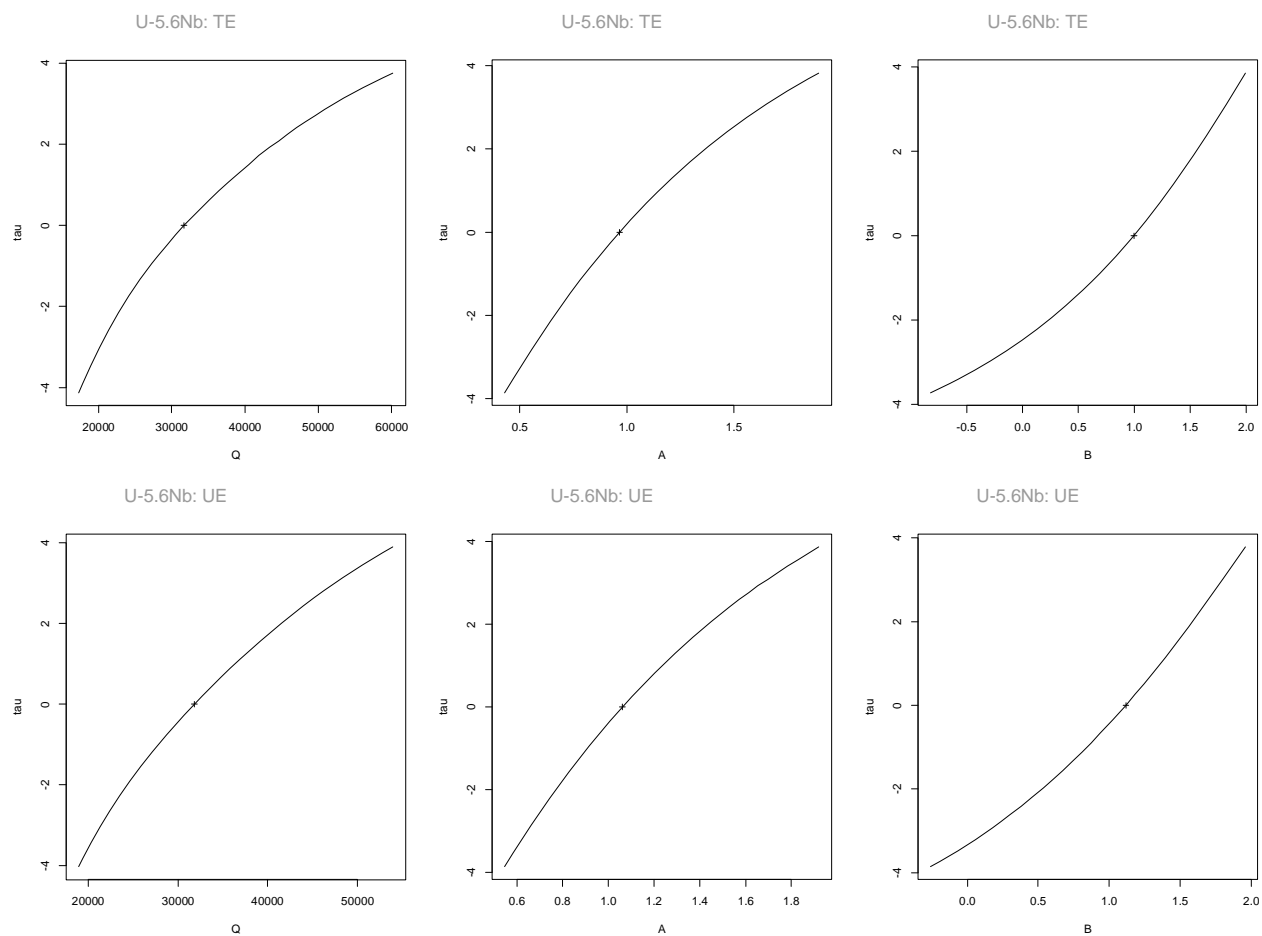


Figure A3.3 (continued). Two-dimensional profiles of the residual sum-of-squares function for U-5.6Nb model fits.

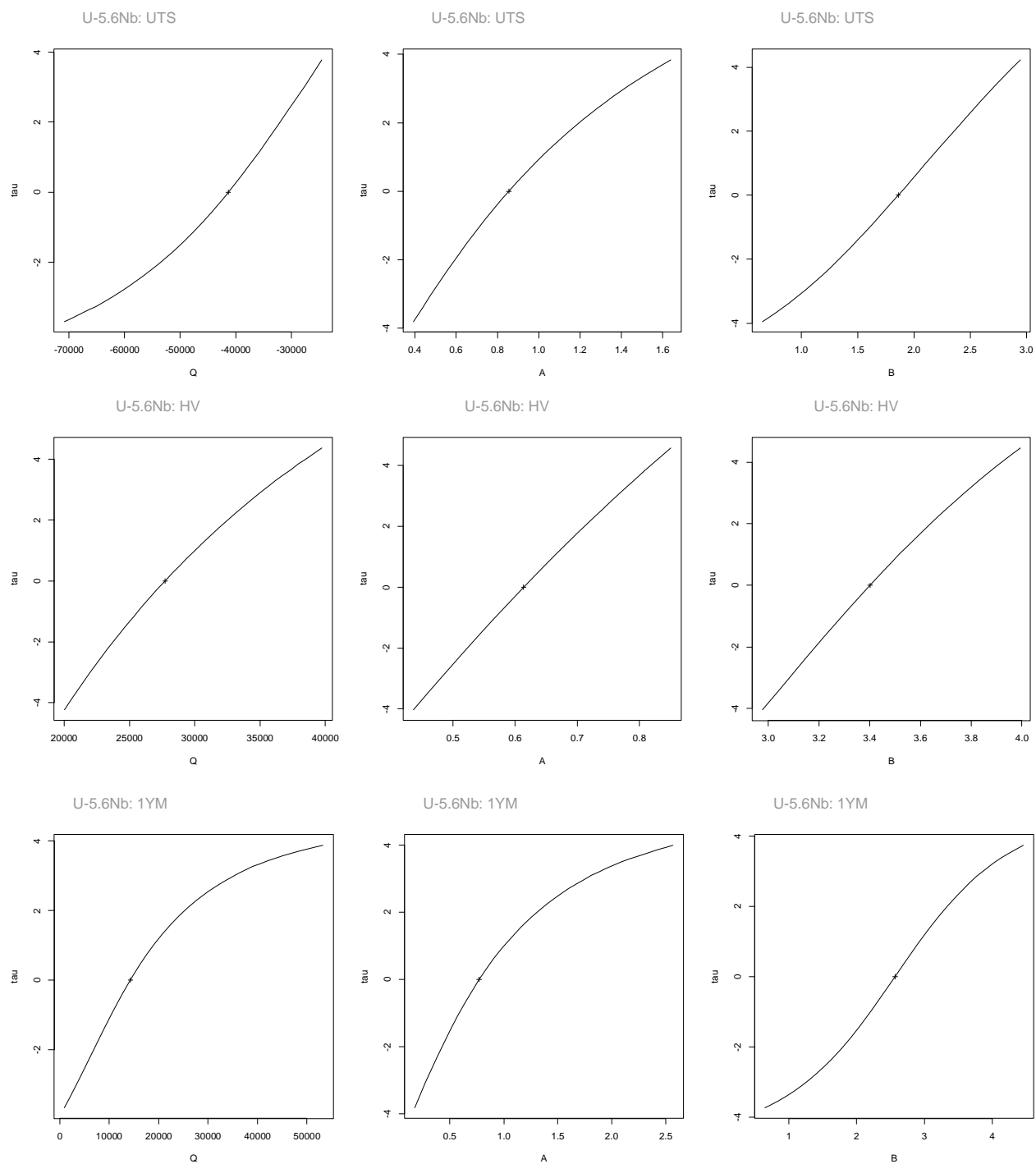


Figure A3.3 (continued). Two-dimensional profiles of the residual sum-of-squares function for U-5.6Nb model fits.

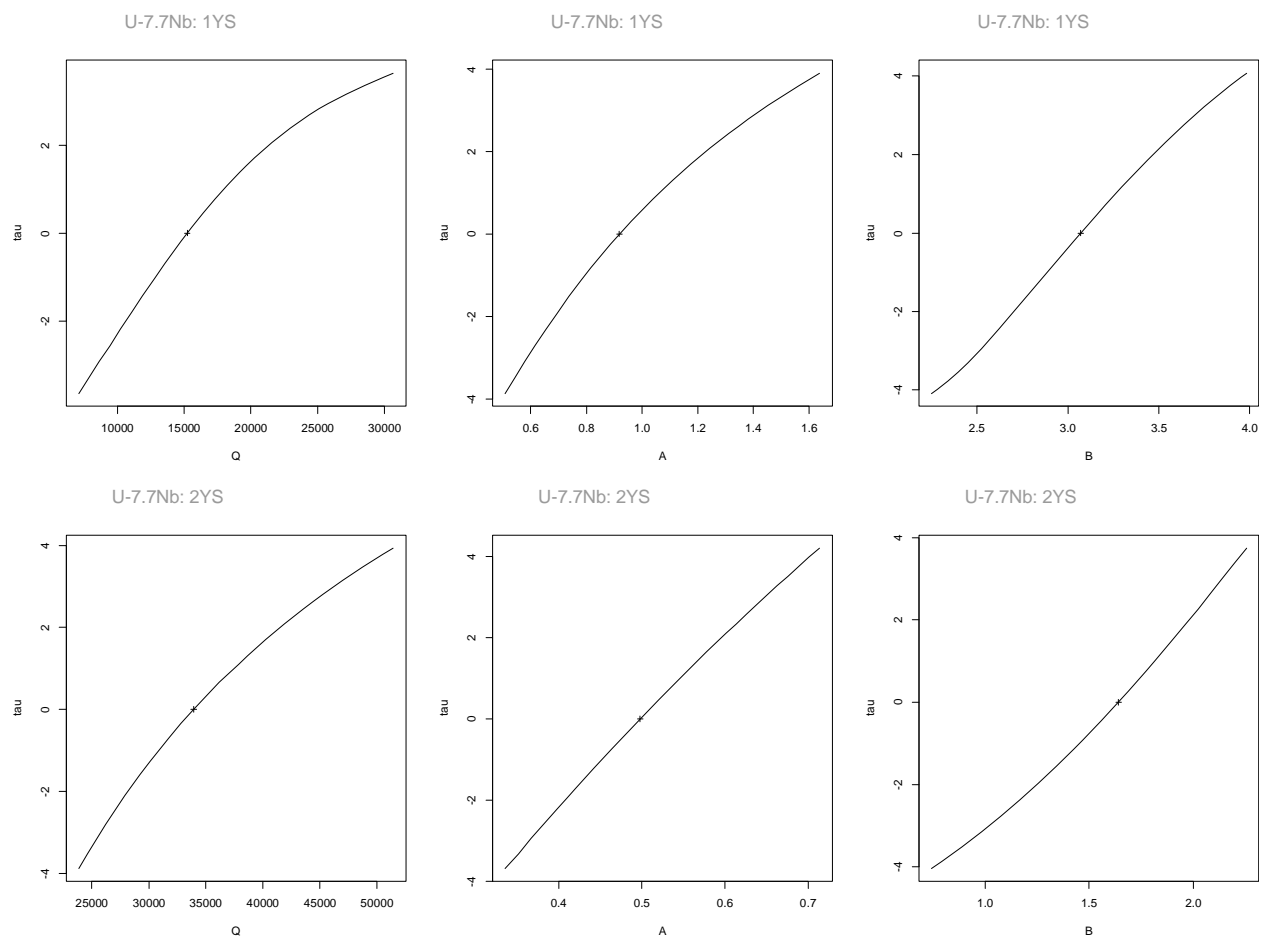


Figure A3.4. Two-dimensional profiles of the residual sum-of-squares function for U-7.7Nb model fits.

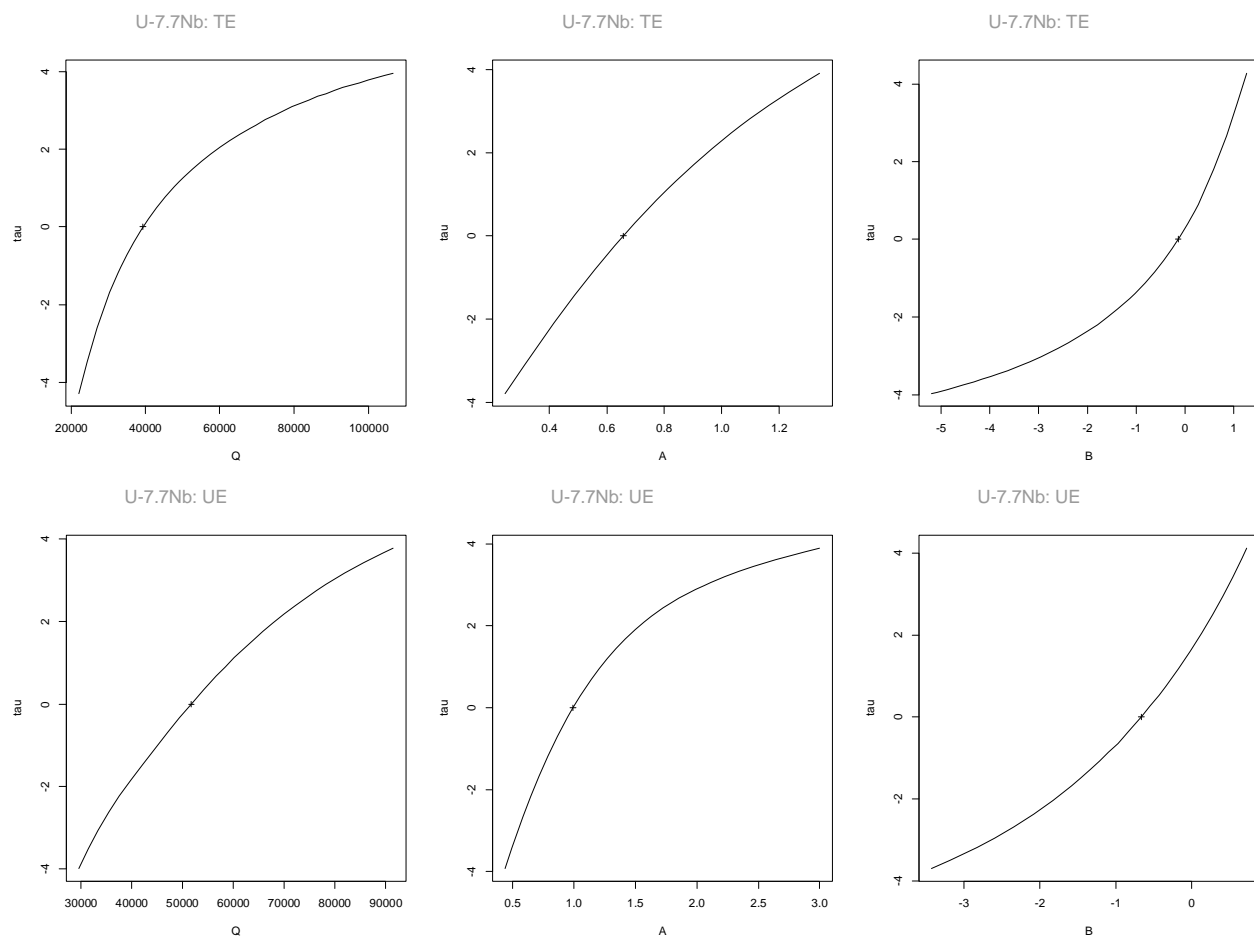


Figure A3.4 (continued). Two-dimensional profiles of the residual sum-of-squares function for U-7.7Nb model fits.

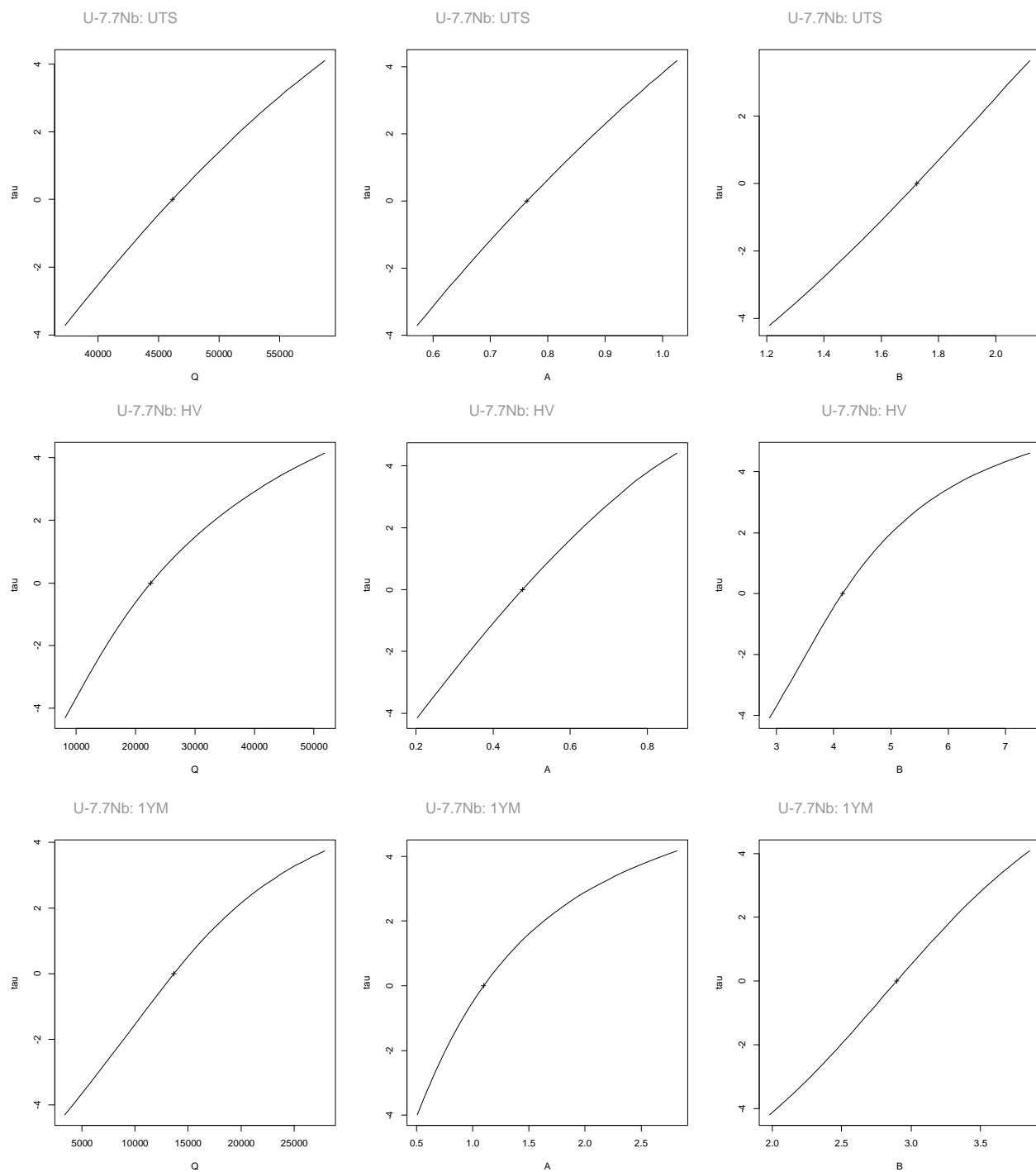


Figure A3.4 (continued). Two-dimensional profiles of the residual sum-of-squares function for U-7.7Nb model fits.

## APPENDIX 4: BACKGROUND ON NONLINEAR MODELS

### A4.1. Nonlinear Regression

Consider the general form of a regression model:

$$y_i = f(\mathbf{X}_i; \boldsymbol{\theta}) + \varepsilon_i \quad \text{Eq. A4.1}$$

where  $y_i$  represents the response variable,  $\mathbf{X}_i$  represents a vector of explanatory variables, and  $\varepsilon_i$  represents the error term at the  $i$ th replicate data point,  $i = (1, 2, \dots, n)$ . The term  $f(\mathbf{X}_i, \boldsymbol{\theta})$  describes a function of the explanatory variables, represented by the vector  $\mathbf{X}_i$ , and the parameters, represented by the vector  $\boldsymbol{\theta}$ . The term  $\varepsilon_i \sim N(0, \sigma^2)$  means that the error is assumed to be normally distributed with mean zero and constant variance  $\sigma^2$  for all values of the explanatory variables represented by  $\mathbf{X}_i$ . It is generally assumed that the errors are independent and identically distributed about the mean zero with constant variance. Independence means that the error at one value is not related to the error at some other value.

Given the validity of the assumption of independent and identically distributed normal error, one can make certain general statements about the least-squares estimators in linear and nonlinear regression models. Least-squares estimators of  $\boldsymbol{\theta}$  are those that minimize the sums of squares of the deviations between the observed values and the predicted values from the model. The maximum likelihood estimates for the parameters in  $\boldsymbol{\theta}$  are least squares estimates.

A nonlinear regression model is distinguished from a linear regression model in that at least one of its parameters appears nonlinearly. In the formal mathematical sense, nonlinear means that at least one of the derivatives of  $y_i$  with respect to the parameters in  $\boldsymbol{\theta}$  is a function of at least one of those parameters.

In general, linear regression models are preferred to nonlinear regression models because of the desirable properties associated with their estimators. For linear models, the estimates of the parameters are unbiased, normally distributed, and have the minimum possible variance. The estimators for nonlinear models do not exhibit these properties, but achieve these properties only asymptotically as the sample size approaches infinity. In addition, exact standard errors and confidence intervals can be computed for linear models, whereas for nonlinear models, these values are only approximate.

For linear models, the estimators of the parameters can be obtained from explicit mathematical expressions, whereas for nonlinear regression models, either an iterative procedure using a mathematical algorithm or an exhaustive search procedure must be used for finding the optimum solution. One commonly used iterative procedure is the Gauss-Newton method.

For a linear model, the solution locus is a line or a plane through the origin and the coordinate system defined by the parameters. It has no curvature. On the other hand, the solution locus for a nonlinear model is a curved surface. The closer such a curved surface is to being linear, the closer the properties of the nonlinear model are to having the properties of a linear model. For such close-to-linear models, the predicted values of the response variable will be virtually unbiased. The least-squares estimators of the parameters will have distributions closely approximating a normal distribution. In addition, the confidence intervals for each parameter will be close to being exact. Additional information on nonlinear models can be found in Ratkowsky [1983rat], Bates and Watts [1988bat], and Draper and Smith [1981dra].

#### **A4.2. Application of Statistical Intervals**

The appropriate choice of a statistical interval depends on the general purpose of the interval and the characteristic of interest. One must decide whether the main interest is in describing the population from which the sample has been selected or in predicting the results of future samples from the same population. Intervals that describe the population include confidence intervals for the population mean or for mean fitted values (such as in regression modeling). In contrast, prediction intervals deal with predicting (or containing) the results of a future sample from the population. See Hahn and Meeker [1982mee, 1991hah] for a more thorough discussion on different types of intervals.

A confidence interval is an interval that can be claimed to contain the mean of a population with a high degree of confidence. For a 95% confidence interval on the mean fitted values of a regression model, it can be said that, for very many repeated experiments, in the long run, one would be correct approximately 95% of the time in claiming that the true regression fit to the population is contained in the calculated confidence interval.

A prediction interval for a single future observation is an interval that will, with a specified degree of confidence, contain the next randomly selected observation from the population. This interval is calculated from the sample data under the important assumption that the previously sampled items and the future ones can be regarded as random samples from the same population. It also assumes similar aging conditions and measurement procedures. If, for example, three future measurements are to be obtained at a specified point in time, then, in the long run after many repeated experiments, one would be correct 95% of the time in claiming that the true values of the future samples, as well as the average of the three samples, would be contained within a 95% prediction interval if the model is truly representative of the population being studied. If a validation point were to fall outside of the prediction interval bounds, then one could conclude either that the sample is different from the population from which the model was obtained, or that the model does not adequately represent the population.

Tables 4.7 to 4.13 contain mean fitted values from the nonlinear regression models and corresponding confidence intervals on these predictions for the times and temperatures both within and outside of the time-temperature space spanned by the model-fitting data. In addition, these tables contain measured values which are the results of ongoing and future validation experiments, occurring at temperatures observed in the first experiment and at temperatures lower than previously studied. These values will be referred to as validation points. For the validation points, prediction intervals are provided. In Tables 4.7 to 4.13, both the confidence intervals on the mean fitted values from the model and the prediction intervals for the validation points have been truncated at the lower and upper bounds for each property (Table 3.1). These intervals have also been truncated in the plots showing the location of the validation points relative to the predicted curves and bounds.

#### **A4.3. Computation of Statistical Intervals**

Assuming that the errors from the model fit are normally distributed, confidence intervals on population parameters can be calculated. The first step in the process of obtaining an approximate confidence interval for the predicted nonlinear model is to obtain the standard errors of the fitted points. To compute these standard errors, the variance-covariance matrix and the equations for the first partial derivatives (gradients) of the model with respect to the three parameters are needed. The gradient equations are provided below, and the variance-covariance

matrix values are provided in Table A4.1. At a given aging time and temperature, the equation for computing the standard error of a fitted value,  $se.fit$ , is as follows:

$$se.fit = \sqrt{P^T * VCV * P} \quad \text{Eq. A4.2}$$

where  $P$  is a  $3 \times 1$  vector containing the first partial derivatives for the estimates of  $Q$ ,  $A$ , and  $B$ , evaluated at a particular time and temperature,  $P^T$  is the transpose of the vector  $P$ , and  $VCV$  is a  $3 \times 3$  matrix containing the variances for the parameters  $Q$ ,  $A$ , and  $B$  along its diagonal and the covariances between parameters on the off-diagonal.

First derivative equations were obtained using S-Plus software licensed by Insightful Corp. See Venables and Ripley [1994ven] for details on the software code. In order to keep the gradient equations readable, the equations have been broken down into the following six expressions:

$$U = \frac{\log(e)}{R} \approx \frac{0.43429}{1.99 \text{ cal/mol}} = 0.218 \text{ mol/cal} \quad \text{Eq. A4.3}$$

$$V = \frac{1}{573.15 \text{ K}} - \frac{1}{T} \quad \text{Eq. A4.4}$$

$$W = x + QUV - B \quad \text{Eq. A4.5}$$

$$X = e^{AW} \quad \text{Eq. A4.6}$$

$$Y = 1 + X \quad \text{Eq. A4.7}$$

$$Z = Y^2 \quad \text{Eq. A4.8}$$

where  $A$ ,  $B$ , and  $Q$  are the Logistic model parameters,  $T$  is in Kelvin, and  $x$  is  $\log_{10}(\text{time})$  as defined in Eq. 3.3.

The gradient equations are as follows:

$$grad(Q) = \frac{AUVX}{Z} \quad \text{Eq. A4.9}$$

$$grad(A) = \frac{WX}{Z} \quad \text{Eq. A4.10}$$

$$grad(B) = -\frac{AX}{Z} \quad \text{Eq. A4.11}$$

The general procedure for computing an approximate lower and upper confidence interval at a given point involves the following steps:

1. Choose a value for time and a value for temperature.
2. Evaluate the gradient equations at the chosen time and temperature. (This produces a  $P$  vector.)
3. Compute the standard error using Eq. A4.2.
4. Use the following equation to compute an approximate confidence interval:

$$CI = pred_i \pm t_{(0.95, df)} * se.fit_i . \quad \text{Eq. A4.12}$$

In this equation,

- $pred_i$  is the predicted or mean fitted value from the model at time  $i$  for the chosen temperature,
- $t_{(0.95, df)}$  is the t-statistic for a 95% confidence level with  $df$  degrees of freedom,
- $df$  (degrees of freedom) is computed as the total number of replicate observations in the data set ( $n$ ) minus the number of parameter estimates ( $p$ ), and
- $se.fit_i$  is the computed standard error of the fitted value at time  $i$ , Eq. A4.2.

The variance-covariance matrices are presented in lower triangular form in Table A4.1.

A prediction interval is wider than a confidence interval. One would expect that an estimate of an individual measurement would have more variability than an estimate of the mean response from a group of measurements. In computing a prediction interval on an actual observed  $y_i$ , there is an additional source of error. It represents the deviation of the individual  $y_i$  values from the mean fitted values from the model. See Kleinbaum and Kupper [1978kle] for more details on the calculation of a prediction interval for regression.

In equation form, the calculation of a prediction interval is as follows:

$$PI = pred_i \pm t_{(0.95, df)} \sqrt{(se.fit_i)^2 + \left(\frac{RSE}{nv}\right)^2}, \quad \text{Eq. A4.13}$$

where  $pred_i$ ,  $t_{(0.95, df)}$ , and  $se.fit_i$  are as defined above. The equation for computing the residual standard error is as follows:

$$RSE = \sqrt{\sum_{i=1}^n \frac{(y_i - pred_i)^2}{(n - p)}}, \quad \text{Eq. A4.14}$$

where  $n$  is the number of samples,  $p$  is the number of parameters in the model, and  $nv$  is the number of future validation points for a given alloy and temperature combination. The  $RSE$  values for each model are provided in Table 4.3.

**Table A4.1 Variance-Covariance Matrices****U-5.6Nb TE**

	$Q$	$A$	$B$
$Q$	24852120		
$A$	-311.5718	0.03008261	
$B$	-1259.116	0.01844140	0.09262537

**U-7.7Nb TE**

	$Q$	$A$	$B$
$Q$	39500890		
$A$	-502.1799	0.01500349	
$B$	-2690.861	0.04079818	0.2308611

**U-5.6Nb UE**

	$Q$	$A$	$B$
$Q$	18541480		
$A$	-199.8689	0.02822474	
$B$	-891.2887	0.01132047	0.06320916

**U-7.7Nb UE**

	$Q$	$A$	$B$
$Q$	41153030		
$A$	-471.5211	0.02680211	
$B$	-2561.475	0.03651868	0.1844366

**U-5.6Nb 1YS**

	$Q$	$A$	$B$
$Q$	3224415		
$A$	-37.06893	0.009140565	
$B$	-150.8623	0.0006613776	0.01281954

**U-7.7Nb 1YS**

	$Q$	$A$	$B$
$Q$	4855980		
$A$	-64.74975	0.015668949	
$B$	-269.6162	-0.002011677	0.03180668

**U-5.6Nb 1YM**

	$Q$	$A$	$B$
$Q$	16677440		
$A$	-248.2645	0.03324399	
$B$	-1041.423	0.001828075	0.1348329

**Table A4.1 (continued).**

U-7.7Nb 1YM

	$Q$	$A$	$B$
$Q$	5346451		
$A$	-73.02778	0.03572418	
$B$	-338.8812	-0.0005889329	0.04206774

U-5.6Nb 2YS

	$Q$	$A$	$B$
$Q$	6605678		
$A$	-58.80722	0.004762360	
$B$	-301.4772	0.002406113	0.02084868

U-7.7Nb 2YS

	$Q$	$A$	$B$
$Q$	9230194		
$A$	-83.27905	0.002097209	
$B$	-416.9067	0.003069187	0.03066215

U-5.6Nb UTS

	$Q$	$A$	$B$
$Q$	24835420		
$A$	285.3534	0.02084541	
$B$	905.9384	0.003800227	0.05845111

U-7.7Nb UTS

	$Q$	$A$	$B$
$Q$	6724107		
$A$	-64.77024	0.002894096	
$B$	-228.1218	0.001549427	0.01245295

U-5.6Nb HV

	$Q$	$A$	$B$
$Q$	5122572		
$A$	-53.36997	0.002207797	
$B$	-91.16910	-0.002040067	0.013020668

U-7.7Nb HV

	$Q$	$A$	$B$
$Q$	16340840		
$A$	-114.2892	0.005124729	
$B$	-416.0291	-0.01342360	0.1063440

This page left blank intentionally.

This page left blank intentionally.

This report has been reproduced directly from the best available copy. It is available electronically on the Web (<http://www.doe.gov/bridge>).

Copies are available for sale to U.S. Department of Energy employees and contractors from:

Office of Scientific and Technical Information  
P.O. Box 62  
Oak Ridge, TN 37831  
(865) 576-8401

Copies are available for sale to the public from:

National Technical Information Service  
U.S. Department of Commerce  
5285 Port Royal Road  
Springfield, VA 22161  
(800) 553-6847

